^{14}C via accelerator mass spectrometry (AMS) as a tracer and dating tool in the study of paddy soil carbon dynamics

Dissertation
zur Erlangung des Doktorgrades
der Mathematisch-Naturwissenschaftlichen Fakultät
der Christian-Albrechts-Universität
zu Kiel

vorgelegt von
Tino Bräuer

Kiel, Juli 2013

Erstgutachter: Prof. Dr. Rainer Duttmann

Zweitgutachter: Prof. Dr. Ingmar Unkel

Tag der mündlichen Prüfung: 23.09.2013

Zum Druck genehmigt:

---

gez.

Die vorliegende Arbeit wurde im Leibniz-Labor für Altersbestimmung und Isotopenforschung der Christian- Albrechts-Universität zu Kiel angefertigt. Finanziert wurde diese Arbeit aus Mitteln der Deutschen Forschungsgemeinschaft im Rahmen der DFG Forschergruppe FOR995 „Biogeochemistry of paddy soil evolution“.

Table of contents

Table of contents

Summary

Soils, globally containing about 2,500 gigatonnes of carbon, are supposed to behave as sink as well as source for atmospheric carbon dioxide (CO_2). Due to a higher carbon (C) sequestration potential compared to vegetation and atmosphere, soils have been suggested as the most appropriate potential sink for atmospheric carbon. Thus, soils are considered to be of outstanding importance within the system of climate change. Thereby, especially the types of land-use and management practices seem to influence the processes that mitigate the loss of soil organic carbon (SOC) and increase C sequestration. One of the most important kinds of land-use is the cultivation of soils with wetland rice (paddy soils), since the staple food of more than 50 percent of the world's population is based on rice. Also in regards to the global carbon cycle paddy soils are of importance. The cultivation of wetland rice leads to decreased decomposition rates in the relevant soils and therefore, supports the accumulation of SOC caused by water logged conditions during flooded periods. The outcomes are high SOC levels observed in topsoils and an assumed high carbon sequestration potential.

Owing to the high potential of paddy soils to sequester carbon, according to a foreseeable increase of the atmospheric CO_2 concentration, and due to a continuous increase in land under wetland rice cultivation it is crucial to understand the mechanisms, which influence the carbon dynamics under paddy management. Hence, soils from a chronosequence of 50 to 2,000 years of agricultural use were sampled and investigated. The study sites belong to one of the oldest paddy soil regions in the world, near the southern coast of Hangzhou Bay around Cixi, Zhejiang Province, China. The parent material consists of estuarine sediment that was deposited in the Hangzhou Bay after passing the Yangtze delta. Its uniform composition provided the comparative investigation of soil carbon dynamics under the land management practice of wetland rice-paddies against upland-crops. For this purpose radiocarbon (^{14}C) measurements by accelerator mass spectrometry (AMS) were made at the Leibniz-Laboratory (Kiel). Particularly, the origin and the distribution of soil organic carbon present in subsoil horizons was investigated in this study.

The parent material is characterized by a total organic carbon (TOC) content of ca. 0.3 % and a ^{14}C concentration of ca. 50 pMC (percent modern carbon). After being diked-in,

gradients in TOC and ^{14}C of the ten investigated soil profiles developed under the influence of an intensified cultivation. Results of ^{14}C measurements reveal the formation of a dense plough pan within the first five decades of paddy rice cultivation and thus, disclose a seriously reduced, but not totally prevented, downward transport of soil organic matter (SOM). In the paddy topsoils the 'original' SOC with a radiocarbon signature depleted in ^{14}C gets replaced by 'fresh' material with modern ^{14}C signals within decades. The equilibrium times for TOC and ^{14}C in the subsoils are in the order of centuries.

To reveal the main source of organic carbon (OC) present in the subsoil the entire SOC pool was chemically fractionated into three SOM fractions: the acid soluble fulvic acid (FA), the alkali soluble humic acid (HA) and the insoluble humin fraction (alkali residue). Results disclose the fulvic acid fraction, which is assumed to be the most mobile fraction among the three groups of humic substances, as the main driver for the input of organic matter into the subsoil. FA's show an average contribution of about 50 % on SOC with a maximum of 65 % in the 2,000-year old paddy soil. The average HA contribution is less than 20 % for all soil profiles, while the humin fraction represents ca. 30 % of the SOC. Since fulvic acids are the major component of dissolved organic matter (DOM), the relocation of organic matter through the plough pan, transported by percolating water, was identified as the main driver for subsoil 'OC-refreshing' in paddy subsoils. A second source for subsoil OC in paddy soils could be identified by plant roots and root exudates with ^{14}C concentrations up to 128 % of the modern standard. The plant remains were found far below the plough pan (1 m) and could be related to *Oryza sativa*, partly by means of DNA isolation and 18S rDNA analysis.

After the quantification of the different SOC fractions, a classification of TOC into two conceptual C pools provided a more detailed insight into SOC dynamics. Based on a time-dependent steady-state box model mean residence times and pool sizes were calculated. Depending on the depth, results reveal a fast cycling SOC pool with residence times ranging from 1.5 to 21 years. The stabilized SOC pool reveals residence times between 150 and 2,000 years. The quantitative relevance of the modeled SOC pools is strongly affected by the initial model parameters. The proportion of the conceptual SOC pools on TOC at the beginning of the time series governs the resulting pool sizes significantly. However, the applied calculations were confirmed as an appropriate tool to estimate turnover rates of SOC in young paddy soils. Furthermore, it was possible to calculate mean

residence times not only for the topsoil but also for deep subsoil horizons. In summary, the results presented in this thesis suggest a dynamic balance of OC fluxes, rather than a long-term stabilization of SOC within paddy soils.

Zusammenfassung

Böden speichern weltweit etwa 2500 Gigatonnen Kohlenstoff (C). Sie fungieren dabei sowohl als Senke als auch als Quelle für atmosphärisches Kohlendioxid (CO_2). Aufgrund ihrer Fähigkeit mehr Kohlenstoff zu binden als die Vegetation und die Atmosphäre wurden Böden als die am besten geeigneten Kohlenstoffsenken ausgemacht. Böden stellen daher einen wichtigen Faktor im System der globalen Klimaveränderung dar. Die Prozesse, die einerseits den Verlust von bodeneigenem Kohlenstoff vermindern und andererseits Kohlenstoffspeicherung in Böden verstärken sind dabei vor allem von der Art der Landnutzung beeinflusst. Eine der weltweit bedeutendsten Landnutzungsformen ist die Bewirtschaftung von Nassreisböden (*paddies*), da diese mehr als der Hälfte der Weltbevölkerung als Hauptnahrungsmittellieferant dienen. Auch in Hinblick auf eine auf den CO_2 Anstieg zurückzuführende globale Erwärmung sind *paddies* aufgrund ihrer Relevanz für den globalen Kohlenstoffkreislauf von Bedeutung. In den betroffenen Böden führt der Anbau von Nassreis zu verminderten Abbauraten der organischen Bodensubstanz (OBS) und die herbeigeführte Wasserüberstauung begünstigt die Anreicherung bodeneigenen Kohlenstoffs. Als Konsequenz ergeben sich hohe Gehalte an organischem Kohlenstoff (OC) in den Oberböden und das bereits erwähnte hohe Potential Kohlenstoff zu speichern.

Aufgrund des hohen Kohlenstoffspeicherungspotentials, eines fortwährenden CO_2 Anstiegs in der Atmosphäre und einer kontinuierlichen Zunahme von Flächen mit Nassreiskultivierung ist es von großer Bedeutung die Mechanismen, die die Kohlenstoffdynamik unter Reisanbau beeinflussen, zu verstehen. Aus diesem Grund wurden Böden einer sich über 2000 Jahre erstreckenden Chronosequenz beprobt und untersucht. Das Untersuchungsgebiet gehört zu einer der ältesten Reisanbauregionen der Welt und liegt an der Südküste der Bucht von Hangzhou, nahe der Stadt Cixi (Provinz Zhejiang), China. Das Ausgangsmaterial besteht aus Sediment, das aus dem Jangtsekiang-Delta kommend, in der Bucht von Hangzhou abgelagert wurde. Seine einheitliche Zusammensetzung ermöglicht die vergleichende Untersuchung der Kohlenstoffdynamik unter der Landnutzungsform Nassreisanbau gegenüber Nicht-Reisanbau. Zu diesem Zweck wurden Radiokohlenstoffmessungen (^{14}C) mittels Beschleuniger-Massenspektrometrie

(AMS) im Leibniz-Labor (Kiel) durchgeführt. In dieser Arbeit wurde insbesondere die Herkunft und Verteilung bodeneigenen Kohlenstoffs im Unterboden untersucht.

Der Gesamtanteil des organischen Kohlenstoffs (TOC) im Ausgangssediment beträgt etwa 0,3 % und die ^{14}C Konzentration beträgt ca. 50 pMC (percent modern carbon). Unmittelbar nach Abschluss von Landgewinnungsmaßnahmen bildeten sich unter dem Einfluss intensivierter Kultivierung OC und ^{14}C Gradienten in den zehn untersuchten Bodenprofilen. ^{14}C Messungen zeigen, dass es durch Nassreisanbau innerhalb der ersten fünf Jahrzehnte zur sukzessiven Bildung einer kompakten Zone (*plough pan*) kommt, welche den nach unten gerichteten Transport der OBS deutlich reduziert aber nicht vollständig unterbindet. Der noch aus dem Ausgangsmaterial stammende, an ^{14}C verarmte Kohlenstoff, wird im Oberboden der *paddies* innerhalb von Jahrzehnten durch „frischen" Kohlenstoff mit modernem ^{14}C Signal ersetzt. Derselbe Prozess nimmt im Unterboden mehrere Jahrhunderte in Anspruch.

Um den Ursprung des im Unterboden befindlichen Kohlenstoffs zu ermitteln, wurde die OBS einer chemischen Fraktionierung unterzogen, resultierend in drei Fraktionen: säurelösliche Fulvinsäuren, basenlösliche Huminsäuren und die unlösliche Huminfraktion. Unter den gewonnen Fraktionen konnte die Fulvinsäure, welche als die mobilste Fraktion unter den Huminstoffen gilt, als hauptverantwortliche Fraktion für die Zufuhr von Kohlenstoff in den Unterboden identifiziert werden. Die Fulvinsäuren machen einen durchschnittlichen Anteil von 50 % an der OBS aus mit einem Maximum von 65 % im ältesten *paddy*. Die Huminsäuren umfassen im Durchschnitt weniger als 20 % der OBS. Die verbleibenden 30 % können den Huminen zugerechnet werden. Da sich die OBS überwiegend aus löslichen Fraktionen zusammensetzt, gelangt ein Großteil des sich im Unterboden befindlichen Kohlenstoffs durch Wassertransport dorthin. Als eine weitere Möglichkeit organisches Material mit modernen ^{14}C Gehalten in den Unterboden zu bringen, konnte die Zufuhr von OC mittels Pflanzenwurzeln nachgewiesen werden. Die Pflanzenreste wurde in Tiefen von bis zu einem Meter gefunden und konnten teilweise durch DNA Analysen als Reis (*Oryza sativa*) identifiziert werden.

Nach der Quantifizierung der verschiedenen OBS Fraktionen wurde der gesamte organische Kohlenstoff in zwei konzeptionelle Kohlenstoffpools eingeteilt, um die C-Dynamik genauer zu untersuchen. Unter Verwendung eines Abbau- und

Verlagerungsmodels wurden Verweildauern und Größen von Kohlenstoffpools berechnet. In Abhängigkeit von der Tiefe ergaben die Berechnungen einen sich schnell umsetzenden C-Pool mit Verweildauern von 1,5 bis 21 Jahren. Der stabilisierte C-Pool ist durch Verweildauern zwischen 150 und 2000 Jahren gekennzeichnet. Dabei ist die Poolgröße in hohem Maße von den Eingangsparametern des Models abhängig. Die Aufteilung des TOC zu Beginn der Berechnungen beeinflusst die sich ergebenen Poolgrößen in erheblicher Weise. Die hier angewendeten Berechnungen erwiesen sich als nützliches Werkzeug zur Bestimmung von OC Umsatzraten in jungen *paddies*. Darüber hinaus war es möglich, Verweildauern nicht nur für Oberböden abzuschätzen, sondern auch für Unterböden. Zusammenfassend lassen die Ergebnisse dieser Arbeit den Schluss zu, dass Nassreisböden eher durch ein dynamisches Gleichgewicht von OC Flüssen gekennzeichnet sind als durch die langfristige Stabilisierung der OBS.

Danksagung

Zunächst danke ich Herrn Prof. Dr. Pieter Meiert Grootes für die Bereitstellung des interessanten Themas und seine Unterstützung bei der Durchführung dieser Arbeit. Sein ständiges Streben nach neuen Erkenntnissen hat mich und diese Arbeit vorangetrieben. Mein Dank gilt weiterhin Prof. Dr. Rainer Duttmann für sein Interesse an meiner Arbeit, seine fachlichen Ratschläge sowie die Übernahme des Erstgutachtens. Dr. Marie-Josée Nadeau danke ich für die angenehme Zusammenarbeit und anregenden Diskussionen während meiner Promotion. Insbesondere möchte ich mich bei meinem Vorgänger, Dr. Alexander Dreves, für die Einführung in das Leibniz-Labor und interessante Diskussionen aus unterschiedlichen fachlichen Sichtweisen, welche meine Arbeit sehr bereichert haben, bedanken. Prof. Dr. Ingrid Kögel-Knabner und Dr. Angelika Kölbl danke ich für die hervorragende Organisation der Forschergruppe 995 „Biogechemistry of paddy soil evolution“.

Für ein angenehmes Arbeitsklima und unterschiedlichste Unterstützung bedanke ich mich herzlich beim gesamten Team des Leibniz-Labors für Altersbestimmung und Isotopenforschung: Monika Gumz und Annette Mintrop danke ich für die Einführung in die chemische Probenaufbereitung, Angelika Oriwall und Katrin Paap-Meiß für ihre Einweisung in die Arbeitsschritte zur Herstellung von Graphit-Targets sowie das Abschmelzen unzähliger Quarzampullen. In diesem Zusammenhang danke ich Nicole (*„…es hat KNACK gemacht…“*) Möckel für die Gelegenheit den Arbeitsschritt der Einwaage, durch die eine oder andere Wiederholung, zu perfektionieren. Weiterhin gilt mein Dank Corinna Tschorn, Andrea Hamann-Wilke, Anke Rieck und Dr. Matthias Hüls für vielfältigen Beistand und Unterstützung. Christian und Andrzej danke ich für mal mehr, mal weniger fachbezogene, aber immer unterhaltsame, Gespräche im Labor, wie auch für arbeitsklimafördernde Maßnahmen außerhalb des Labors.

Meinen Eltern danke ich von Herzen für ihre umfassende Unterstützung in allen Lebenslagen, und für ihr mir immer gegenwärtiges Vertrauen. Mein größter Dank gilt meiner kleinen Familie. Nancy danke ich für die Unterstützung während der letzten Jahre. Du hast mich immer bestärkt und mehr als einmal motivierende Worte für mich gefunden. Emma danke ich dafür, dass sie die letzten Monate meiner Promotion zu der aufregendsten Zeit meines bisherigen Lebens gemacht hat. Ich liebe euch!

List of manuscripts

This study comprises two introducing chapters (chapter I and II), and three stand-alone papers, chapters III to V, which are published to refereed international scientific journals or in preparation for submission (in prep.). They may therefore be subject to revision. Each of the chapters contains a separate introduction, description of methods, presentation of data and discussion, as well as a separate reference list. Main results of this study are summarized in the concluding chapter VI.

The titles and authors of the Chapters III, IV, and V are briefly listed below:

CHAPTER III
Title: Downward carbon transport in a 2000-year rice paddy soil chronosequence traced by radiocarbon measurements
Authors: T. Bräuer, P. M. Grootes, M.-J. Nadeau & N. Andersen
Status: published in Nuclear Instruments and Methods in Physics Research Section B: Beam Interactions with Materials and Atoms 294, 584-587 (2013).

CHAPTER IV
Title: Origin of subsoil carbon in Chinese paddy soil chronosequence.
Authors: T. Bräuer, P. M. Grootes & M.-J. Nadeau
Status: published in Radiocarbon 55 (3-4), xxxx.

CHAPTER V
Title: Modeling of soil organic carbon dynamics in paddy soils of different ages
Authors: T. Bräuer, A. Dreves, P. M. Grootes & M.-J. Nadeau
Status: in preparation

I contributed to these papers by field work in China and sample preparation, by processing and interpreting of the field and experimental data. All analyses, the writing and preparation of manuscripts and graphical presentation were done by Tino Bräuer under the supervision of Prof. Dr. Pieter M. Grootes, Dr. Marie-J. Nadeau and Dr. Alexander Dreves.

In addition to the work presented in Chapters III - V, I cooperated with members of the Forschergruppe (FOR 995) and contributed to the following publications, which are not part of this thesis.

Title: The carbon count of 2,000 years of rice cultivation.
Authors: Kalbitz K, Kaiser K, Fiedler S, Kölbl A, Amelung W, Bräuer T, Cao ZH, Don A, Grootes PM, Jahn R, Schwark L, Vogelsang V, Wissing L, Kögel-Knabner I.
Status: published in Global Change Biology 19, 1107-1113.

Title: Decalcification increases the accessibility of soil mineral surfaces for organic carbon accumulation in paddy soils.
Authors: Wissing L, Kölbl A, Schad P, Bräuer T, Cao ZH, Kögel-Knabner I.
Status: submitted to Geoderma

Chapter I

General Introduction

Significance of soils within the global carbon cycle

The Intergovernmental Panel on Climate Change (IPCC) reported significant climate changes, including an increased global surface temperature by 0.8°C, a sea-level rise of 15-23 cm during the twentieth century, and notable impacts on ecosystems, caused by elevated greenhouse gas (GHG) levels (Schellnhuber 2006; IPCC 2007). With a contribution of around 64 % to the radiative forcing by GHGs, carbon dioxide (CO_2) is the most important anthropogenic gas in the atmosphere (WMO 2012). The increase in CO_2 is supposed to be caused by human activities due to fossil fuel burning, soil cultivation, deforestation and land-use changes. Thus, the continuous increase in CO_2 is directly associated with the increase in human population, especially from the pre-industrial time until the present day. The observed rise in atmospheric CO_2 amounts to ca. 40 %, starting with ca. 280 ppm (parts per million, number of molecules of the greenhouse gas per million molecules of air) in 1850 and increasing to 390.9 ppm in 2011, with a current increase of 2.0 ppm per year (IPCC 2007; WMO 2012). Lal (2004) estimated the emissions of carbon from fossil fuel burning to the atmosphere for the post industrial era with 270 ± 30 Pg (1Pg = 10^{15}g) and the contribution of terrestrial ecosystems (e.g. land-use changes) to be 136 ± 55 Pg. With an annual emission of 9.1 ± 0.5 Pg carbon (C) the combustion of fossil fuels is considered as the main driver of the observed CO_2 increase, followed by emissions from land-use changes, mostly due to tropical deforestation of 0.9 ± 0.7 Pg C (WMO 2012). This is known from direct measurements of atmospheric CO_2 since the 1950's and analyses of atmospheric air trapped in ice cores (Leuenberger et al. 1992; Keeling et al. 2001; IPCC 2007). Within the global carbon cycle, the amount of C linked to the atmospheric C pool is relatively small compared to the four remaining C pools (cf. Figure 1.1)

Estimates by Schimel et al. (2001) reveal an annual deficit in the global carbon budget ranging from 2 to 4 Pg C per year for the 1990's by comparing the CO_2 emissions with the

carbon uptake by the oceans and the terrestrial biosphere. Considering the potential of this unknown C sink, which could turn into a C source and enhance the CO_2 concentration in the atmosphere, it is important to know where the so-called 'missing' carbon is sequestered. Despite the ongoing controversial discussion about the fate of the 'missing' carbon, results mainly regarding the 1990's suggest an uptake of the carbon in terrestrial ecosystems of the northern hemisphere (Ciais et al. 1995; Keeling et al. 1996; Brown und Schroeder 1999; White et al. 2000; McGuire et al. 2001). According to recent studies, a crucial role regarding the additional C uptake is accorded to forest ecosystems (Lal 2005).

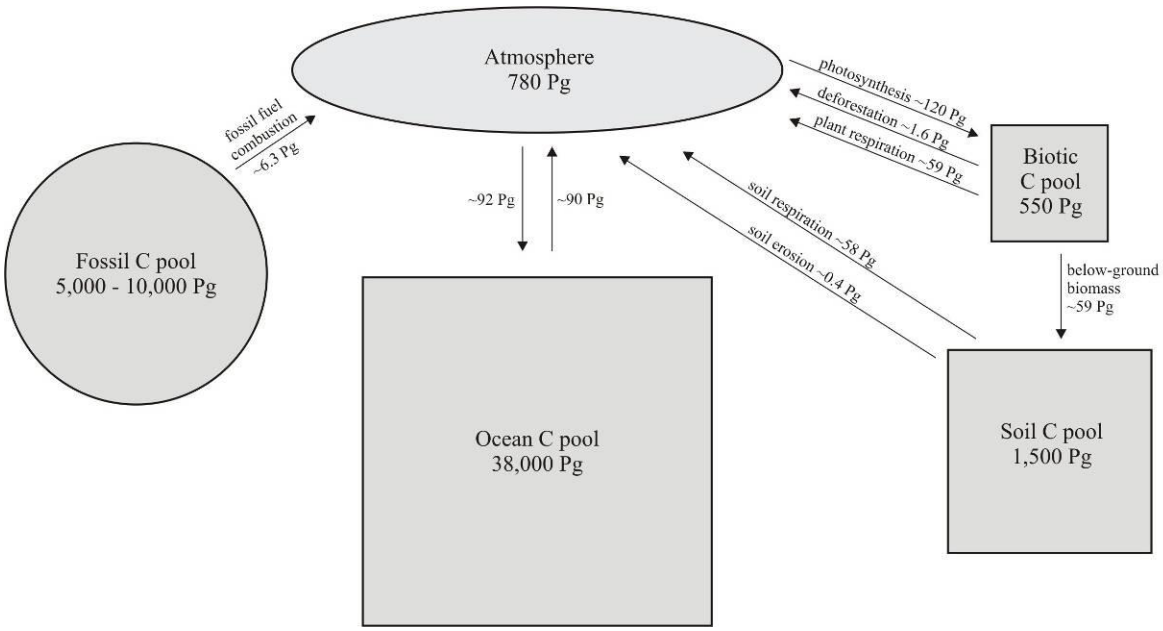

Figure 1.1: Global carbon reservoirs and major CO_2 exchanges between them in Pg of carbon per year. As a consequence of natural cycles and human activities the different C pools are not constant, and exchanges between the geochemical compartments take place. The carbon stocks in each C pool and the data of CO_2 fluxes were obtained from Houghton (2007) and IPCC (2007).

With a proportion of about two-thirds of the global terrestrial carbon pool, consisting of the biotic and the pedological pool, the soil organic carbon (SOC) pool is the largest active pool within the global carbon cycle (Batjes 1996; Lal 2008). It is two times the size of the atmospheric C pool and nearly three times the size of the biotic C pool (Lal 2004). Considering the geological C reservoirs as part of the terrestrial carbon cycle, storing more than 4,000 Pg carbon in form of fossil organic carbon, soils are the second largest C pool. The amount of organic carbon (OC) in the upper 100 cm in the world's soils is estimated to be about 1,550 Pg, yet considering a depth of 3 m soils contain ca. 2,300 Pg OC (Batjes 1996; Jobbágy and Jackson 2000). Soils exchange large amounts of carbon with other reservoirs within a few months to several thousand years and are regarded as a medium-term sink for the atmospheric CO_2 (Schlesinger 1997; Houghton 2000). The annual SOC overall balance between C gain by organic deposits and C loss by soil respiration is nearly equalized, whereat several authors provide different amounts of exchanged C, ranging from ca. 60 Pg (Houghton 2007, cf. Fig. 1.1) to 75 Pg (Schlesinger and Andrews 2000).

Soils are supposed to behave as a sink as well as a source for carbon. Considered as carbon source, soils are assumed to enforce the process of global warming by releasing CO_2 due to an accelerated decomposition of SOC stored below the surface (Kirschbaum 2000; Davidson and Janssens 2006). Disturbance of soils (e.g. ploughing) led to decreased soil carbon sequestration potentials and to an increased release of carbon to the atmosphere (Six et al. 2002; Rethemeyer 2004). Carbon losses from the soil into the atmosphere of up to 50 % within five decades were caused by conversion of natural forests to cropland (Scholes and Scholes 1995; Houghton 2000). In addition, Jenkinson et al. (1991) and Trumbore et al. (1996) indicate increased decomposition rates and the loss of SOC due to rising global surface temperatures.

A measure to mitigate the projected global warming, which attracts more and more attention during the last decade, is the long-term withdrawal of carbon from the atmosphere by sequestration to another sink (Ingram and Fernandes 2001). Soils, considered as a carbon sink, provide the opportunity to sequester carbon in form of SOC and, furthermore, are supposed to play a key role in reducing the atmospheric CO_2 concentration and mitigate the positive feedback on global warming (Amundson 2001). Due to a higher C sequestration potential compared to vegetation and atmosphere, soils have been suggested as the most desirable potential sink for atmospheric carbon (Bellamy

et al. 2005). Several studies, including those of Lal (2004, 2008), Feller and Bernoux (2008), Mondini and Sequi (2008), Macías and Camps Arbestain (2010) and Srivastava et al. (2012), examined a broad range of soils regarding their C sequestration potential. Especially land-use and management practices seem to influence the processes that mitigate SOC loss and increase C sequestration (West and Post 2002; Lal 2004).

Soil organic matter (SOM)

Concerning cultivated croplands and the maintenance of soil fertility, soil organic matter (SOM) is of significant importance, since it affects soil properties like pH, redox potential, soil structure, and microbial activity (Stevenson 1994; Swift 2001). SOM comprises a very large number of organic compounds, including easily mineralisable plant remains as well as recalcitrant products from biotic and abiotic transformation processes, and the microbial biomass (Kögel-Knabner 2002; Scheffer/Schachtschabel 2010). The term soil organic matter describes a mixture of components of different forms and types of biotic origin, and comprehends the living and the dead organic matter (Coleman et al. 1989; Stevenson 1994). Up to 4 % of the total organic carbon is accounted for by the living constituents, which include plant roots, macro- and microorganisms (Shibu et al. 2006). The non-living organic matter can be sub-divided into non-humic and humic substances. Non-humic substances are composed of different, well characterized compound classes, including carbohydrates, fats, waxes, and proteins (Stevenson 1994). The humic substances are organic compounds of high molecular weight and can be classified by their chemical properties (Kononova 1966). Traditionally, they are divided into alkali-soluble humic acids, acid-soluble fulvic acids, and a humin fraction, which is resistant to both acid and alkali (Stevenson 1994).

The carbon sequestration potential of soils is governed by the long-term preservation of soil organic matter from oxidative and microbial decomposition (Swift 2001). Thus, the stabilization of SOM is the basis for the sequestration of carbon in soils and the associated withdrawal from the exchange between soil and atmosphere. Physical interactions between the mineral phase and SOM, like soil aggregation, and chemical factors like chemical composition and structure, are assumed to influence the stability of SOM (von Lützow et al. 2008). Stabilized SOM can outlast periods ranging from decades to millennia

(Scharpenseel and Becker-Heidmann 1992; Jenkinson et al. 1992). In general, three factors are assumed to be responsible for the stabilization of SOM, (i) the chemical structure and molecular composition of organic matter components, (ii) the spatial inaccessibility of organic matter to microbes and oxygen, and (iii) the interaction between organic matter and inorganic soil matrix (Oades 1995; Six et al. 2001; Kögel-Knabner 2002; von Lützow et al. 2006). However, these mechanisms and the relevance of particular processes are still not completely understood. Still, quantitative information regarding SOM turnover can only be obtained by modeling, while the complex mechanisms of organic matter stabilization and relocation in soils are not completely understood. Several approaches are available that model carbon dynamics in soils and can be used to simulate the effect of different management practices on SOM (Smith et al. 1997). Usually, models divide SOM into two or more pools, ranging from fast turnover, labile or active SOM, to very slow turnover rates, stable or passive SOM fractions (Elzein and Balesdent 1995; Jenkinson and Coleman 2008). However, most carbon dynamic models consider only the uppermost 30 cm of soils.

Paddy soils

In general, agricultural soils are characterized by lower SOM contents compared to natural soils, due to the removal of the major portion of plant material after harvest and consequently lower organic carbon (OC) inputs. Exceptions to this are the largest anthropogenic wetlands on earth - paddy soils. The formation of paddy soils is the result of submerged rice cultivation in bunded fields. 75 % of the world's rice production can be assigned to irrigated lowland rice cropping (IRRI 2012). Paddy soils are the most important agricultural soils in the world, since the staple food of more than 50 percent of the world's population is based on rice (MacLean et al. 2002). In 2011 the total harvested area amounted to approximately 163 million hectares, with a production of more than 720 million tons (FAOSTAT 2011). Rice is the major crop in the tropics and sub-tropics, whereas China represents the predominant rice producer with about 30 % of the global rice production and 18 % of the total world rice paddy area (FAOSTAT 2011). In 2008 ca. 136 million ha were cultivated as paddy soils, which represents about 80 % of the total rice growing area in Asia (IRRI 2012). Main parts of the rice production are located in the southern part of China in the Yangtze and Huaihe River Valley, where sufficient water

supply is available. Many areas in south-eastern China are able to provide two or three crops of rice per year due to high temperatures and abundant rainfall. Especially the rice growing areas in the Yangtze River Valley are characterized by a rice-wheat or other winter upland crop rotation (Zhang et al 2012; Cao and Zhang 2004; Lin et al 2004).

Due to the semi-aquatic ancestry of cultivated rice (*Oryza sativa*) and the high sensitivity to water deficiency, the cultivation of rice is less depending on the nature of the soil than on the moisture conditions under which the plant grows (Ikehashi 2007; Vaughan et al. 2008). Prior soil conditions, like nutrient status and texture, affect rice plants slightly (Kawaguchi and Kyuma 1977; Barnes 1990). Thus, paddy soil formation is governed by the specific soil management practices, which disguise the original character of soils (Kirk 2004). Paddy soils are characterized by increased SOC stocks, caused by large carbon input via straw incorporation, plant residues, and organic fertilizers (Tanji et al. 2003; Rui and Zhang 2010). The specific soil management practices, namely the artificial flooding and drainage, ploughing, puddling, organic manuring, and fertilization lead to decreased decomposition rates and, therefore, support the accumulation of SOC caused by water logged conditions during flooded periods (Neue et al. 1997; Kirk and Olk 2000; Kirk 2004; Huang and Sun 2006; Kögel-Knabner et al. 2010). In the context of mitigating the increase of atmospheric GHGs, like carbon dioxide and methane, paddy soils are considered of outstanding importance due to the high SOC level observed in paddy topsoils and the assumed high carbon sequestration potential (Pan et al. 2003; Liu et al. 2006; Xu et al. 2011; Baek et al. 2011; Zhang et al. 2012). The mean level of organic carbon in the top soils of lowland rice soils ranges from 20 g kg^{-1} in tropical Asia (Kirk, 2004) to 29 g kg^{-1} (Shirato, 2005) in Japan. The Chinese Yangtze River Valley comprises 27 - 41 g kg^{-1} (Cao and Zhang, 2004; Lin et al., 2004; Pan et al., 2008). Pan et al. (2003) take advantage of the 2nd State Soil Survey carried out in China during 1979 - 1982 and from the nationwide arable soil monitoring system established since then. The area-weighted mean density amounts to 44 t C ha^{-1}, which is comparable to the value of the US grasslands and which is higher than that of the cultivated drylands in China and the US. The total topsoil SOC pool was estimated with 1.3 Pg. Xie et al. (2004) estimated a SOC stock of 2.9 Pg in the upper 100 cm and 0.9 Pg in the upper 20 cm for Chinese paddy soils. Wang et al. (2000) reported that the SOC level of paddy soils in China amounts to 3.1 Pg. Liu et al. (2006) used the 1:1,000,000 digital soil map of China as well as data from 1,490 paddy soil profiles to determine a mean SOC density of 111.4 t C ha^{-1} for paddy soils at a

depth of 1 m and a SOC stock of 5.1 Pg. Considering the upper 20 cm of paddy soil profiles, the SOC density amounts to 37.6 t C ha^{-1}, with a SOC stock of 1.7 Pg. Kimura et al. (2004) estimated mean amounts of potential CO_2 and methane (CH_4) production from Japanese and Thai rice fields. Their calculations for CO_2 resulted in a mean production of about 1.5 t C ha^{-1} in Japanese rice fields and 1.8 - 2.1 t C ha^{-1} in Thai rice fields during a season of rice cultivation. The mean amounts of CH_4 production during a rice cultivation period ranged from 24 to 54 kg C ha^{-1} for Japanese rice fields and from 30 to 93 kg C ha^{-1} for Thai rice fields respectively, which were about one third or less of the reported CH_4 evolved amounts from rice fields in the world (Bouwman, 1990).

The change of oxic and anoxic conditions, caused by alternation of flooded and dry periods, results in temporal and spatial variations in redox reactions (Cheng et al. 2009). Most of the times of rice growth anoxic conditions dominate. After drainage, before harvest, the redox potential increases and reduced compounds are oxidized (Jäckel et al. 2001; Krüger et al. 2001). After rice cultivation, when upland crops are grown, oxic conditions are prevailing over a longer period of time. The shift of redox potentials results in an increased dispersion of clay particles, which reinforces the migration of clay in paddy soils (Li et al. 1997). In addition to the relocation of clay into the bottom of the plough layer, the mechanical pressure caused by buffalos and tractors leads to the formation of a plough pan (Bouman and Tuong 2001). Continuous puddling over a period of many years reduces small pores and meso pores in the plough pan and enhances the plant available water capacity in the puddle layer (Janssen et al. 2006). The water retention characteristics of the puddled layer are affected by the puddling intensity, which correlates with the reduction of macropores and the increase of micropores (Eickhorst and Tippkötter 2009). Furthermore, the period the soil is under paddy management has a large effect on the hydraulic properties of the plough pan (Lennartz et al. 2009). With increasing age of paddy soils, strongly decreasing infiltration rates were reported by Janssen and Lennartz (2006; 2007).

The particular paddy management, described above, leads to the development of diagnostic horizons that are specific to paddy soils (cf. Figure 1.2). According to IUSS Working Group WRB (2007) the paddy soil profile can be divided into an anthraquic horizon and a hydragric horizon. With an average range over the upper 20 cm, the anthraquic horizon comprises the puddle layer and the plough pan and is defined as a

human induced topsoil formed by wet cultivation. The hydragric horizon is dominated by reduction features (IUSS Working Group WRB 2007). The water regime of the underlying B or C horizons (subsoil) is governed by the hydraulic properties of the plough pan. The subsoil horizons may have either oxic or reducing conditions.

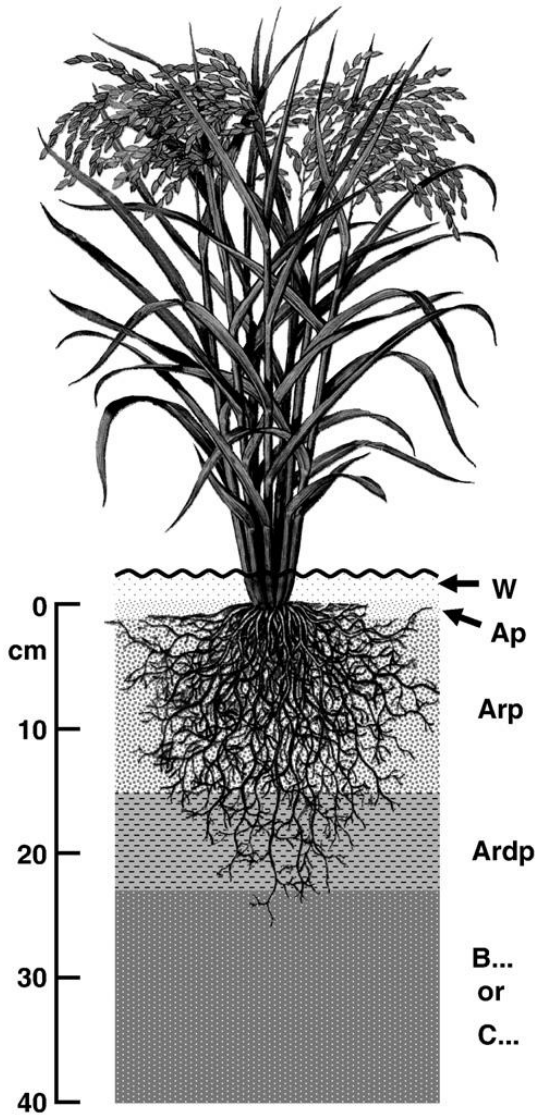

Figure 1.2: Depiction and description of a soil profile under paddy management. Figure was taken from Kögel-Knabner et al. (2010), page 3. **W**: layer of ponded water. **Ap** and **Arp**: the puddle layer with varying oxic and anoxic conditions. During the flooded period the Arp is characterized by mainly reduced conditions. **Ardp**: the plough pan is a dense layer, compacted by the specific paddy management.

Objectives

This study was conducted to reveal the influence of the described rice-paddy management regime on carbon cycling in soils. For this purpose the doubling of the atmospheric ^{14}C concentration, caused by the release of ^{14}C due to atmospheric nuclear weapon test from the late 1950's to the early 1960's, the so-called 'bomb-^{14}C spike' was used to quantify fluxes and cycling of SOM (O'Brien 1984; Harrison 1996). The determination of ^{14}C contents was carried out by accelerator mass spectrometry (AMS) providing the advantage of analyzing samples with very low carbon amounts (< 1 mg).

The objective of this thesis was to (i) quantify the rice cultivation effect on SOM dynamics using the radioactive isotope ^{14}C as a tracer, (ii) to reveal SOC stabilization mechanisms (C inclusion in iron-manganese (Fe-Mn) concretions) and SOM fluxes with special attention to paddy subsoils, and (iii) to examine to what extent the application of SOC modeling is able to predict or reproduce reliable SOC turnover rates and residence times for entire vertical paddy soil profiles. The aims and topics of this PhD thesis as outlined above are presented in three separate articles in Chapter III to V.

In chapter III, the characteristic SOC depth gradients under paddy management were investigated. For that purpose the first and the last member of a 2,000-year paddy soil chronosequence were analyzed regarding their ^{14}C depth distribution. Furthermore, ^{14}C concentrations of bulk soil samples were used to reveal effects of different management practices with increasing soil depth. Although, no 'pre-bomb' soil samples collected before 1954 were available, ^{14}C could be used as tracer due to the knowledge of soil profile development and available soil samples of the parent material. Chapter IV deals with the comparison of different chemically isolated SOM fractions from different depth intervals. Moreover, this section assesses the mechanisms which are responsible for the observed SOC depth gradients of the different soil profiles and emphasizes the spatial heterogeneity of SOM under paddy management by radiocarbon analysis of different SOM constituents. Chapter V discusses the application of a time dependent two-pool model to quantify SOC turnover rates. ^{14}C data of entire soil profiles, at least down to 1 m depth, were used to reveal mean residence times of SOC pools.

References

Amundson R. 2001. The Carbon Budget In: Soils. Annual Review of Earth and Planetary Sciences 29, 535-562.

Baek WJ, Kim YJ, Yun SI, Lee SI, Lim SS, Kim HY, Yoon KS, Choi SM, Choi WJ. 2011. Sequestration of Roots-derived Carbon in Paddy Soil under Elevated CO_2 with Two Temperature Regimes as Assessed by Isotope Technique. Journal of the Korean Society for Applied Biological Chemistry 54, 403-408.

Barnes GL. 1990. Paddy soils now and then. World Archaeol. 22, 1–17.

Batjes NH. 1996. Total carbon and nitrogen in the soils of the world. European Journal of Soil Science 47, 151-163.

Bellamy PH, Loveland PJ, Bradley RI, Lark RM, Kirk GJD. 2005. Carbon losses from all soils across England and Wales 1978-2003. Nature 437, 245-8.

Bouman B, Tuong T. 2001. Field water management to save water and increase its productivity in irrigated lowland rice. Agricultural Water Management 49, 11-30.

Bouwman AF. 1990. Exchange of greenhouse gases between terrestrial ecosystems and the atmosphere. In: Bouwman AF. (Ed.). Soils and the Greenhouse Effect, Wiley, Chichester, pp. 61–127.

Brown SL, Schroeder PE. 1999. Spatial Patterns of Aboveground Production and Mortality of Woody Biomass for Eastern U.S. Forest. Ecological Applications 9, 968-980.

Cao ZH, Zhang HC. 2004. Phosphorus losses to water from lowland rice fields under rice-wheat double cropping system in the Tai Lake region. Environ. Geochem. Hlth. 26, 229-236.

Chen SK, Liu CW. 2002. Analysis of water movement in paddy rice fields (I) experimental studies. Journal of Hydrology 260, 206–215.

Cheng YQ, Yang LZ, Cao ZH, Ci E, Yin S. 2009. Chronosequential changes of selected pedogenic properties in paddy soils as compared with non-paddy soils. Geoderma 151, 31-41.

Ciais P, Tans PP, Trolier M, White JW, Francey RJ 1995. A Large Northern Hemisphere Terrestrial CO_2 Sink Indicated by the $^{13}C/^{12}C$ Ratio of Atmospheric CO_2. Science (New York, N.Y.) 269, 1098-102.

Coleman DC, Oades JM, Uehara G. 1989. Dynamics of Soil Organic Matter in Tropical Ecosystems. University of Hawaii Press, Honolulu.

Davidson EA, Janssens IA. 2006. Temperature sensitivity of soil carbon decomposition and feedbacks to climate change. Nature 440, 165-73.

Eickhorst T, Tippkötter R. 2009. Management-induced structural dynamics in paddy soils of south east China simulated in microcosms. Soil Till. Res. 102, 168–178.

Elzein A, Balesdent J. 1995. Mechanistic Simulation of Vertical Distribution of Carbon Concentrations and Residence Times in Soils. Soil Sci. Soc. Am. J. 59, 1328-1335.

FAOSTAT (Food and Agricultural Organization of the United Nations). 2011. Online, URL: http://faostat.fao.org/

FAO. 2006. Guidelines for soil description, 4th edition (Publishing Management Service, Information Division, FAO, Rome, 2006), 110 pp.

Feller C, Bernoux M. 2008. Historical advances in the study of global terrestrial soil organic carbon sequestration. Waste management 28, 734-40.

Frenzel P, Rothfuss F, Conrad R. 1992. Biology and Fertility of Soil Oxygen profiles and methane turnover in a flooded rice microcosm. Biology and Fertility of Soils 14, 84-89.

Harrison KG. 1996. Using bulk soil radiocarbon measurements to estimate soil organic matter turnover times: implications for atmospheric CO_2 levels. Radiocarbon 38, 181-190.

Hintermaier-Erhard G, Zech W. 1997. Wörterbuch der Bodenkunde: Systematik, Genese, Eigenschaften, Ökologie und Verbreitung von Böden. Spektrum Akademischer Verlag, Stuttgart, pp.338.

Houghton RA. 2007. Balancing the Global Carbon Budget. Annual Review of Earth and Planetary Sciences 35, 313-347.

Houghton RA. 2000. A new estimate of global sources and sinks of carbon from landuse change. Eos 81. 281.

Huang Y, Sun W. 2006. Changes in topsoil organic carbon of croplands in mainland China over the last two decades. Chinese Science Bulletin 51, 1785-1803.

Ikehashi H. 2007. The origin of flooded rice cultivation. Rice Science 14 (3), 161-171.

Ingram JSI, Fernandes ECM. 2001. Managing carbon sequestration in soils: concepts and terminology. Agriculture, Ecosystems & Environment 87, 111-117.

IPCC. 2007. Climate Change 2007: An Assessment of the Intergovernmental Panel on Climate Change. IPCC's Fourth Assessment Report, 12-17.

IRRI. 2012. (http://beta.irri.org/statistics).

IUSS Working Group WRB. 2007. World reference base for soil resources. World Soil Resources Reports, Vol. 103. FAO: Rome. 145 p.

Jäckel U, Schnell S, Conrad R.2001. Effect of moisture, texture and aggregate size of paddy soil on production and consumption of CH_4. Soil Biol. Biochem. 33, 965–971.

Janssen I, Peng X, Horn R. 2006. Physical soil properties of paddy fields as a function of cultivation history and texture. Adv. Geo. Ecol. 38, 446-455.

Janssen M, Lennartz B. 2006. Horizontal and vertical water fluxes in paddy rice fields of subtropical China. Adv. Geo. Ecol. 38, 344–354.

Janssen M, Lennartz B. 2007. Horizontal and vertical water and solute fluxes in paddy rice fields. Soil Till. Res. 94, 133–141.

Jenkinson DS, Adams D, Wild A. 1991. Model estimates of CO_2 emissions from soil in response to global warming. Nature 351, 304-306.

Jenkinson DS, Harkness D, Vance ED, Adams D, Harrison AF. 1992. Calculating net primary production and annual input of organic matter to soil from the amount and radiocarbon content of soil organic matter. Soil Biology and Biochemistry 24, 295-308.

Jenkinson DS, Coleman K. 2008. The turnover of organic carbon in subsoils. Part 2. Modelling carbon turnover. European Journal of Soil Science 59, 400-413.

Jobbagy EG, Jackson RB. 2000. The vertical distribution of soil organic carbon and its relation to climate and vegetation. Ecological Applications 10, 423-436.

Kawaguchi K, Kyuma K. 1977. Paddy soils in tropical Asia: their material nature and fertility. The University Press of Hawaii, Honolulu.

Keeling CD, Piper SC, Bacastow RB, Wahlen M, Whorf TP, Heimann M, Meijer HA. 2001. Exchanges of Atmospheric CO_2 and $^{13}CO_2$ with the Terrestrial Biosphere and Oceans from 1978 to 2000. Scripps Inst. Oceanogr., Tech. Rep. SIO Ref. Ser., No. 01-06, San Diego.

Keeling R, Piper S, Heimann M. 1996. Global and hemispheric CO_2 sinks deduced from changes in atmospheric O_2 concentration. Nature 381, 218-221.

Kimura M, Murase J, Lu Y. 2004. Carbon cycling in rice field ecosystems in the context of input, decomposition and translocation of organic materials and the fates of their end products (CO_2 and CH_4). Soil Biology and Biochemistry 36, 1399-1416.

Kirk G, Olk DC. 2000. Carbon and Nitrogen Dynamics in Flooded Soils. IRRI, Los Banos, Philippines, p. 194.

Kirk G. 2004. The biogeochemistry of submerged soils. Wiley, Chichester, p. 293.

Kirschbaum M. 2000. Will changes in soil organic carbon act as a positive or negative feedback on global warming? Biogeochemistry 48, 21-51.

Kögel-Knabner I. 2002. The macromolecular organic composition of plant and microbial residues as inputs to soil organic matter. Soil Biology and Biochemistry 34, 139-162.

Kögel-Knabner I, Amelung W, Cao Z, Fiedler S, Frenzel P, Jahn R, Kalbitz K, Kölbl A, Schloter, M. 2010. Biogeochemistry of paddy soils. Geoderma 157, 1-14.

Kononova MM. 1966. Soil Organic Matter. London: Pergamon Press.

Krüger M, Frenzel P, Conrad R. 2001. Microbial processes influencingmethaneemission from rice fields. Global Change Biology 7, 49–63.

Lal R. 2004. Soil carbon sequestration impacts on global climate change and food security. Science 304, 1623-7.

Lal R. 2005. Forest soils and carbon sequestration. Forest Ecology and Management 220, 242-258.

Lal R. 2008. Carbon sequestration. Philosophical transactions of the Royal Society of London. Series B, Biological sciences 363, 815-30.

Lennartz B, Horn R, Duttmann R, Gerke HH, Tippkötter R, Eickhorst T, Janssen I, Janssen M, Rüth B, Sander T, Shi X, Sumfleth K, Taubner H, Zhang B. 2009. Ecological safe management of terraced rice paddy landscapes. Soil Till. Res. 102, 179–192.

Leuenberger M, Siegenthaler U, Langway C. 1992. Carbon isotope composition of atmospheric CO_2 during the last ice age from an Antarctic ice core. Nature 357, 488-490.

Li ZH, Horikawa Y, Tamagawa S. 1997. Stability behavior of soil colloidal suspensions in relation to sequential reduction of soils. I. Turbidity of soil colloidal suspension and change induced by submergence of paddy soils. Soil Sci. Plant Nutr. 43, 719–728.

Libby WF. 1946. Atmospheric helium three and radiocarbon from cosmic radiation. Physical
Review 69, 671-672.

Lin XG, Yin R, Zhang HY, Huang JF, Chen RR, Cao ZH. 2004. Changes of soil microbiological properties caused by land use changing from rice-wheat rotation to vegetable cultivation. Environ. Geochem. Hlth. 26, 119–128.

Liu QH, Shi XZ, Weindorf DC, Yu DS, Zhao YC, Sun WX, Wang HJ. 2006. Soil organic carbon storage of paddy soils in China using the 1:1,000,000 soil database and their implications for C sequestration. Global Biogeochemical Cycles 20, n/a-n/a.

Macías F, Camps Arbestain, M. 2010. Soil carbon sequestration in a changing global environment. Mitigation and Adaptation Strategies for Global Change 15, 511-529.

MacLean JL, Dawe DC, Hardy B, Hettel GP. 2002. Rice Almanac: Source Book for the Most Important Economic Activity on Earth. Wallingford: CABI Publishing. p. 270.

McGuire D, Sitch S, Clein JS, Dargaville R, Esser G, Foley J, Heimann M, Joos F, Kaplan J, Kicklighter DW, Meier R, Melillo JM, Moore B, Prentice IC, Ramankutty N, Reichenau T, Schloss A, Tian H, Williams LJ, Wittenberg U. 2001. Carbon balance of the terrestrial biosphere in the Twentieth Century: Analyses of CO_2, climate and land use effects with four process-based ecosystem models. Global Biogeochemical Cycles 15, 183-206.

Mondini C, Sequi P. 2008. Implication of soil C sequestration on sustainable agriculture and environment. Waste management (New York, N.Y.) 28, 678-84.

Neue HU, Gaunt J, Wang Z, Becker-Heidmann P, Quijano C. 1997. Carbon in tropical wetlands. Geoderma 79, 163-185.

Oades JM. 1995. An overview of processes affecting the cycling of organic carbon in soils. In: Zepp RG, Sonntag C. (Eds.), The role of nonliving organic matter in the earth's carbon cycle, Wiley, Chichester, pp. 293-303.

O´Brien BJ. 1984. Soil organic carbon fluxes and turnover rates estimated from radiocarbon. Soil Biology and Biochemistry 16, 115-120.

Pan G, Wu L, Li L, Zhang X, Gong W, Wood Y. 2008. Organic carbon stratification and size distribution of three typical paddy soils from Taihu Lake Region, China. Journal of environmental sciences (China) 20, 456-63.

Pan G, Li L, Wu L, Zhang X. 2003. Storage and sequestration potential of topsoil organic carbon in China's paddy soils. Global Change Biology 10, 79-92.

Rethemeyer J. 2004. Organic carbon transformation in agricultural soils : Radiocarbon analysis of organic matter fractions and biomarker compounds, Thesis CAU Kiel, p.165.

Rui W, Zhang W. 2010. Effect size and duration of recommended management practices on carbon sequestration in paddy field in Yangtze Delta Plain of China: A meta-analysis. Agriculture, Ecosystems & Environment 135, 199-205.

Scharpenseel HW, Becker-Heidmann P. 1992. Twenty-five years of radiocarbon dating soils: paradigm of erring and learning. Radiocarbon 34, 541-549.

Scheffer F, Schachtschabel P. 2010. Lehrbuch der Bodenkunde. 16th ed. Spektrum Akademischer Verlag, Heidelberg.

Schellnhuber HJ, Cramer W, Nakicenovic N. (Eds). 2006. Avoiding dangerous climate change. Cambridge University Press, Cambridge, UK p. 406.

Schimel DS, House JI, Hibbard A, Bousquet P, Ciais P, Peylin P, Braswell BH, Apps MJ, Baker D, Bondeau A, Canadell J, Churkina G, Cramer W, Denning S, Field CB, Friedlingstein P, Goodale C, Heimann M, Houghton R, Melillo JM, Moore B, Murdiyarso D, Noble I, Pacala SW, Prentice IC, Raupach MR, Rayner PJ, Scholes RJ, Steffen WL, Wirth C. 2001. Recent patterns and mechanisms of carbon exchange by terrestrial ecosystems. Nature 414, 169-72.

Schlesinger WH. 1997. Biogeochemistry: an analysis of global change. Academic Press, San Diego, p. 588.

Schlesinger WH, Andrews JA. 2000. Soil respiration and the global carbon cycle. Biogeochemistry 48, 7-20.

Scholes RJ, Scholes MC. 1995. The effect of land use on nonliving organic matter in the soil. In: Zepp RG, Sonntag C. (Eds.), The role of nonliving organic matter in the earth's carbon cycle, Wiley, Chichester, pp. 209-226.

Shibu ME, Leffelaar PA, Van Keulen H, Aggarwal PK. 2006. Quantitative description of soil organic matter dynamics - A review of approaches with reference to rice-based cropping systems. Geoderma 137, 1-18.

Shirato Y. 2005. Testing the suitability of the DNDC model for simulating long-term soil organic dynamics in Japanese paddy oils. Soil Sci. Plant Nutr. 51, 183-192.

Six J, Feller C, Denef K, Ogle S, Moares Sa J, Albrecht A. 2002. Soil organic matter, biota and aggregation in temperate and tropical soils - Effects of no-tillage. Agronomie 22, 755-775.

Six J, Guggenberger G, Paustian K, Haumaier L, Ellliot E, Zech W. 2001. Sources and composition of soil organic matter fractions between and within soil aggregates. European Journal of Soil Science 52, 607-618.

Smith P, Smith JU, Powlson DS, McGill WB, Arah JRM, Chertov OG, Coleman K, Franko U, Frolking S, Jenkinson DS, Jensen LS, Kelly RH, Klein-Gunnewiek H, Komarov AS, Li C, Molina JAE, Mueller T, Parton WJ, Thornley JHM, Whitmore AP. 1997. A comparison of the performance of nine soil organic matter models using datasets from seven long-term experiments. Geoderma 81, 153-225.

Srivastava P, Kumar A, Behera SK, Sharma YK, Singh, N. 2012. Soil carbon sequestration: an innovative strategy for reducing atmospheric carbon dioxide concentration. Biodiversity and Conservation 21, 1343-1358.

Stevenson FJ. 1994. Humus Chemistry - Genesis, composition, reactions. 2nd edition. John Wiley, New York.

Swift R. 2001. Sequestration of carbon by soil. Soil Science 166, 858-871.

Tanji KK, Gao S, Scardaci SC, Chow AT. 2003. Characterizing redox status of paddy soils with incorporated rice straw. Geoderma 114, 333-353.

Trumbore SE, Chadwick OA, Amundson R. 1996. Rapid exchange between soil carbon and atmospheric carbon dioxide driven by temperature change. Science 272, 393-396.

Vaughan DA, Bao-Rong L, Tommoka N. 2008. The evolving story of rice evolution. Plant Science 174, 394-408.

von Lützow M, Kögel-Knabner I, Ekschmitt K, Matzner E, Guggenberger G, Marschner B, Flessa H. 2006. Stabilization of organic matter in temperature soils: mechanisms and their relevance under different soil conditions - a review. European Journal of Soil Science 57, 426-445.

von Lützow M, Kögel-Knabner I, Ludwig B, Matzner E, Flessa H, Ekschmitt K, Guggenberger G, Marschner B, Kalbitz K. 2008. Stabilization mechanisms of organic

matter in four temperate soils: Development and application of a conceptual model. Journal of Plant Nutrition and Soil Science 171, 111-124.

Wang SQ, Zhou CH, Xia J. 2000. USGCRP latest trend in the study of carbon cycle. Advance in Geoscience 15 (5), 592-597.

West TO, Post W. 2002. Soil Organic Carbon Sequestration Rates by Tillage and Crop Rotation: A Global Data Analysis. Soil Science Society of America Journal 66, 1930-1946.

White A, Cannell M, Friend A. 2000. CO 2 stabilization , climate change and the terrestrial carbon sink. Global Change Biology 6, 817-833.

WMO. 2012. WMO Greenhouse Gas Bulletin. World Meteorological Organization.

Xie XL, Sun B, Zhou HZ. 2004. Soil organic carbon storage and affecting factors under different vegetations in China. Journal Soil Science 41 (5), 667-699.

Xu S, Shi X, Zhao Y, Yu D, Li C, Wang S, Tan M, Sun W. 2011. Carbon sequestration potential of recommended management practices for paddy soils of China, 1980-2050. Geoderma 166, 206-213.

Zhang W, Xu M, Wang X, Huang Q, Nie J, Li Z, Li S, Hwang SW, Lee KB. 2012. Effects of organic amendments on soil carbon sequestration in paddy fields of subtropical China. Journal of Soils and Sediments 12, 457-470.

Chapter II

Materials and Methods

Study sites and soil sampling

This study is part of the Research Unit FOR995 'Biogeochemistry of paddy soil evolution', which has been established by the Deutsche Forschungsgemeinschaft (DFG; German Science Foundation) in 2009, to improve the understanding of the cycling and storage of organic matter at different stages of paddy soil evolution, as well as the dynamics of hydrological and microbial mediated redox processes. For this purpose, two soil chronosequences derived from the same uniform parent material were sampled. One chronosequence comprises differently aged paddy soils (50 yrs; 100 yrs; 300 yrs; 500 yrs; 700 yrs; 1,000 yrs; 2,000 yrs), characterized by an annual cropping rotation of rice cultivation under flooded conditions alternated by a non-inundated upland crop. The corresponding upland chronosequence was only used for non-inundated crop production (50 yrs; 100 yrs; 300 yrs; 500 yrs; 700 yrs).

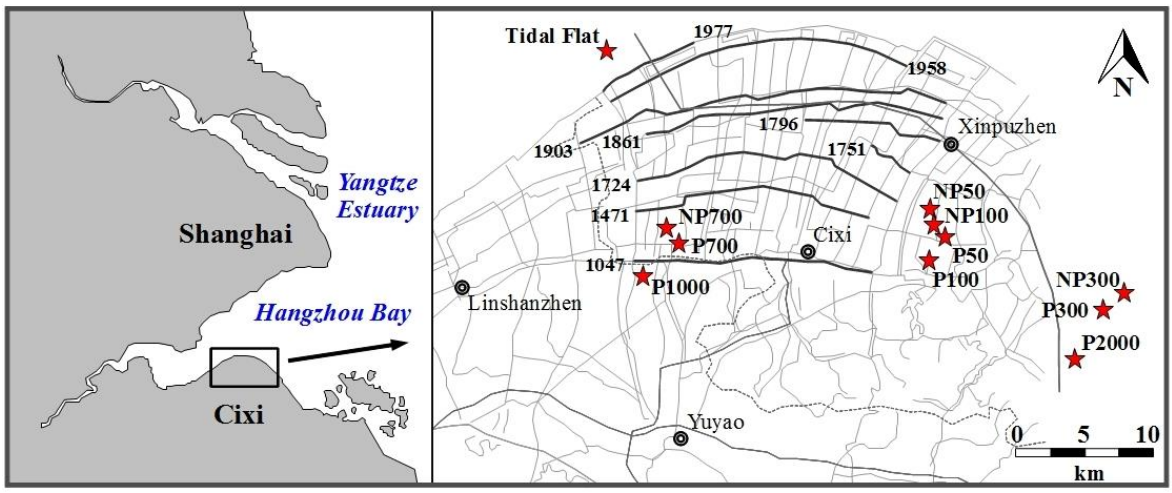

Figure 2.1: Map of study area, depicting generations of dikes constructed for land reclamation and sampling points of paddy and non-paddy soils.

The study area (cf. Figure 2.1) belongs to one of the oldest paddy soil regions in the world on the south bank of Hangzhou Bay around Cixi, Zhejiang Province, PR China (Cao et al. 2006). With a longitude range of 121°05'- 121°30' and a latitude range of 30°06' - 30°19' the investigated area has an overall size of 433 km^2 (in 1988) and an elevation ranging from 2.6 to 5.7 m above sea level (Zhang et al. 2004). The mean annual precipitation is 1,325 mm with higher values from April to October (Cheng et al. 2009). Due to a total evaporation of 1,000 mm, irrigation is needed to maintain standing water during rice growing season. During the past centuries the deposited estuarine material of Hangzhou Bay was converted into new farmland through continuous land reclamation by the construction of protective dikes. The conversion of wetlands into agricultural lands is a traditional, customary, and worldwide applied procedure to supply the need for cultivable land of people living in coastal areas (Healy and Hickey 2002; Ellis and Atherton 2003). In China, the thousands of years old tradition of coastal wetland reclamation is still in progress. Mainly due to reclamation for agricultural purposes, the area of natural coastal wetlands decreased by 51 % since 1949 (An et al. 2007). Thus, the Chinese mainland increased by $1.19 \cdot 10^6$ ha new land between the 1950's and 1980's (He and Zhang 2001). The convex shaped south shore of Hangzhou Bay has accreted continuously at an average rate of 20 m y^{-1} over the last 600 years (Su and Wang 1989).

The age of the sampling sites was recapitulated from the time of embankment and dike construction. Thus, the investigated soil chronosequences were determined according to records found in the Country Annals of the Zhejiang Province, as well as in Cixi, Shangyu and Yuyao Counties. These records comprise information regarding the dikes, the position, and the year of dike construction, and were written between 1621 and 1627 (Cheng et al. 2009). According to the commencement of rice cultivation, we are able to study the uptake and relocation of OC with atmospheric ^{14}C composition and identify the influence of agricultural management on comparable sites at different stages of pedogenesis. A glance at the map, with sampling points and dikes, raises doubts about the reliability of the given duration times. Especially the 50-year old sites do not fit into the scheme, since P50 and NP50 should be expected closer to the coastal line. This deceptive circumstance was explained by the Chinese partners with the removal of thick topsoil layers in the late 1950's. The excavation comprises enough material to lay open undisturbed parent material. In spite of the misleading spatial location of some sampling points, later results obtained by the Research unit FOR995, reveal the given ages as appropriate information.

Paddy (P50-P2000) and Non-Paddy (NP50-NP700) soils were described by FAO guidelines for soil description and classified according to the IUSS Working Group WRB (2007). Soil profile description and soil classification in the field were made by Reinhold Jahn and Peter Schad, both members of the Research Unit FOR995. The identified soil types and the geographical locations of the sampling sites are given in Table 2.1. Due to early analytical data showing higher contents of total sodium (Na) and calcium (Ca) and lower contents of aluminum (Al), potassium (K) and iron (Fe), compared with the other sites, and doubts of the Chinese partners that the site fits into the chronosequence, the 500 year old sites were excluded from further investigations.

As well as paddy and non-paddy sites, the tidal flat was sampled as a representative of the parent material. The parent material of the study site mainly consists of estuarine sediment, which originates from the Yangtze River and furthermore of holocene marine and lagoonal to limnic deposits. The original sediment is characterised by a silty texture (SiL), containing 3.5 to 4 % of total Fe, of which about 20 to 30 % are bound in oxyhydroxides. The deposits contain quartz, feldspars, calcite as well as dolomite, and the clay fraction is dominated by illite followed by kaolinite. More detailed information about the single soil profiles are given in the appendix (Table A1 and A3).

Table 2.1 Characteristics of investigated sampling sites

Site description	**Sampling location**		**Soil classification**
	North	**East**	
P50	30°11.031´	121°21.366´	Stagnic Endogleyic Cambisol
P100	30°09.827´	121°20.971´	Endogleyic Cambisol
P300	30°06.437´	121°30.280´	Endogleyic Cambisol
P700	30°10.408´	121°09.180´	Endogleyic Stagnosol
P1000	30°09.763´	121°06.957´	Endogleyic Stagnosol
P2000	30°05.425´	121°26.775´	Endogleyic Stagnosol
NP50	30°13.152´	121°21.382´	Endogleyic Cambisol
NP100	30°11.884´	121°21.196´	Endogleyic Cambisol
NP300	30°06.932´	121°30.646´	Haplic Cambisol
NP700	30°10.967´	121°08.706´	Haplic Cambisol
tidal wetland	30°19.557´	121°08.691´	Tidalic, Salic Fluvisol

Figures 2.2 - 2.4 depict photographs of sampled soil profiles. According to IUSS Working Group WRB (2007), the original soils are Fluvisols. Soil formation leads rapidly to the development of a genuine soil structure replacing the original stratification and to the formation of Cambisols. Under paddy use, redox processes transform the Cambisols into Stagnosols. Due to some missing characteristics of an anthraquic horizon, the described soils cannot be classified as Anthrosols, and thus remain Stagnosols.

In P700 and P1000, fossil A horizons have been found below 50 cm giving rise to the hypothesis that in some cases continuous soil development may have been interrupted by receiving new parent material. This disturbance in the soil profile formation will be apparent consistently in the following chapters by means of differing results (i.e. TOC, ^{14}C, mean residence times, turnover rates).

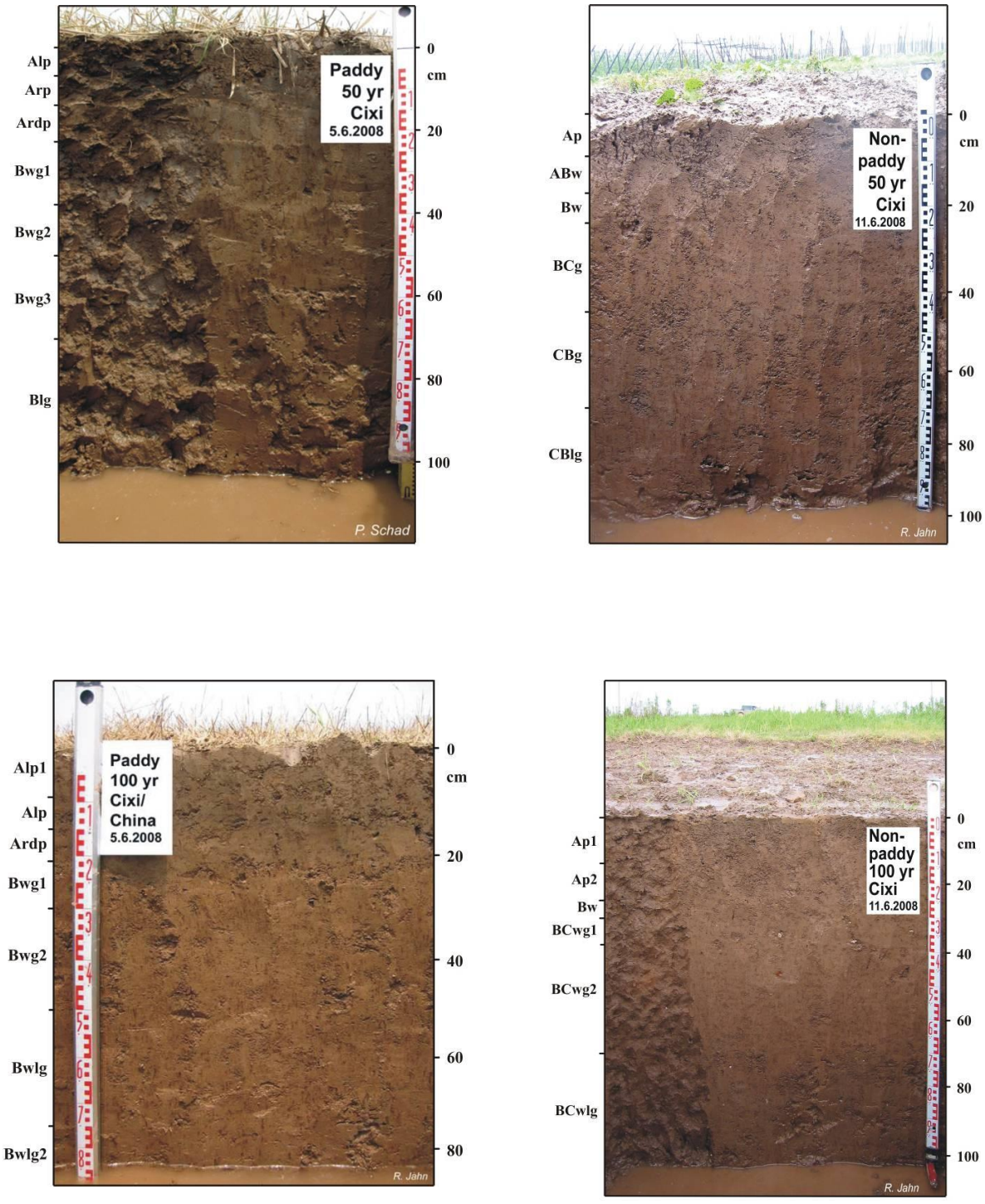

Figure 2.2: Soil profiles of the chronosequence (50 and 100 years) used for growing lowland rice (left hand side) and upland crops (right hand side). Soils were classified according to IUSS Working Group WRB 2007. For further details regarding soil profile description see Appendix (Table A1 and A3). The photographs were taken and kindly provided by Reinhold Jahn (Institute for Soil Sciences, Martin Luther University Halle-Wittenberg) and Peter Schad (Institute for Soil Sciences, Center of Life and Food Sciences Weihenstephan, TUM Munich).

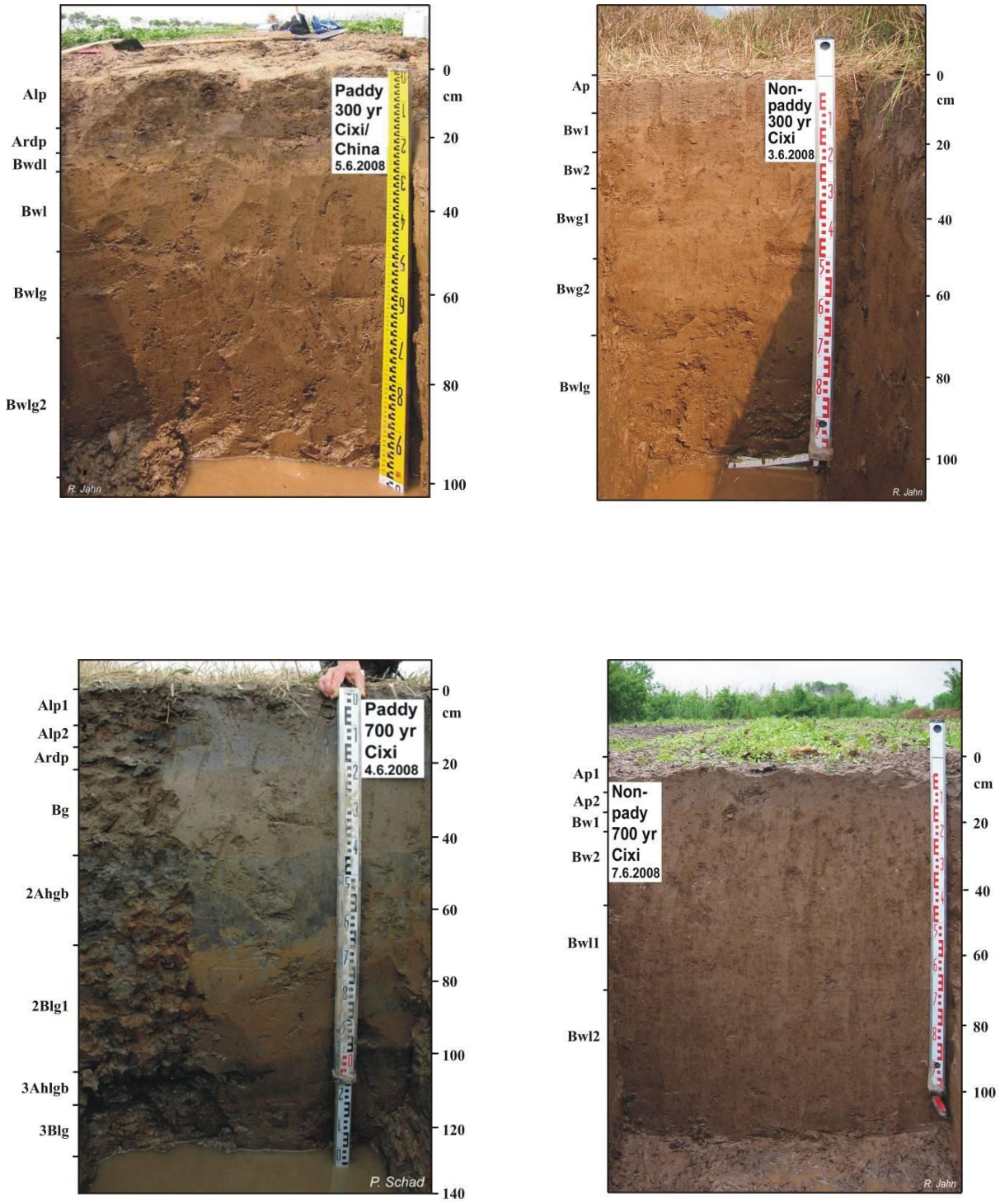

Figure 2.3: Soil profiles of the chronosequence (300 and 700 years) used for growing lowland rice (left hand side) and upland crops (right hand side). Soils were classified according to IUSS Working Group WRB 2007. For further details regarding soil profile description see Appendix (Table A1 and A3). The photographs were taken and kindly provided by Reinhold Jahn (Institute for Soil Sciences, Martin Luther University Halle-Wittenberg) and Peter Schad (Institute for Soil Sciences, Center of Life and Food Sciences Weihenstephan, TUM Munich).

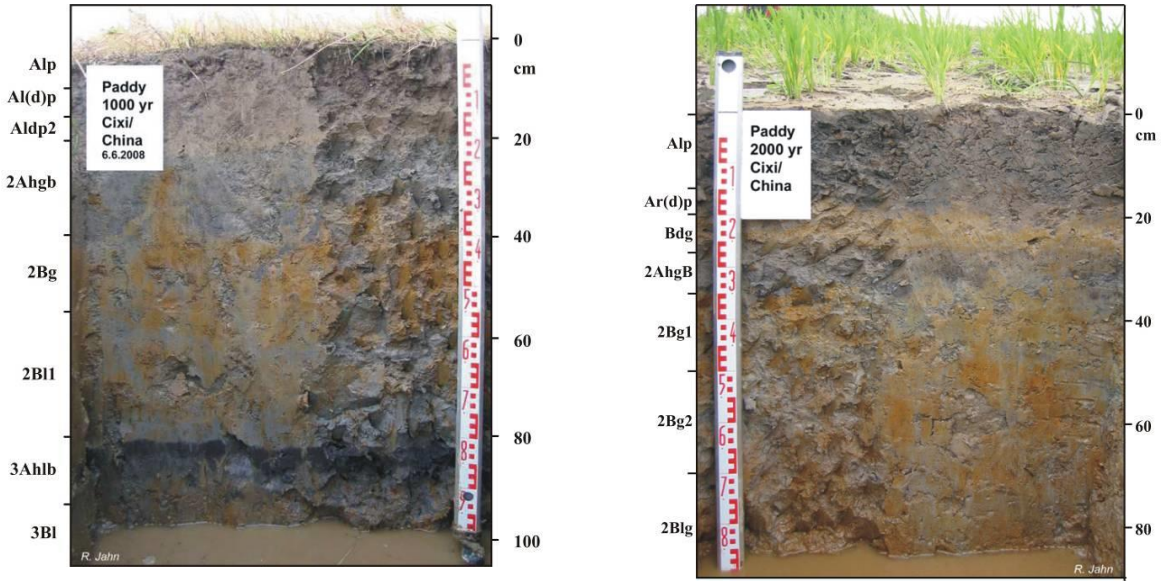

Figure 2.4: Soil profiles of the chronosequence (1,000 and 2,000 years) used for growing lowland rice. Soils were classified according to IUSS Working Group WRB 2007. For further details regarding soil profile description see Appendix (Table A1 and A3). The photographs were taken and kindly provided by Reinhold Jahn (Institute for Soil Sciences, Martin Luther University Halle-Wittenberg) and Peter Schad (Institute for Soil Sciences, Center of Life and Food Sciences Weihenstephan, TUM Munich).

Principles of radiocarbon analysis

Natural carbon isotope abundances as tracers for SOM dynamics

Under natural conditions, carbon occurs in three isotopes that have different numbers of neutrons and thus different masses. The most abundant isotope is ^{12}C with an approximate percentage of 98.89 % of all carbon in nature. The abundance of the stable isotope ^{13}C is ca. 1.11%. The radioactive ^{14}C is present in merely very small quantities of $1.176 \cdot 10^{-12}$ atoms per atom ^{12}C (Karlén et al., 1968). By studying the ratios of the two stable isotopes as well as of the radioactive and a stable carbon isotope in soil organic matter, it is possible to decipher processes and rates of organic carbon production, transformation, and degradation in soils.

The stable isotope abundance is reported as the relative deviation in the $^{13}C/^{12}C$ ratio of a sample from that of an international standard, expressed as $\delta^{13}C$ in ‰ PDB:

$$\delta^{13}C\ (‰\ PDB) = [(^{13}C/^{12}Csample) / (^{13}C/^{12}C_{reference}) - 1] \cdot 1000 \qquad (1)$$

The reference material is the carbonate shell of the mollusk *Bellemnitella americana* from the cretaceous Pee Dee formation (PDB) in South Carolina ($\delta^{13}C = 0‰$). Since the original material does not exist anymore, it was replaced by a new carbonate (NBS-19) with a exact known $\delta^{13}C$ value compared to PDB. Radiocarbon data are also reported relative to the $^{14}C/^{12}C$ or $^{14}C/^{13}C$ ratio of a standard, but corrected for the effect of isotopic fractionation.

Principles of radiocarbon dating

In the late 1940's, Willard Libby (1946; 1953) demonstrated the existence of ^{14}C and its use as a dating tool. His work was honored with the Nobel Prize in chemistry in 1960. In general, the radiocarbon method is suitable for age determination up to 50,000 years. For conventional decay counting methods this range has been extended by isotopic enrichment to ca. 75,000 years (Grootes 1978). Völker et al. (2000) correlated climatic records and ^{14}C ages of the planktonic foraminifera of a deep-sea sediment core from the Iceland Sea and hence, demonstrated the extension to 60,000 years for AMS radiocarbon dating.

^{14}C is produced under the release of a proton (p) in the lower stratosphere by the collision of nitrogen atoms with low energy neutrons (n) originating from cosmic rays:

$$^{14}N + n \rightarrow {}^{14}C + p$$

The newly formed ^{14}C is oxidized rapidly to ^{14}CO, which is also oxidized to $^{14}CO_2$ within months and distributed in the atmosphere. By assimilation of CO_2 for photosynthesis ^{14}C enters the plant biomass, and, consequently, the heterotrophic organisms via the food chain. Exchange between the atmosphere, the biosphere, and the hydrosphere results in a dynamic equilibrium between ^{14}C production and decay. Exchange rates between the different reservoirs differ greatly depending on the respective carbon dynamics.

After the death of an organism, the exchange with the atmosphere stops and the ^{14}C concentration starts to decrease through radioactive decay with a half-life of 5,730 ± 40 years (Godwin 1962). ^{14}C decays under the release of an electron (β^-) and an antineutrino (ν):

$$^{14}C \rightarrow {}^{14}N + \beta^- + \nu$$

The residual ^{14}C concentration of a sample at a certain time is defined by the radioactive decay equation:

$$N(t) = N_0 \cdot e^{-\lambda t} \qquad (2)$$

with: N: the number of atoms at a time t

N_0: the initial number of atoms

λ: the decay constant of ^{14}C

If the initial number of atoms (N_0) is known, the age of a sample can be calculated according to equation (3). Since the initial number of atoms is not known, N_0 is estimated via a modern standard.

$$t = -\frac{1}{\lambda} \cdot \ln \frac{N(t)}{N_0} \qquad (3)$$

with: $\frac{1}{\lambda} = \frac{t_{1/2}}{\ln 2}$, describing the mean-life and $t_{1/2}$ the half-life of ^{14}C.

For the calculation of the conventional ^{14}C age, instead of the more precise half-life of 5,730 years reported by Godwin (1962), the original half-life of 5,568 years determined by Libby (1946; 1953) is used according to an international agreement to ensure the comparability of ^{14}C dates independent of the year of publication.

Basic assumptions regarding the ^{14}C method

The determination of absolute or calendar ages requires several general assumptions underlying the ^{14}C method, which are listed below:

1. The production of ^{14}C has been constant (over a period of more than 10^5 years).
2. The carbon reservoirs are well mixed, which requires a rapid exchange between the C pools (atmosphere, biosphere, and ocean) compared to the half-live of ^{14}C.
3. Carbon isotope ratios in samples represent the ratio of their environment before the exchange stopped.
4. After the death of organisms, or the deposition of carbonates, no further exchange with the environment takes place.
5. The decay of ^{14}C is constant and not affected by its chemical or physical surroundings.

These assumptions are only partly fulfilled. The atmospheric ^{14}C concentration has varied with time due to changes in the ^{14}C production (de Vries 1958). Reasons are variations of the earth's magnetic field (Stuiver et al. 1991; Sternberg 1992), the sunspot cycle (Stuiver

and Quay 1980), and cosmic ray fluxes (Suess 1986; Stuiver et al. 1991; Kocharov et al. 1992). Among these factors, the most significant effect is attributed to the variations of the earth's magnetic field (Hagstrum and Champion 1995). The terrestrial magnetic field screens the earth and the atmosphere from cosmic rays. With increasing intensity of the magnetic field, the shielding effect increases, and therefore the ^{14}C production rate becomes reduced.

Furthermore, the Suess effect has led to a dilution of ^{14}C in the atmosphere by release of $^{12}CO_2$ caused by fossil fuel burning since the late 19th century (Suess 1955). In contrast, ^{14}C was released in large quantities to the atmosphere due to atmospheric testing of nuclear weapons since the late 1950's. In 1963 the atmospheric radiocarbon concentration reached a maximum in the northern hemisphere (about 200 pMC; pMC = percent modern carbon) nearly doubling the value from 1950 (Nydal and Lövset 1983; Levin and Kromer 1997). After ceasing atmospheric nuclear weapon tests and due to the incorporation of CO_2 into oceans, the atmospheric ^{14}C concentration decreased exponential (Levin und Kromer 2005, Naegler et al. 2006). The 'bomb-^{14}C spike' can be used as a tracer to follow the transformation of organic carbon in SOM, since it entered the vegetation and SOM by photosynthesis (O'Brien and Stout 1978; O'Brien 1984; Dörr and Münnich 1986; Trumbore 1996; Levin and Hesshaimer 2000).

In addition to changes of the natural ^{14}C production and the human activity, the ^{14}C concentration of the atmosphere is also affected by varying exchange rates between the different reservoirs. Thus, the increased release of CO_2 depleted in ^{14}C during the last glacial epoch results in a dilution of the ^{14}C concentration of the northern hemisphere (Sarnthein et al. 2007). Furthermore, the third assumption is not entirely fulfilled, since different organic components have slightly different initial ^{14}C concentrations due to isotopic fractionation, e.g. during photosynthesis plants discriminate against heavier carbon isotopes.

Another crucial condition, especially for SOM analyzing, which is not fulfilled is the closed system assumption (4). Recently fixed CO_2 in plant tissues is continuously added to the SOC pool while carbon gets lost from this pool by mineralization of organic matter as well as via losses of dissolved organic carbon leached into the ground water. Thus, soils continuously exchange carbon with the atmosphere and with the hydrosphere.

Application of ^{14}C analysis on SOM

Radiocarbon dating applied to soil samples and SOM has already been used since the 1960's (Scharpenseel et al. 1968; 1969; Perrin et al. 1964). Since SOM is a mixture of organic constituents in various stages of decomposition and, thus, contains compounds of different origin and ages. The results of ^{14}C measurements of bulk SOM reflect the 'apparent mean ages of the carbon comprised in soils. Therefore, the investigation of SOM requires a fractionation of the organic matter into pools of different stability (Trumbore et al. 1989; Trumbore and Zheng 1996; Tonneijck et al. 2006). The ^{14}C method is helpful for investigating organic matter sources, their transformation and stabilization in soils. Scharpenseel and Becker-Heidmann (1989) for example, examined the effect of bioturbation by the analysis of bulk soil ^{14}C distribution in soil profiles. Several studies determined ^{14}C concentrations of different physical and chemical fractions in soils to examine C sources at different depth levels (Trumbore 1993; Baisden et al. 2002; Rethemeyer et al. 2005; Dreves et al. 2007; Prior et al. 2007; Inoue et al. 2011).

Furthermore, ^{14}C values can be applied to verify physically and chemically defined SOM pools of different stabilities (Trumbore et al. 1989; Huang et al. 1999). In addition, ^{14}C concentrations have been used to estimate carbon turnover times in bulk soil as well as in different chemically or physically defined SOM pools. In principle, this is possible on different time-scales, (i) from several days up to a few years by the priming with artificial, ^{14}C-enriched substances as tracer (Bhupinderpal-Singh et al. 2005), (ii) from several years up to decades by using the 'bomb-^{14}C' as a tracer, and (iii) for time scales exceeding 100 years by using the natural decay of ^{14}C. The determination of 'bomb-^{14}C' has been used in numerous studies to trace organic carbon cycling in bulk soil (O'Brien und Stout 1978; O'Brien 1984, 1986; Harkness et al. 1986, 1991; Harrison 1996, 1998; Rumpel et al. 2003), whereas other studies took advantage of the possibilities provided by the AMS technique and measured 'bomb-^{14}C' concentrations of physical and chemical SOM fractions with very low carbon contents (Römkens et al. 1998; Rethemeyer 2004).

^{14}C measurement by accelerator mass spectrometry (AMS)

To measure natural ^{14}C levels mass spectrometrically, tandem accelerators have been used since the end of the 1970's (Nelson et al. 1977; Bennett et al. 1977). The most striking

advantage of AMS compared to the conventional decay counting methods is the about 10,000-times higher sensitivity. This is achieved by the direct detection of all ^{14}C atoms instead of only those which decay, as it is done in conventional decay counting methods such as liquid scintillation or proportional gas counters which detect β^--particles emitted during radioactive decay of ^{14}C. Thus, AMS provides the opportunity to measure samples with a very small size (1 milligram C instead of 1 gram C) within a shorten time (1 hour instead of days).

The AMS technique is an extension of conventional isotope ratio mass spectrometry (IR-MS) in which a magnetic field is used to separate the ionized carbon isotopes by their different masses so that they can be quantified separately. The lower abundance limit of IR-MS, however, is set by the presence of mass interfering isotopes and molecular fragments (isobars). Thereby carbon isotope ratios down to about $1:10^{-9}$ can be measured and thus conventional IR-MS cannot be used to detect ^{14}C. The measurement of rare natural isotopes with relative abundances of 10^{-9} to 10^{-16} requires the discrimination against unwanted isobars, which are in the case of radiocarbon the mass-14 interfering molecular fragments ^{13}CH and $^{12}CH_2$, and the nitrogen isotope ^{14}N. This is possible by starting with negative ions and thus discriminating against ^{14}N, which does not form a stable negative ion. Furthermore, the use of a tandem electrostatic accelerator, equipped with a terminal stripper for charge exchange to positive ions, makes it possible to destroy isobaric molecular ions (Vogel and Nelson 1995; Tuniz et al. 1998). The mass spectrometric determination of isotope ratios uses relative measurements made against an international standard of known isotope ratio. The contamination introduced during sample preparation and during AMS analysis is determined and corrected for by background measurements.

The AMS system of the Leibniz-Laboratory at Kiel

The ^{14}C measurements of this study were made at the Leibniz-Laboratory (Christian-Albrechts-University of Kiel) with a 3 million volt (MV) Tandetron 4130 AMS system installed by High Voltage Engineering (HVE). A schematic depiction is given in Figure 2.5. A detailed description of the system can be found in Nadeau et al. (1997).

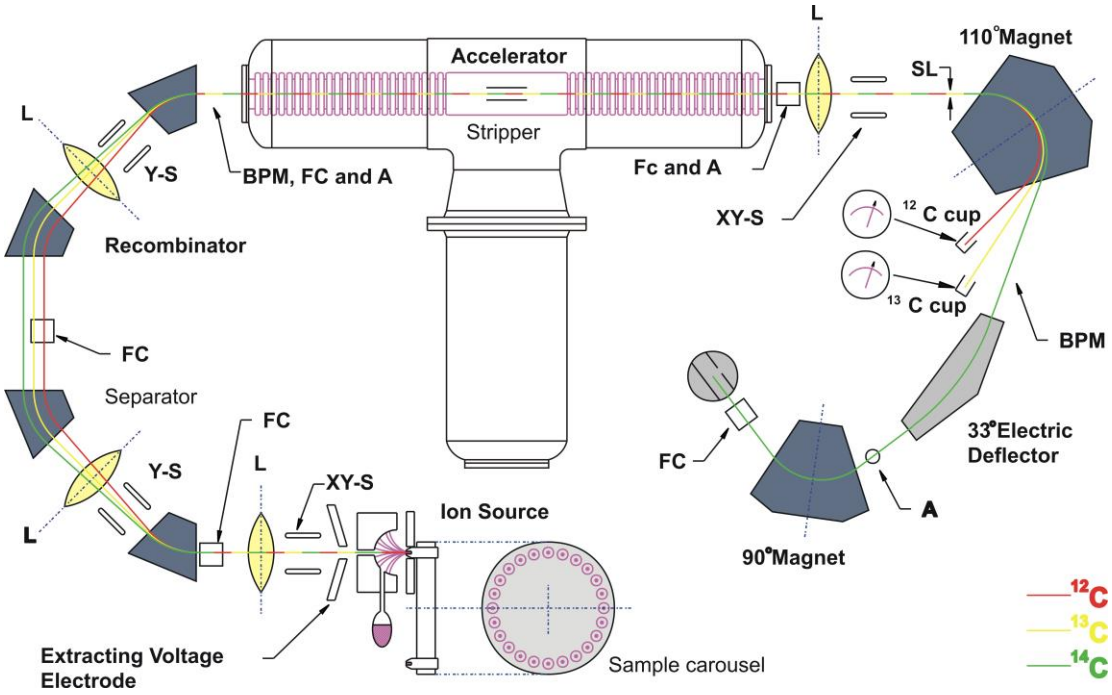

Figure 2.5: The HVE AMS system of the Leibniz-Laboratory (Kiel) with a separator-recombinator unit for simultaneous acceleration of the three carbon isotopes. The symbols indicate: L - a lens, Y-S - one pair, and XY-S - two pairs of steerers (horizontal and vertical), BPM - a beam profile monitor, FC - faraday cups, SL - vertical slits, and A - aperture. Schematic modified from Nadeau et al. (1997).

The sample graphite is pressed into aluminum target holders which are placed in a sample carousel for up to 59 targets. The graphite was recovered by reducing the sample gas (CO_2) with H_2 at 600°C. When measuring, successive target holders are automatically pushed into and removed from the ion source, which remains under high vacuum. In the ion source, the sample graphite is sputtered with caesium (Cs^+) ions producing a negative ion beam which consists of ^{12}C-, ^{13}C-, ^{14}C- and other elemental and molecular negative ions. This procedure discriminates against ^{14}N, as this isobar does not form stable negative ions. In order to simultaneously accelerate the three carbon masses, the AMS system of the Leibniz-Laboratory uses a separator-recombinator unit (Nadeau et al., 1997): The ions emerging with a low-energy of 35 kilo electron volt (keV) from the source pass through an analyzer where they are split into mass 12, 13, and 14 and other, unwanted, masses are eliminated. Then the ^{12}C- beam is reduced to about 1 % of its intensity by a mechanical

chopper, to prevent overloading of the accelerator, and after that the three masses are recombined. Subsequently, the negative ion beam is accelerated toward the terminal in the centre of the accelerator which is at +2.5 MV thus gaining 2.5 million electron volts (MeV) energy. There the beam passes through a low-density gas stripper (argon). The stripper removes several electrons from the ions and thereby multiple positive ions are produced, and molecular isobars are destroyed. The positively charged ions, mainly +3, are then further accelerated from 2.5 MV to earth potential gaining another 7.5 MeV. A 110° magnet separates the ion beam into the three masses at charge +3 and eliminates other ions. The relative abundances of the stable, abundant isotopes ^{12}C and ^{13}C are measured as charge deposited in Faraday cups. The rare ^{14}C isotopes pass an electrostatic analyzer (33° deflection) and a 90° magnet to remove residual products of the molecular ions and scattering before they are counted in a gas-ionization chamber. Particle identification is possible by determination of their energy loss rate and total energy. The particle count rate and the Faraday cup currents of the AMS measurement are used to calculate a ratio of $^{14}C/^{12}C$ and $^{13}C/^{12}C$ for samples as well as for the reference standard.

Calculation of ^{14}C data

^{14}C concentrations are calculated from the measured $^{14}C/^{12}C$ ratio of the sample compared to that of an international standard and commonly expressed in percent modern carbon (pMC) (equation 4). As radiocarbon dating reference standard 95 % of the activity of the oxalic acid standard (Ox I; decay corrected to 1950, corrected to $\delta^{13}C$ of -19 ‰ PDB) is internationally accepted (Stuiver and Polach 1977). The correction adjusts the isotope ratio of Ox I (105.26 pMC) in 1950, to that of pre-industrial wood from 1859 AD, containing no fossil fuel-derived carbon. Therefore, 'modern' carbon is defined as the $^{14}C/^{12}C$ ratio in 1950 AD, which is conventionally considered as 100 pMC. The IAEA (International Atomic Energy Agency, Vienna, Austria) provided a new standard (Ox II; 134.07 pMC), since the original material can no longer be supplied. Consequently, the isotope ratio of Ox II has to be corrected to that of the primary Ox I standard (correction factor: 1.2736; Mann 1983) and adjusted to pre-industrial wood (= 0.95/1.2736).

According to Stuiver and Polach (1977) the ^{14}C content is expressed as follows:

$$pMC = (R_{sample*}) / (R_{Ox*}) \cdot 100 \quad (4)$$

with: $R_{sample*} = R_{sample} \cdot [(1 - 25/1{,}000) / (1 + \delta^{13}C/1{,}000)]^2$

$R_{Ox*} = 0.95 \cdot R_{Ox\,I} [(1 - 19/1{,}000) / (1 + \delta^{13}C/1{,}000)]^2$

$= 0.7459 \cdot R_{Ox\,II} [(1 - 25/1{,}000) / (1 + \delta^{13}C/1{,}000)]^2$

where R_{sample} is the $^{14}C/^{12}C$ ratio of the sample, R_{Ox} that of the oxalic acid standard, and $R_{sample*}$ and R_{Ox*} are the respective values corrected for isotopic fractionation as defined in equation (4) and described below.

Correction for isotopic fractionation

^{14}C results have to be corrected to constant $\delta^{13}C$ values to account for mass-dependent isotopic fractionation arising from natural processes. By convention ^{14}C results ($R_{sample*}$) are normalized to $\delta^{13}C$ of -25 ‰ relative to PDB and results of the oxalic acid standard (R_{Ox*}) are corrected to $\delta^{13}C$ of -19 ‰ PDB (Ox I) and to $\delta^{13}C$ of -25 ‰ PDB (Ox II), respectively, (Mook and van der Plicht 1999; Mann 1983). The $^{13}C/^{12}C$ ratio of the sample and of the oxalic acid standard, which is measured by the AMS system simultaneously with the $^{14}C/^{12}C$ ratio, is used for the correction. $\delta^{13}C$ of sample and standard are calculated according to equation (1) relative to the reference standard (PDB).

Correction for background

The process blank, i.e. the contamination introduced during chemical sample treatment, combustion, and graphitization, is determined by measuring prepared anthracite, which is ^{14}C-free due to its high age. The blank value correction is subtracted from the $\delta^{13}C$ corrected ^{14}C data. The effect of the sample contamination on the ^{14}C result depends on the amount of carbon in the sample and on the age difference between the contaminant and the sample.

Measurement uncertainty

Radiocarbon measurements are reported with ± 1-σ (σ = standard deviation) measurement uncertainty. This accords the confidence interval in which the true value is to be expected with 68.3 % probability (Stuiver and Polach 1977). Depending on the value, either the reproducibility of the 8 to 9 measurements of each sample during a single run or the Poisson counting statistics, based on the total number of ^{14}C counts for each sample, whichever is larger, is combined with the uncertainty of the blank correction as measurement uncertainty for ^{14}C results at the Leibniz laboratory (Nadeau et al. 1998).

Calculation of the conventional radiocarbon age and the calendar age

The conventional radiocarbon age (t) in years before present (BP) is calculated following equation (3):

$$\text{t (years BP)} = -\frac{1}{\lambda} \cdot \ln\left(\frac{R_{sample*}}{R_{Ox*}}\right), \qquad (5)$$

where $1/\lambda$ represents the mean lifetime of ^{14}C (8033 years based on the original half-life of 5,568 years). The 1-σ statistical uncertainty in the measured $R_{sample*}$ and R_{Ox*} are then used to calculate the ± 1-σ uncertainties in ^{14}C age.

The conventional ^{14}C age do not correspond to the historical age, due to the mentioned ^{14}C variations in the atmosphere and the "falsely" accepted Libby-half-life. To obtain historical ages (cal AD, cal BP) the conventional ^{14}C age needs to be calibrated. This is carried out by using an international tree ring calibration data set (Stuiver et al. 1998) which is included in different calibration programs (e.g. CALIB, Stuiver et al. 2003 or IntCal09, Reimer et al. 2009). Calendar ages based on ^{14}C ages can also be determined for the time after the additional production of 'bomb-^{14}C' by aboveground nuclear weapon tests (Reimer et al. 2004). The used calibration curves are obtained by determination of the conventional ^{14}C age of dendrochronological investigated tree rings. In doing so, the variation of the atmospheric ^{14}C concentration during the last millennia can be reconstructed.

The German oak and pine chronologies (Spurk et al. 1998) play a crucial role. The German oak chronology provides absolute counts of dendro-years back to ca. 10,300 cal BP. This chronology could be extended to 11,857 cal BP by matching the latest part of a floating German pine chronology to the earliest absolutely dated German oak. Errors in the matching may amount to 20 cal years (Kromer and Spurk 1998). Additional calibration data for up to 20,000 cal BP can be obtained by the uranium-thorium (U-Th) dating of corals (Bard et al. 1998; Burr et al. 1998).

Sample pretreatment and preparation

Since SOM is a heterogeneous mixture of organic components accumulating and decaying at different rates, which is reflected by ^{14}C ages of organic components from recent to more than 20,000 years (Scharpenseel and Becker-Heidmann, 1992). Furthermore, soils are open systems which continuously receive organic carbon as plant residues and loose gaseous and dissolved carbon via mineralization and leaching, respectively. Hence, radiocarbon data of SOM do not represent the soil age and as a consequence of this numerous physical and chemical fractionation methods have been used with the objective to isolate a 'passive' SOM fraction that turns over on time scales of millennia and thus, is least influenced by recently introduced organic matter and can be used as an indicator for the soil age (Scharpenseel, 1972, 1977; Huang et al., 1996; Pessenda et al., 2001).

Depending on the required amount of material, which can be estimated i.e. by the sample color, dried soil samples, SOM fractions (fulvic acids, humic acids, humins) and macrofossils were transferred into small (inner diameter: 0.4 cm ; length: 6 cm) or large (inner diameter: 0.6 cm ; length: 6 cm) quartz combustion tubes. Furthermore, 450 mg of copper oxide, supplying oxygen, and, depending on sample size, 150 mg to 450 mg of silver wool, for removal of sulfur and halogens, were added for combustion. Afterwards, the combustion tubes were transferred into larger outside quartz tubes of 0.7 - 0.9 cm inner diameter, and ca. 35 cm length.

The tubes were evacuated on a vacuum line for about 10 hours down to a pressure of about 10^{-4} mbar and subsequently flame sealed. All samples were combusted in a muffle furnace at 900°C for 4 hours. The resulting CO_2 was purified cryogenically in a vacuum line and collected in glass bottles, which were placed in a cold trap with liquid nitrogen (-196°C).

To graphitize the cleaned CO_2 the bottles were then transferred to a separate vacuum manifold with multiple parallel reduction systems. About 10 % excess of hydrogen was added to the sample CO_2. The reaction tubes, which contained 2 mg cleaned (0.7 bar O_2 at 400°C for 15 min.; 0.7 bar H_2 at 400°C for 30 min.) iron powder as catalyst, were then heated at 600°C for about 2 to 3 hours until the reaction was completed. (Nadeau et al. 1998). The water released during the reaction ($CO_2 + 2H_2 \rightarrow C + 2H_2O$) was removed cryogenically. The obtained graphite-iron powder mixture was pressed into 1.5 mm diameter cavities in aluminum target holders using a pneumatic press (Nadeau et al., 1998). The graphite targets were stored in small glass bottles filled with argon before they were placed in a target wheel for AMS measurement.

AMS ^{14}C measurement and reporting of ^{14}C results

A sample carousel for AMS measurement contains in Kiel usually 42 'unknown' sample targets, 8 oxalic acid standard (Ox II) targets, 2 IAEA standards of known ^{14}C content, 4 background targets, 1 graphite blank, and 1 target used as 'caesium beam dump' (Nadeau et al., 1998). The ^{14}C results were checked for natural isotopic fractionation via the $^{13}C/^{12}C$ ratio of the sample compared to a standard, measured by AMS simultaneously with the $^{14}C/^{12}C$ ratio (Nadeau et al., 1998). The long-term stability of the AMS measurements was evaluated by IAEA standards with known ^{14}C contents, which are included in each sample carousel. ^{14}C results are expressed according to Stuiver and Polach (1977) in percent modern carbon (pMC) with ± 1-σ measurement uncertainty as described before.

The precision of the radiocarbon measurement is limited by the process blank, the contamination of the samples with modern CO_2 during sample preparation and graphitization, as well as by the stability of the AMS system. Details of the laboratory blank and the machine background at the Leibniz-Laboratory have been described in detail by Schleicher et al. (1998) and Nadeau et al. (1998). The machine background, which was determined by measuring pure graphite, is about 0.03 pMC. The contamination introduced by reduction and graphitization is about 0.05 to 0.06 pMC. The overall background equals ca. 4 µg modern carbon which is equivalent to about 0.3 pMC for samples containing 1.5 - 2.0 mg of carbon.

Methods of C determination

The determination of carbon (C) is essential for a wide range of research areas, such as geochemistry, agronomy, oceanography and ecology. Especially in soil science, measurements of total carbon (TC), inorganic carbon (IC) and organic carbon (OC) are used to characterise soils and sediments. There are two basic forms of carbon in soils and sediments: organic carbon and inorganic carbon. The OC fraction originates from animals, plants and microorganisms in various stages of decomposition. Also elemental C in form of coal, charcoal, graphite or soot is attributed to the organic fraction (Page et al., 1982; Ballesteros et al., 1997). The IC fraction is commonly present as carbonate and derived in most cases from the parent material of the soil or sediment. Calcite ($CaCO_3$) and (less) dolomite ($CaMg(CO_3)_2$) are the most common representatives of carbonate minerals in the IC fraction. Due to their characteristics (alkalinity, solubility and buffering properties) carbonate minerals are of great importance for soils and the IC measurement is part of the standard procedure of soil analysis (Scheffer/Schachtschabel, 2010). Since TC is the sum of IC and OC, IC determination is always linked to OC determination if TC is involved. TC is measured by oxidation and liberation of all carbon in the sample. Removing OC from the sample and measuring the remaining carbon reveals the IC content and vice versa. This results in different methods, which all have one common problem - the precise separation of the IC from the OC fraction (Weliky et al., 1983).

Five laboratories, involved in the research unit FOR995 ‘Biogeochemistry of paddy soil evolution’, jointly investigated soil samples from a paddy and non-paddy chronosequence regarding their IC, OC and TC content. Comparison of the results reveals differences between the applied methods. Overall six methods for IC determination were used: two volumetric approaches, three methods using thermal conductivity with a C-analyzer and an infrared detection method. Effects of the different methods on IC contents are, unfortunately, not known, although each method gives seemingly consistent results. However, IC values are crucial for calculation of total organic carbon (TOC) values, particularly in subsoils having relatively low-TOC and high-IC concentrations. To provide a detailed comparison of the applied IC measurements, four soil samples were chosen for a round-robin test. Table 2.2 provides an overview of the different approaches. Detailed information about the C determination methods are specified at Kalbitz et al. 2013.

Table 2.2: Applied C determination methods within the research unit FOR 995

Method	C detection	IC measurement	OC measurement	Device
I	volumetric	direct	TC - IC	Scheibler apparatus
II	volumetric	direct	direct (combustion)	Vacuum system AMS (Leibniz-laboratory, Kiel)
III	thermal conductivity	direct	TC-IC	Elemental analyzer: Vario EL III with TIC module SoliTIC
IV	thermal conductivity	TC - OC	direct*	Elemental analyzer: Carlo Erba NA 2000
V	thermal conductivity	direct**	TC - IC	Elemental analyzer: Vario EL element analyzer
VI	photometric	direct	TC - IC	infrared spectrometer: C-MAT 5500, Ströhlein GmbH

*IC fraction was removed and the remaining C was measured as OC.
**OC fraction was removed and the remaining C was measured as IC.

The C data, used in this study were obtained by method II. Thus, the IC content of a sample is determined by dissolution of carbonates with 5 % HCl in an evacuated glass ampoule overnight at 80 °C, freeze trapping of the CO_2 with liquid nitrogen and removal of other gases, repetition of the procedure to purify the CO_2, and volumetric quantification of CO_2 (limit of determination ca. 0.05 mg C g^{-1} soil). The removal of carbonates with HCl is routinely applied to obtain total organic carbon-derived CO_2 for ^{14}C analysis by accelerator mass spectrometry (Grootes et al., 2004). The OC content of the sample was recovered by the combustion of the material, left after carbonate dissolution, and following volumetric quantification of CO_2.

The results of the methods I - VI are summarized in Figure 2.6. Clearly the TC values obtained are quite similar, with an average deviation for TC across all samples and methods of less than 6 %. Thus the method of CO_2 quantification is of little relevance. The difference between the methods is rather in the classification of the TC into OC and IC.

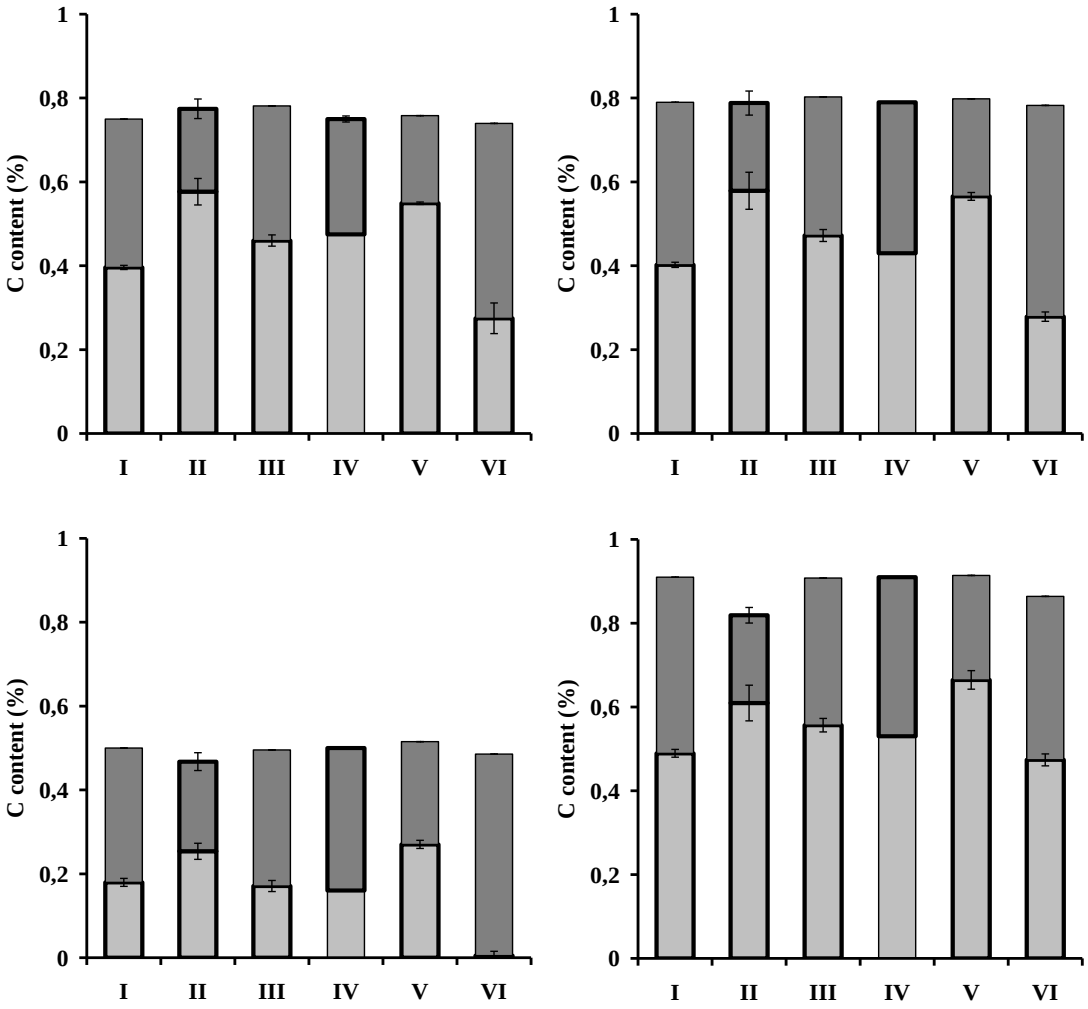

Figure 2.6 Total carbon divided in IC (light grey) and OC (dark grey) determined with six different methods. All bars give the arithmetic mean of at least two and at most eight replicates. Direct measurements are marked with a black frame. Method II gives the sum of IC and OC. Method I, III, V and VI result from TC and IC measurements. Method IV gives measured TC and OC values. Top left = sample 1; top right = sample 2; bottom left = sample 3; bottom right = sample 4.

Table 2.3 shows the average IC content of the four test samples after repeated measurements using the six described methods. The large differences between the IC contents, especially those measured with method II and V and those of Method VI, are obvious. Method II quantifies IC and OC individually volumetrically. The other methods determine TC and IC (Methods I, III, V, and VI) or OC (IV) and derive OC or IC, respectively, as the difference with TC.

Table 2.3: Carbonate content (IC) measured with six different methods. All numbers give the arithmetic mean of at least two and at most eight replicates with standard deviation.

Sample	IC_I (%)	IC_{II} (%)	IC_{III} (%)	IC_{IV} (%)	IC_V (%)	IC_{VI} (%)
1	0.40 ±0.01	0.58 ±0.03	0.46 ±0.01	0.48* ±n.d.	0.55 ±0.01	0.27 ±0.04
2	0.40 ±0.01	0.58 ±0.04	0.47 ±0.01	0.43* ±n.d.	0.57 ±0.01	0.28 ±0.01
3	0.18 ±0.01	0.25 ±0.02	0.17 ±0.01	0.16* ±n.d.	0.27 ±0.01	0.01 ±0.01
4	0.49 ±0.01	0.61 ±0.04	0.56 ±0.02	0.53* ±n.d.	0.66 ±0.02	0.47 ±0.01

* Method IV provides calculated IC values after TC and OC determination.

A problem which is inherent for all methods working with acid treatment is the assumption that all IC in the sample is present in form of uniform, fast reacting carbonates like calcite or aragonite. However, some carbonates, such as dolomite, often occurring in soils, require heat for a complete reaction and are only slowly decomposed by acid treatment in the cold (van Moort & de Vries, 1970). Al-Aasm et al., 1990 reported a required dolomite removal time six times longer than for calcite, using 100 % H_3PO_4 at 50°C. A problem is thus, the time needed for a complete reaction between sample and acid (Caughey et al., 1995) for an unknown soil mixture. The reaction time for the "Scheibler apparatus" (method I) is usually chosen between 10 and 40 minutes, yet the time for this experiment, using 15 % HCl, was set at several minutes. Method III used 480 seconds with 10 % HCl at 50°C, and Method VI 450 seconds with 42 % H_3PO_4 at room temperature. Method II provided a reaction time with 5 % HCl at 80°C in a shaking bath of several hours (over night). Reaction time and temperature could be responsible for the lower carbonate yield of method I, III, and VI compared to method II. The higher viscosity of H_3PO_4 may be an additional complication for Method VI and a reason it produced the lowest IC values of the round-robin test.

Method I and IV are based on the same TC measurements. Yet, for method IV, OC is measured in an elemental analyzer after removal of the IC with acid. Since the amount of HCl for carbonate dissolution in method IV is estimated from the IC results of method I, the lower IC yield of method I could result in a low amount of acid, leading to incomplete

removal of IC. An erroneously high OC, incorporating some IC, would explain the lower IC yield of method IV compared to method II.

Method V used LOI (loss over ignition) to remove OC, so IC can be measured directly in an elemental analyzer, like in Method IV. Due to easy handling and relatively low costs, the LOI method is widespread. However, the assumption that only the OC fraction is removed by combustions around 500°C was disproved by several studies. Clay, gypsum and sesquioxides release chemically combined water in such temperature range (Dean, 1974). Moreover, Bendor & Banin, 1989 reported carbonate decomposition after prolonged heating at 400°C. Thus LOI must be considered of questionable reliability to quantify OC. Nonetheless, the results of method V suggest that for these samples LOI functioned effectively, since the measured IC values belong, with those of Method II, to the highest values obtained in the round-robin test.

We attribute the revealed significant differences between the described IC determination methods to the different reaction times and temperatures during carbonate dissolution by acid. However, we suppose the longest reaction time, applied for our method (II), as an advantage for the determination of reliable IC and OC values.

References

Al-Aasm, I.S., Taylor, B.E. and South, B., 1990. Stable isotope analysis of multiple carbonate samples using selective acid extraction, Chemical Geology (Isotope Geoscience Section) 80,119-125

An S, Li H, Guan B, Zhou C, Wang Z, Deng Z, Zhi Y, Liu Y, Xu C, Fang S, Jiang J, Li H. 2007. China's Natural Wetlands: Past Problems, Current Status, and Future Challenges. AMBIO: A Journal of the Human Environment 36, 335-342.

Baisden WT, Amundson R, Brenner DL, Cook AC, Kendall C, Harden JW. 2002. A multiisotope C and N modeling analysis of soil organic matter turnover and transport as a function of soil depth in a California annual grassland soil chronosequence. Global Biochemical Cycles 16 (4), 8210-8226.

Ballesteros, E., Rios A. and Valcárcel, M., 1997. Integrated Automatic Determination of Nitrate, Ammonium and Organic Carbon in Soil Samples, Analyst 122, 309–313

Bard E, Arnold M, Hamelin B, Tisnerat-Laborde N, Cabioch G. 1998. Radiocarbon calibration by means of mass spectrometric $^{230}Th/^{234}U$ and ^{14}C ages of corals: An updated

database including samples from Barbados, Mururoa and Tahiti. Radiocarbon 40 (3), 1085-1092.

Bendor, E. and Banin, A., 1989. Determination of organic-matter content in arid-zone soils using a simple loss-on-ignition method, Communications in Soil Science and Plant Analysis 20 (15/16), 1675-1695

Bennett CL, Beukens RP, Clover MR, Gove HE, Liebert RP, Litherland AE, Purser KH, Sondheim WE. 1977. Radiocarbon dating using electronic accelerators: negative ions provide the key. Science 198, 508-510.

Bhupinderpal-Singh, Hedley MJ, Saggar S. 2005. Characterization of recently ^{14}C pulse labeled carbon from roots by fractionation of soil organic matter. European Journal of Soil Science 56, 329-341.

Burr GS, Beck JW, Taylor FW, Recy J, Edwards RL, Cabioch G, Correge T, Donahue DJ, O'Malley JM. 1998. A high-resolution radiocarbon calibration between 11,700 and 12,400 calendar years BP derived from ^{230}Th ages of corals from Espiritu Santo Island, Vanuatu. Radiocarbon 40 (3), 1093-1105

Cao ZH, Ding JL, Hu ZY, Knicker H, Kögel-Knabner I, Yang LZ, Yin R, Lin XG, Dong YH. 2006. Ancient paddy soils from the Neolithic age in China's Yangtze River Delta. Die Naturwissenschaften 93, 232-6.

Caughey, M.E., Barcelona, M.J., Powell, R.M., Cahill, R.A., Gron, C., Lawrenz, D. and Meschi, P.L., 1995. Interlaboratory study of a method for determining nonvolatile organic carbon in aquifer materials, Environmental Geology 26, 211-219

Cheng YQ, Yang LZ, Cao ZH, Ci E, Yin S. 2009. Chronosequential changes of selected pedogenic properties in paddy soils as compared with non-paddy soils. Geoderma 151, 31-41.

Dean, W. E. Jr., 1974. Determination of carbonate and organic matter in calcareous sediments and sedimentary rocks by loss on ignition: Comparison with other methods. Journal of Sedimentary Petrology 44, 242–248

de Vries H. 1958. Variations in concentration of radiocarbon with time and location on earth. Proceedings of the Koninklijke Nederlandse Akademie van Wetenschappen B 61, 267-281.

Dörr H, Münnich KO. 1986. Annual variations of the ^{14}C content of soil CO_2. Radiocarbon 28, 338-345.

Dreves A, Andersen N, Grootes PM, Nadeau MJ, Garbe-Schönberg CD. 2007. Colloidal matter in water extracts from forest soils. Environmental Chemistry 4, 424-429.

Ellis S, Atherton JK. 2003. Properties and development of soils on reclaimed alluvial sediments of the Humber estuary, eastern England. Catena 52, 129-147.

Godwin H. 1962. Half-life of radiocarbon. Nature 19, 984.

Grootes PM. 1978. Carbon-14 time scale extended. Comparison of chronologies. Science 200,11-15.

Grootes PM, Nadeau, MJ, Rieck A. 2004. ^{14}C-AMS at the Leibniz-Labor: radiometric dating and isotope research. Nuclear Instruments and Methods in Physics Research B 223-224, 55–61.

Hagstrum JT, Champion DE. 1995. Late quaternary geomagnetic secular variation from historical and 14C- dated lava flows on Hawaii. Journal of Geophysical Research 100 (B12), 24,393-24,403.

Harkness DD, Harrison AF, Bacon PJ. 1986. The temporal distribution of 'bomb' ^{14}C in a forest soil. Radiocarbon 28, 328-337.

Harkness DD, Harrison AF, Bacon PJ. 1991. The Potential of Bomb-^{14}C Measurements for Estimating Soil Organic Matter Turnover. In: Wilson WS, (Editor). Advances in soil organic matter research: The impact on agriculture and the environment. Cambridge: Royal Society of Chemistry. p. 239-251.

Harrison KG. 1996. Using bulk soil radiocarbon measurements to estimate soil organic matter turnover times: implications for atmospheric CO_2 levels. Radiocarbon 38, 181-190.

Harrison KG. 1998. Using bulk soil radiocarbon measurements to estimate soil organic matter turnover time. In: La R, Kimble JM, Follet RF, Stewart BA, (Editor). Soil Processes and the carbon cycle. Boca Raton: CRC Press. p.549-560.

He Y, Zhang M. 2001. Study on the wetland loss and its reasons in China. Chinese Geographical Science 11, 241-245.

Healy MG, Hickey KR. 2002. Historic land reclamation in the intertidal wetlands of the Shannon estuary, western Ireland. Journal of Coastal Research, 365-373.

Huang Y, Li B, Bryant C, Bol R, Eglinton G. 1999. Radiocarbon Dating of Aliphatic Hydrocarbons: A New Approach for Dating Passive-Fraction Carbon in Soil Horizons. Soil Science Society of America Journal 63, 1181-1187.

Huang Y, Bol R, Harkness DD, Ineson P, Eglinton G. 1996. Post-glacial variations in distributions, ^{13}C and ^{14}C contents of aliphatic hydrocarbons and bulk organic matter in three types of British upland soils. Organic Geochemistry 24, 273-287.

Inoue Y, Hiradate S, Sase T, Hosono M, Morita S, Matsuzaki H. 2011. Using ^{14}C dating of table humin fractions to assess upbuilding pedogenesis of a uried Holocene humic soil horizon, Towada volcano, Japan. Geoderma 167-168, 85-90.

IntCal09. http://www.radiocarbon.org/IntCal09.htm

IUSS Working Group WRB. 2007. World reference base for soil resources. World Soil Resources Reports, Vol. 103. FAO: Rome. 145 p.

Kalbitz K, Kaiser K, Fiedler S, Kölbl A, Amelung W, Bräuer T, Cao Z, Don A, Grootes P, Jahn R, Schwark L, Vogelsang V, Wissing L, Kögel-Knabner I. 2013. The carbon count of 2,000 years of rice cultivation. Global Change Biology 19, 1107-1113.

Karlén I, Olsson IU, Kållburg P, Kilici S. 1968. Absolute determination of the activity of two ^{14}C dating standards. Arkiv Geofysik 4, 465-471.

Kocharov GE, Peristykh AN, Kereselidze PG, Lomtatidze ZN, Metskhvariskvii RY, Tagauri ZA, Tsereteli SL, Zhorzholiani LV. 1992. Variation of radiocarbon content in tree rings during the Maunder minimum of solar activity. Radiocarbon 34, 213-217.

Kromer B, Spurk M. 1998. Revision and tentative extension of the tree-ring based ^{14}C calibration, 9200-11,855 cal BP. Radiocarbon 40 (3), 1117-1125.

Levin I, Kromer B. 1997. Twenty years of atmospheric 14CO2 observations at Schauinsland station, Germany. Radiocarbon 39, 205-218.

Levin I, Hessheimer V. 2000. Radiocarbon - A unique tracer of global carbon cycle dynamics. Radiocarbon 42, 69-80.

Levin I, Kromer B. 2005. The Tropospheric 14CO2 Level in Mid-Latitudes of the Northern Hemisphere (1959–2003). Radiocarbon 46, 1261-1272.

Libby WF. 1953. Radiocarbon dating. Chicago: University of Chicago Press.

Libby, W. F., 1946. Atmospheric helium three and radiocarbon from cosmic radiation. Physical Review 69, 671-672.

Mann WB. 1983. An international reference material for radiocarbon dating. Radiocarbon 25, 519-522.

Mook WG, van der Plicht J. 1999. Reporting 14C activities and concentrations. Radiocarbon
41, 227-239.

Nadeau MJ, Schleicher M, Grootes PM, Erlenkeuser H, Gottdang A, Mous DJW, Sarnthein JM, Willkomm H. 1997. The Leibniz-Labor AMS facility at the Christian-Albrechts University, Kiel, Germany. Nuclear Instruments and Methods in Physics Research B 123, 22-30

Nadeau MJ, Grootes PM, Schleicher M, Hasselberg P, Rieck A, Bitterling M. 1998. Sample throughput and data quality at the Leibniz-Labor AMS facility. Radiocarbon
40, 239-245.

Naegler T, Ciais P, Rodgers K, Levin I. 2006. Excess radiocarbon constraints on air-sea gas exchange and the uptake of CO2 by the oceans. Geophysical Research Letters 33 (doi:10.1029/2005GL025408).

Nelson DE, Korteling RG, Stott WR. 1977. Carbon-14 direct detection of natural concentrations. Science 198, 507-508.

Nydal R, Lövseth K. 1983. Tracing bomb-14C in the atmosphere 1962-1980. Journal of Geophysical Research 88, 3621-3642.

O´Brien BJ. 1984. Soil organic carbon fluxes and turnover rates estimated from radiocarbon. Soil Biology and Biochemistry 16, 115-120.

O'Brien BJ. 1986. The use of natural and anthropogenic ^{14}C to investigate the dynamics of soil organic carbon. Radiocarbon 28, 359-362.

O'Brien BJ, Stout JD. 1978. Movement and turnover of soil organic matter as indicated by carbon isotope measurements. Soil Biology and Biochemistry 10, 309-317.

Page, A.L., Miller, R.H. and Keeney, D.R., 1982. Methods of Soil Analysis - Part 2: Chemical and Microbiological Properties, 2nd ed. (American Society of Agronomy and Soil Science Society of America, Madison, WI)

Perrin R, Willis E, Hodge C. 1964. Dating of humus podzolz by residual radiocarbon activity. Nature 202, 165-166.

Pessenda, L.C.R., Gouveia, S.E.M., and Aravena, R., 2001. Radiocarbon dating of total soil organic matter and humin fraction and its comparison with 14C ages of fossil charcoal. Radiocarbon 43 (2b), 595-601.

Prior CA, Baisden WT, Bruhn F, Neff JC. 2007. Using a soil chronosequence to identify soil fractions for understanding and modeling soil carbon dynamics in New Zealand. Radiocarbon 49 (2), 1093-1102.

Reimer PJ, Brown TA, Reimer RW. 2004. Discussion: reporting and calibration of post-bomb ^{14}C data. Radiocarbon 46, 1299-1304.

Reimer PJ, Baillie MGL, Bard E, Bayliss A, Beck JW, Blackwell PG, Bronk Ramsey C, Buck CE, Burr GS, Edwards RL, Friedrich M, Grootes PM, Guilderson TP, Hajdas I, Heaton TJ, Hogg AG, Hughen KA, Kaiser KF, Kromer B, McCormac FG, Manning SW, Reimer RW, Richards DA, Southon JR, Talamo S, Turney CSM, van der Plicht J,Weyhenmeyer CE. 2009. IntCal09 and Marine09 radiocarbon age calibration curves, 0-50,000 years cal BP. Radiocarbon 51, 1111-1150.

Rethemeyer J. 2004. Organic carbon transformation in agricultural soils : Radiocarbon analysis of organic matter fractions and biomarker compounds, Thesis CAU Kiel, p.165.

Rethemeyer J, Kramer C, Gleixner G, John B, Yamashita T, Flessa H, Andersen N, Nadeau MJ, Grootes PM. 2005. Transformation of organic matter in agricultural soils: radiocarbon concentration versus soil depth. Geoderma 128, 94-105.

Römkens PFAM, Hassink J, van der Pflicht J. 1998. Soil organic ^{14}C dynamics: effects of pasture installation an arable land. Radiocarbon 40, 1023-1031.

Rumpel C, Balesdent J, Grootes P, Weber E, Kögel-Knabner I. 2003. Quantification of ligniteand vegetation-derived soil carbon using 14C activity measurements in a forested chronosequence. Geoderma 112, 155-166.

Sarnthein M, Grootes PM, Kennett JP, Nadeau M-J. 2007. ^{14}C reservoir ages show deglacial changes in ocean currents and carbon cycle. In: Schmittner A, Chiang JCH, Hemming SR, Hrsg. Ocean circulation: Mechanisms and impacts - Past and future changes of meridional overturning. Washington: American Geophysical Union. p. 175-196.

Scharpenseel HW, Becker-Heidmann P. 1989. Shifts in ^{14}C patterns of soil profiles due to bomb carbon, including effects of morphogenetic and turbation processes. Radiocarbon 31 (3), 627-636.

Scharpenseel HW, Becker-Heidmann P. 1992. Twenty-five years of radiocarbon dating soils: paradigm of erring and learning. Radiocarbon 34, 541-549.

Scharpenseel HW, Pietig, F. 1968. Altersbestimmung von Boden durch die Radiokohlenstoffdatierungsmethode Teil 3. 122, 145-152.

Scharpenseel HW, Pietig, F. 1969. Einfache Boden- und Wasserdatierung durch Messung der ^{14}C- oder Tritiumkonzentration. Geoderma 2, 273-289.

Scharpenseel, H.W., 1972. Messung der natürlichen C-14 Konzentration in der organischen Bodensubstanz von rezenten Böden. Zeitschrift für Pflanzenernährung und Bodenkunde 133 (3), 241-263.

Scharpenseel, H.W., 1977. The search for biologically inert and lithogenic carbon in recent soil organic matter. Proceedings of IAEA Conference on soil organic matter studies, Vienna, SM 211 (71), 193-200.

Scheffer F, Schachtschabel P. 2010. Lehrbuch der Bodenkunde. 16th ed. Spektrum Akademischer Verlag, Heidelberg.

Schleicher, M., Grootes, P.M., Nadeau, M.J., and Schoon, A., 1998. 14C backgrounds and their components at the Leibniz AMS facility. Radiocarbon 40 (1), 85-93.

Spurk M, Friedrich M, Hofmann J. 1998. Revisions and extension of the Hohenheim oak and pine chronologies: New evidence about the timing of the Younger Dryas/Preboreal transition. Radiocarbon 40 (3), 1107-1116.

Sternberg R.S., 1992. Radiocarbon fluctuations and the geomagnetic field. In: Taylor R.E., Long A., and Kra R.S. (eds.), Radiocarbon After Four Decades. An Interdisciplinary Perspective. Springer, New York, pp. 93-116.

Stuiver M, Polach HA. 1977. Discussion: reporting of ^{14}C data. Radiocarbon 19, 355-363.

Stuiver M, Quay PD. 1980. Changes in atmospheric carbon-14 attributed to a variable sun. Science 207, 11-19.

Stuiver M, Braziunas TF, Becker B, Kromer B. 1991. Late-glacial and Holocene atmospheric $^{14}C/^{12}C$ change: climate, solar, oceanic and geomagnetic influences. Quaternary Research 35, 1-24.

Stuiver M, Reimer PJ, Bard E, Beck JW, Burr GS, Hughen KA, Kromer B, McCornmac G, van der Plicht J, Spurk M. 1998. INTCAL 98 Radiocarbon age calibration, 24,000-0 cal BP.
Radiocarbon 40, 1041-1083.

Stuiver M, Reimer PJ, Reimer R. 2003. CALIB – Radiocarbon calibration, Version 4.4. (http://radiocarbon.pa.qub.ac.uk/calib/).

Su J, Wang K. 1989. Changjiang river plume and suspended sediment transport in Hangzhou Bay. Continental Shelf Research 9, 93-111.

Suess HE. 1955. Radiocarbon concentration in modern wood. Science 122, 415-417.

Suess HE. 1986. Secular variations of cosmogenic ^{14}C on earth: Their discovery and interpretation. Radiocarbon 28, 259-265.

Tonneijck FH, Van der Plicht J, Jansen B, Verstraten JM, Hooghiemstra H. 2006. Radiocarbon dating of soil organic matter fractions in andosols in northern ecuador. Radiocarbon 48, 337-353.

Trumbore SE, Vogel JS, Southon JR. 1989. AMS 14C measurements of fractionated soil organic matter: an approach to deciphering the soil carbon cycle. Radiocarbon 31, 644-654.

Trumbore SE. 1993. Comparison of carbon dynamics in tropical and temperate soils using radiocarbon measurements. Global Biogeochemical Cycles 7, 275-290.

Trumbore SE.1996. Applications of accelerator mass spectrometry to soil science. In: Boutton, T.W. and Yamaski, S.I. (eds.), Mass spectrometry of soils. Marcel Dekker, New York, pp. 311-340.

Trumbore SE, Zheng S. 1996. Comparison of fractionation methods for soil organic matter 14C analysis. Radiocarbon 38, 219-229.

Tuniz C, Bird JR, Fink D, Herzog GF. 1998. Accelerator Mass Spectrometry. Boca Raton: CRC Press.

van Moort, J.C. and De Vries, D., 1970. Rapid carbon determination by dry combustion in soil science and geochemistry, Geoderma 4, 109-118

Vogel JS, Nelson DE. 1995. Accelerator mass spectrometry. Analytical Chemistry 67, 353 359.

Völker A, Grootes PM, Nadeau M-J, Sarnthein M. 2000. Radiocarbon levels in the Iceland sea from 25-53 kyr and their link to the earth's magnetic field. Radiocarbon 42, 437-452.

Weliky, K., Suess, E., Ungerer, C.A., Muller, P.J. and Fischer, K., 1983. Problems with accurate carbon measurements in marine sediments and particulate matter in sea water - a new approach, Limnology and Oceanography 28 (6), 1252-1259

Zhang M, Lu H, Zhao XJ, Li RA. 2004. A comparative study of soil fertility change of upland soil in Cixi County. Chinese Journal of Soil Science 35, 91-93.

Chapter III

Downward carbon transport in a 2,000-year rice paddy soil chronosequence traced by radiocarbon measurements

Status: Published in Nuclear Instruments and Methods in Physics Research Section B: Beam Interactions with Materials and Atoms 294, 584-587 (2013).

Abstract

Paddy and non-paddy soils from a chronosequence of 50 to 2000 years of agricultural use, developed on former estuarine sediments of the Yangtze River, were sampled near Cixi, Zhejiang Province, China, in the framework of the Research Unit "Biogeochemistry of paddy soil evolution" of the German Research Foundation (DFG). In addition samples of Yangtze River estuarine sediments were obtained. The parent sediment shows a fairly homogeneous composition with ca. 0.3 % TOC and a ^{14}C concentration of ca. 50 pMC. After being diked-in, gradients in soil organic carbon and ^{14}C concentration develop under the influence of vegetation and cultivation. In the non-paddy soil, a ^{14}C gradient with concentration decreasing with increasing depth from modern (>100 pMC) to original sediment values around 50 pMC is already established after 50 years and can also be observed in the older sites. In contrast, the 50 years old paddy soil shows organic carbon and ^{14}C enrichment only in the A-horizon and a nearly constant TOC and ^{14}C stock of original sediment below the plough pan. To test the basic approach that the soil profile development started on homogeneous sediment, an isotope and mass balance calculation was used. The results show a quite similar age composition of different sample sites. Paddy rice cultivation quickly leads to a dense plough pan, which seriously reduces, but not totally prevents, downward transport of organic matter. The equilibrium times for TOC and ^{14}C in paddy soil profiles are short (decades) in the topsoil and in the order of centuries in the subsoil, underlining the dynamic character of soil organic carbon

Introduction

Rice paddies are of major importance for the world food production. Today, rice is the staple food for nearly half the world population (MacLean et al. 2002). Currently, the total area of lowland rice paddy in China is about 29.5 million ha, which represents 19 % of the total world rice paddy area. With about 30 % of the global rice production China is the world's largest rice producer, followed by India (22 %) and Indonesia (9 %) (FAOSTAT 2010).

Rice paddies are wetlands characterized by a specific management with alternating flooded and dry phases. During the puddling process the topsoil gets plowed under waterlogged conditions. This leads to homogenized topsoils and a nearly impermeable plough pan (Bouman and Tuong 2001; Sharma et al. 1988). This dense layer is one of the major factors that affect the redox conditions and C stabilization processes in paddy soils (Neue et al. 1997). The submergence induces a temporal variation of the redox potential. This leads to changing oxic and anoxic conditions during the season and a high content of soil organic matter (SOM) (Frenzel et al. 1992). SOM has great influence on many soil processes and also plays a key role in the global carbon cycle. SOM is generally a mixture of a wide variety of compounds of different origin and age. Consequently, its average ^{14}C concentration is determined by the mixing ratio and ^{14}C contents of its components. Especially, after the atmospheric tests of nuclear weapons over the years 1954 to 1962 led to highly elevated ^{14}C concentrations in the atmosphere that changed from year to year, SOM ^{14}C concentrations no longer indicate a SOM age. Yet, ^{14}C concentrations of bulk soil, used as a tracer, can provide an insight into the SOM fluxes within the soil profile, especially when values above 100 pMC indicate incorporation of bomb carbon. The objective of this study is to quantify how rice cultivation affects the stabilization and turnover of organic carbon, using the radioactive isotope ^{14}C as a tracer. The chronosequence also offers the possibility to study how fast the effects of rice cultivation get established.

China has a millennia-old history of rice cultivation, and therefore has a range of rice growing areas from very old to very young, only a few decades old (Zong et al. 2007). In the framework of the DFG Research Unit FOR 995 "Biogeochemistry of paddy soil evolution", paddy soils from a chronosequence of 50 to 2000 years of agricultural use were

sampled. To ascertain the effects of paddy management, additional samples of soils not used for lowland rice cultivation (non-paddy) from 50 to 700 years of agricultural use were obtained. The comparison between paddy and non-paddy will show to what extent carbon dynamics is affected by paddy soil management.

The study sites are located around Cixi (30° 10′ N, 121° 14′ E), Zhejiang Province, China, approximately 180 km south of Shanghai and 150 km east of Hangzhou (Figure 3.1). This region is one of the earliest lowland rice cultivation regions in the world (Cao et al. 2006). With a mean annual temperature of 16.3°C and a mean precipitation of 1325 mm per year the climate is classified as subtropical with periodical monsoon rain (Cheng et al. 2009). The total evaporation is 1000 mm. Therefore, irrigation is needed to maintain standing water during rice growing. The elevation ranges from 2.6 to 5.7 m above sea level (Zhang et al. 2004). The major cropping system in the region of Cixi is rice in summer and wheat or vegetables in winter. More detailed information regarding ground water table, geography, and geochemistry of the study area is given by Cheng et al. (2009).

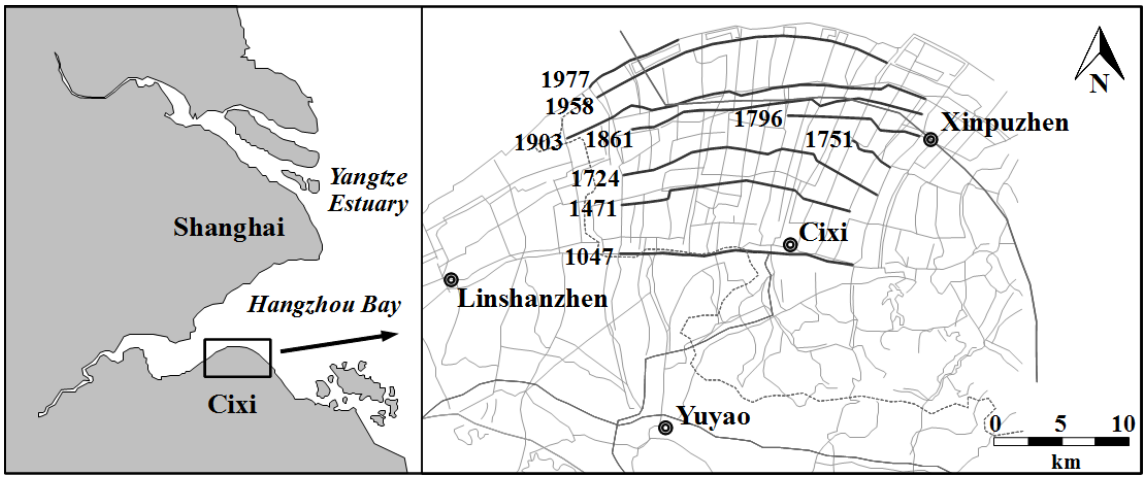

Figure 3.1: Geographical location of the investigation area at the south coast of Hangzhou Bay. Dark lines in the large scale clipping represent protective dikes together with the year of construction.

The parent material of this region consists of estuarine sediment, which originated from the largest river in China, the Yangtze River. With a sediment load of ca. 480 million tons per year, the Yangtze is the main source of sediment delivered to the East China Sea

(Millimann et al. 1985; Wang et al. 2008). After passing the Yangtze delta, the sediments are relocated into the Hangzhou Bay under the influence of the Taiwan Warm Current and the Zhejiang–Fujian Coastal Current (Cheng et al. 2009; Liu et al. 2007). To convert the deposited estuarine material into usable land, land reclamation by building protective dikes was carried out. This is a common practice to satisfy the economic expansion in coastal areas. After diking, followed by leaching, the land becomes arable. Parts of the reclaimed land were used for paddy rice, other parts for a variety of non-irrigated crops. The time of dike construction is recorded in the Cixi County Annals written in the first half of the 17th century. The same documents reveal, that the first rice was cultivated in this area between 25 and 27 A.D. (Cheng et al. 2009). These dates, provided by the Chinese partners, were the basis for the determination of duration of cultivation. Depending on the time since diking, a chronosequence of soil formation developed

The soil chronosequence consists of soils formed on the same substrate under comparable conditions of climate, topography and vegetation (Harden 1982). The use of such soil chronosequences for the investigation of rates and direction of soil development is a proven approach (Huggett 1998) revealing changes in soil properties over time. This has been shown for different environments like pasture (Kieft 1994) or marine terraces (Aniku and Singer 1990). Baisden et al. (2002) and Baisden and Parfitt (2007) used chronosequences to document the gradual accumulation of bomb carbon in the subsoil. Reports by Cheng et al. (2009) and Ma et al. (2010) are related to paddy soils. The fact that the soil formation of all our sampled sites started on the same homogeneous estuarine sediment, with a fairly uniform ^{14}C concentration about half that of the atmosphere, provides a unique opportunity to study the establishing of a ^{14}C concentration-depth gradient by uptake and transport of organic carbon (OC) with atmospheric ^{14}C composition.

Methods

In this study, ^{14}C is used as a tracer for the stabilization and turnover of soil organic carbon and not as a dating tool. Thereto we measured the radiocarbon and total organic carbon (TOC) content of bulk soil samples. The soil profiles of the chronosequence, reported here, were excavated in a joint sampling campaign in June 2008. The complete soil horizons

were described by P. Schad and R. Jahn, members of FOR 995, according to FAO (2006). The paddy soil profiles were divided into topsoil and subsoil. Topsoils are represented by puddle layer and plough pan (A-horizons) and obtain average depths between 20 and 25 cm. The subsoils consist of several B-horizons. More detailed information regarding the soil profile description is given by Wissing et al. (2011).

Multiple samples within single soil horizons were taken to reveal gradients in TOC and ^{14}C. A total of 12 soil profiles were sampled up to a depth of 1 m; 7 paddy soil profiles (50, 100, 300, 500, 700, 1000, 2000 years of lowland rice cultivation: P 50 - P 2000) and 5 non-paddy soil sites (50, 100, 300, 500, 700 years of agricultural use without lowland rice: NP 50 - NP 700). In addition different wetland sites and a tidal flat (estuarine sediment) were sampled. The latter represents the parent material from which soils developed in this region. Sites with a non-paddy cultivation history older than 700 years could not be found.

The soil samples were air-dried and sieved through 2 mm mesh size to homogenize the material. Non soil-derived particles as well as identifiable plant residues were removed and kept for further studies. The bulk soil was treated with 4 ml dilute (1 %) hydrochloric acid per gram of soil to remove carbonates and freeze dried without washing. The samples were transferred into pre-combusted quartz tubes, evacuated, subsequently flame sealed and combusted with CuO and silver wool at 900 °C for 4 hours. The resulting CO_2 was reduced to graphite. The ^{14}C measurements were made with the 3 Million Volt HVE Tandetron AMS (accelerator mass spectrometry) system at Leibniz-Laboratory in Kiel (Germany), with a 1-σ precision of about 0.25 pMC (Nadeau et al. 1997). The ^{14}C contents are stated in percent modern carbon (pMC) (Stuiver and Polach 1977).

The initial results for the tidal flat and subsoil samples indicate that the soil profile development of the chronosequence started on a fairly homogeneous estuarine sediment with ca. 0.3 % TOC and a ^{14}C concentration of organic material of ca. 50 pMC. The low ^{14}C value of 50 pMC reflects a large contribution of old reworked organic carbon, transported in the sediments, to the tidal flats. An isotope and mass balance calculation can be used to estimate the contribution of reworked old carbon in tidal flat and subsoils over time and thus the homogeneity of the chronosequence substrate. The initially homogeneous TOC and ^{14}C depth distribution, with a ^{14}C concentration quite different from that of photosynthetic organic matter added by agriculture, is the basis for the

interpretation of the profiles of the chronosequence. For the mass balance calculation we used the following equation:

$$A_s = (A_m (1 - X) + A_e \cdot X) \, e^{-\lambda \cdot t} \qquad \text{(pMC)} \qquad (6)$$

where A_s is the measured ^{14}C content of sediment and subsoil, A_m the ^{14}C content of OC in equilibrium with the atmosphere and, A_e that of the eroded, reworked carbon at the time of sedimentation t (0 for the tidal flat, 2000 for Paddy 2000), X is the percentage of old reworked carbon, and λ the ^{14}C decay constant (1/8267 yr^{-1}).

Results and Discussion

The OC and ^{14}C observed for the first and the last member of the chronosequence, the 50-yr and the 2000-yr profiles, are shown in Figure 3.2 and 3.3, together with the values obtained for the parent material, the tidal flat. After the onset of paddy/non-paddy management, a soil profile rapidly forms. Already after 50 years, the low ^{14}C signature of the tidal flat sediments has been replaced in the top soils by modern ^{14}C values, and OC contents have increased significantly when compared to the parent material.

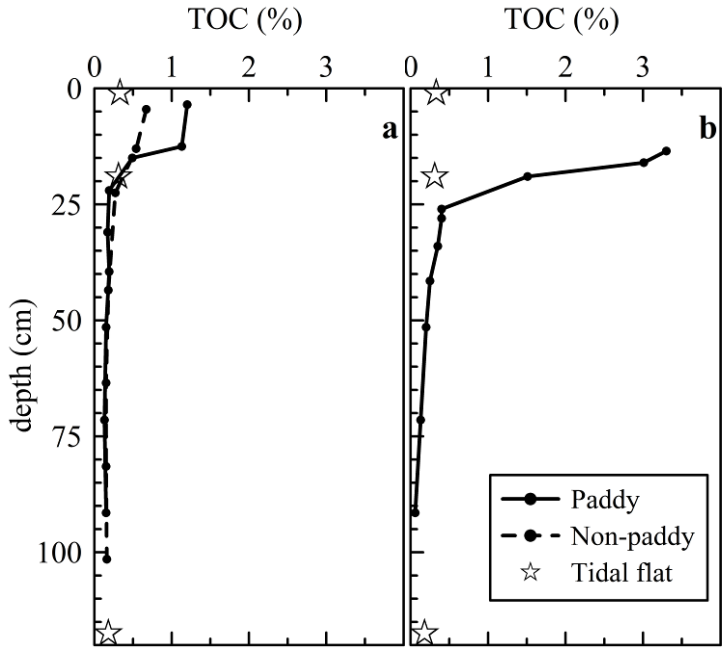

Figure 3.2: TOC content of bulk soil samples from paddy and non-paddy sites with different ages; a (50 years), b (2000 years) and tidal wetland.

The OC increase is more important in the paddy than in the non-paddy (Figure 3.2). Across the low permeability plough pan, which develops in paddy soils due to puddling, we see in the 50-yr paddy a strong decrease in ^{14}C and OC concentrations, with virtually unchanged values of the tidal flat in the subsoil. For the NP 50 profile, the less restricted water transport has already led in the subsoil to slightly increased OC and the establishment of a ^{14}C-depth gradient down to tidal flat values at 80 cm depth.

After 2000 years, the paddy profile also shows a gradual decrease in ^{14}C with increasing depth (Figure 3.3). Other studies observed similar ^{14}C gradients with soil depth (Scharpenseel et al. 1989; Paul et al. 1997) at other sites. Such gradients were, however, generally interpreted as the result of gradual sediment accumulation over time instead of OC transport. The OC values are quite high in the P 2000 topsoil, but drop rapidly in and just below the plough pan. They decrease to below those of the tidal flat below ca. 40 cm, which indicates a loss of organic carbon in the deeper subsoil under paddy management.

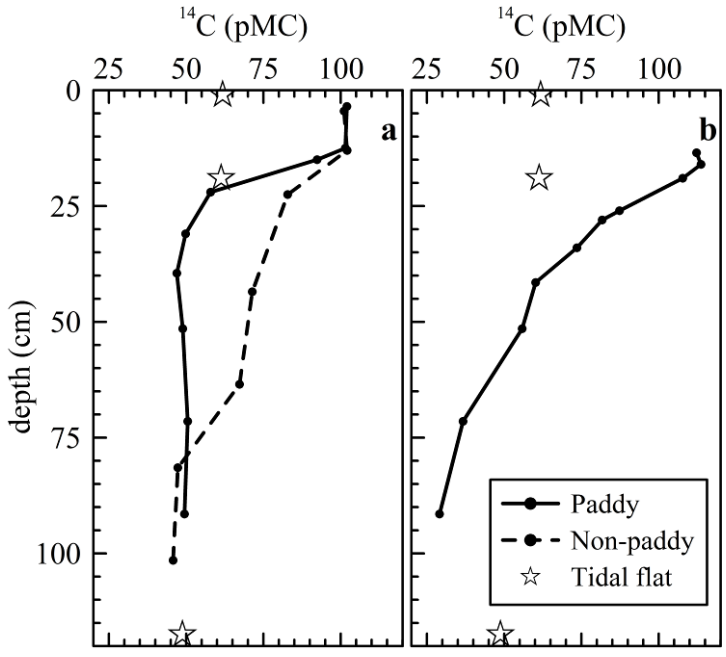

Figure 3.3: Radiocarbon content of bulk soil samples from paddy and non-paddy sites with different ages; a (50 years), b (2000 years) and tidal wetland.

The three tidal flat samples show fairly uniform OC and low ^{14}C values, similar to those in the deeper subsoil of the chronosequence profiles. Considering the large sediment load of the Yangtze River (Milliman et al. 1985; Wang et al. 2008), the relatively stable conditions of sediment production and transport (Yang et al. 2001), and the frequent dike building, it is likely that, for the 2000 years covered by the chronosequence, the time needed to accumulate 1 m of sediment column was relatively short, of the order of a century, compared to the ^{14}C half-life of 5,730 years.

To check the assumed homogeneity of the tidal flat sediments deposited over time, we used Eq. 6 to calculate the admixed fraction of old reworked carbon from the measured ^{14}C concentrations of the three tidal flat samples and the deepest parts of the soil profiles. For the two tidal flat top samples, A_m was assumed to be 120 pMC, the mean ^{14}C concentration of OC in topsoil samples after 1954 (Rethemeyer 2004); for all other samples a value of 100 pMC was chosen. We chose A_e zero, which facilitates calculations and provides the minimum amount of reworked carbon needed. For more realistic mixtures of younger and older eroded material, the reworked fraction increases with increasing A_e. The calculations yield 49 % admixture to the tidal flat surface and 51 % at depth. The P 50 profile gave values from 49 % to 53 % below the plough pan and NP 50 52-54 % at depth. Similar admixtures calculated for other profiles of the chronosequence support our assumption that for each of these at time zero soil development started on a uniform old sediment column, thus providing an ideal substrate to study the effects of management on soil development. The very low radiocarbon content of the total inorganic carbon (TIC) of the tidal flat samples (Table 3.1) indicates around 95 % dead carbonate admixture, which strengthens the argument that the deposited sediment originated from the Chinese inland.

Table 3.1: ^{14}C and C contents of tidal flat samples with standard deviation.

sample	depth (cm)	^{14}C of TOC (pMC)	^{14}C of TIC (pMC)	TOC (%)
tidal flat	0-2	61.78 ± 0.19	7.08 ± 0.08	0.33 ± 0.03
	18-20	61.32 ± 0.21	6.67 ± 0.08	0.31 ± 0.03
	115-120	48.74 ± 0.20	4.93 ± 0.08	0.18 ± 0.02

The difference between paddy and non-paddy sites regarding their ^{14}C depth gradients is caused by the paddy management, which quickly leads to the development of a slightly permeable plough pan. This dense layer works like a barrier, which seriously reduces, but not totally prevents the downward transport of OC. Especially the comparison between P 50 and NP 50 shows this effect very clearly. With increasing time of cultivation, paddy soils show increased ^{14}C contents for the subsoils, signaling an increased penetration of OC with higher ^{14}C values. After 100 years of paddy management, ^{14}C concentrations similar to P 50 values on plough pan level are observed 20 cm below the plough pan. The longer a site is under paddy management the more its ^{14}C depth distribution seems to converge to the ^{14}C depth distribution of a non-paddy site. Thus, a differentiation between paddy and non-paddy soils, by means of their radiocarbon depth gradients, becomes more and more difficult with increasing time of cultivation. Therefore, it can not be excluded that an old paddy soil was used as non-paddy for a short period in its agricultural history. Increasing ^{14}C concentrations in the subsoil at constant or decreasing TOC values document the replacement of original estuarine TOC by OC transported from above (Figure 3.2 and 3.3).

It is thus evident that the observed age-depth profiles for the older members of the chronosequence, with ^{14}C values decreasing with increasing depth, are the result of post depositional transport processes and were not derived by sedimentation over a long time. This emphasizes the importance of (vertical) OC transport for soil organic carbon dynamics. More data are needed to understand the carbon dynamics under paddy management. These are being collected and will indicate the role of plant remains, especially rootlets with their exudates, and DOC for the input of fresh SOC into the subsoil. Several reports brought up the relevance of SOM input into the sub soil by fresh plant remains (Baisden et al. 2002; Baisden and Parfitt 2007; Sanderman et al. 2008).

Conclusions

The chronosequence started on fairly uniform sediments, which were significantly depleted in ^{14}C relative to the atmosphere. Results reveal a ^{14}C-documented replacement of “old” carbon by “modern” carbon over time. Thus, the observed TOC and ^{14}C gradients are the result of OC mobility and relocation instead of accumulation, as usually assumed.

Especially the first decades of paddy management highlight the differences between soil formation under paddy and non-paddy management and accent the reduced transport of OC through the plough pan into the subsoil. Paddy topsoils show a higher TOC content than non-paddies. Yet, the increased accumulation of OC in the topsoil does not inevitably lead to a higher OC content in the paddy subsoil, even after 2000 years of rice cultivation. The OC and ^{14}C depth profiles reflect a dynamic equilibrium between OC import, export, and stabilization on a time scale of decades. At this time it is not yet known, which parts of the OC are responsible for the observed TOC replacement and to which of the functional OC pools they belong.

Acknowledgement

We thank the German Research Foundation (DFG) for funding this project. Furthermore, the authors gratefully acknowledge the support of Prof. Z.-H. Cao (Institute of Soil Science, Chinese Academy of Sciences, Nanjing), who provides the chance to work on the described soil chronosequence. The comments by two reviewers further contributed to the paper.

References

Aniku JRF, Singer MJ. 1990. Pedogenic iron oxide trends in a marine terrace chronosequence. Soil Sci. Soc. Am. J. 54, 147-152.

Baisden WT, Amundson R, Brenner DL, Cook AC, Kendall C, Harden JW. 2002. A multiisotope C and N modeling analysis of soil organic matter turnover and transport as a function of soil depth in a California annual grassland soil chronosequence. Global Biochemical Cycles 16 (4), 8210-8226.

Baisden WT, Parfitt RL. 2007. Bomb ^{14}C enrichment indicates decadal C pool in deep soil. Biogeochemistry 85, 59-68.

Bouman B, Tuong T. 2001. Field water management to save water and increase its productivity in irrigated lowland rice. Agricultural Water Management 49, 11-30.

Cao ZH, Ding JL, Hu ZY, Knicker H, Kögel-Knabner I, Yang LZ, Yin R, Lin XG, Dong YH. 2006. Ancient paddy soils from the Neolithic age in China's Yangtze River Delta. Die Naturwissenschaften 93, 232-6.

Cheng YQ, Yang LZ, Cao ZH, Ci E, Yin S. 2009. Chronosequential changes of selected pedogenic properties in paddy soils as compared with non-paddy soils. Geoderma 151, 31-41.

FAO. 2006. Guidelines for soil description, 4th edition (Publishing Management Service, Information Division, FAO, Rome, 2006), 110 pp.

FAOSTAT (Food and Agricultural Organization of the United Nations). 2011. Online, URL: http://faostat.fao.org/

Frenzel P, Rothfuss F, Conrad R. 1992. Biology and Fertility of Soil Oxygen profiles and methane turnover in a flooded rice microcosm. Biology and Fertility of Soils 14, 84-89.

Harden JW. 1982. A quantitative index of soil development from field descriptions: Examples from a chronosequence in central California. Geoderma 28, 1-28.

Huggett R. 1998. Soil chronosequences, soil development, and soil evolution: a critical review. Catena 32, 155-172.

Kieft TL. 1994. Grazing and plant-canopy effects on semiarid soil microbial biomass and respiration. Biology and Fertility of Soils 18, 155-162.

Liu JP, Xu KH, Li AC, Milliman JD, Velozzi DM, Xiao SB, Yang ZS. 2007. Flux and fate of Yangtze River sediment delivered to the East China Sea. Geomorphology 85, 208-224.

Ma L, Xu R, Jiang J. 2010. Adsorption and desorption of Cu(II) and Pb(II) in paddy soils cultivated for various years in the subtropical China. Journal of Environmental Sciences 22, 689-695.

MacLean JL, Dawe DC, Hardy B, Hettel GP. 2002. Rice Almanac: Source Book for the Most Important Economic Activity on Earth. Wallingford: CABI Publishing. p. 270.

Milliman JD, Huang-Ting S, Zuo-Sheng Y, Meade RH. 1985. Transport and deposition of river sediment in the Changjiang estuary and adjacent continental shelf. Continental Shelf Research 4, 37-45.

Nadeau MJ, Schleicher M, Grootes PM, Erlenkeuser H, Gottdang A, Mous DJW, Sarnthein JM, Willkomm H. 1997. The Leibniz-Labor AMS facility at the Christian-Albrechts University, Kiel, Germany. Nuclear Instruments and Methods in Physics Research B 123, 22-30.

Neue HU, Gaunt J, Wang Z, Becker-Heidmann P, Quijano C. 1997. Carbon in tropical wetlands. Geoderma 79, 163-185.

Paul EA, Follett RF, Leavitt SW, Halvorson A, Petersen GA, Lyon DJ. 1997. Radiocarbon dating for determination of soil organic matter pool sizes and dynamics. Soil Science Society of America Journal 61, 1058-1067.

Rethemeyer J. 2004. Organic carbon transformation in agricultural soils : Radiocarbon analysis of organic matter fractions and biomarker compounds, Thesis CAU Kiel, p.165.

Sanderman J, Baldock J, Amundson R. 2008. Dissolved organic carbon chemistry and dynamics in contrasting forest and grassland soils. Biogeochemistry 89, 181-198.

Scharpenseel HW, Becker-Heidmann P, Neue HU, Tsutsuki K. 1989. Bomb-carbon, ^{14}C-dating and ^{13}C-measurements as tracers of organic matter dynamics as well as of morphogenetic and turbation processes. The Science of the Total Environment 81/82, 99-110.

Sharma PK, De Datta SK, Redulla CA. 1988. Tillage effects on soil physical properties and wetland rice yield. Agronomy Journal 80, 34-39.

Stuiver M, Polach HA. 1977. Discussion: reporting of ^{14}C data. Radiocarbon 19, 355-363.

Wang H, Yang Z, Wang Y, Saito Y, Liu JP. 2008. Reconstruction of sediment flux from the Changjiang (Yangtze River) to the sea since the 1860s. Journal of Hydrology 349, 318-332.

Wissing L, Kölbl A, Vogelsang V, Fu JR, Cao ZH, Kögel-Knabner I. 2011. Organic carbon accumulation in a 2000-year chronosequence of paddy soil evolution. Catena 87, 376-385.

Yang S, Li C, Zhao Q, Yoshiki S, Kazuaki H. 2001. Element geochemistry of Holocene sediment and paleoenvironmental change in the Changjiang Estuary. Science in China (Series B) 44, 40-46.

Zhang M, Lu H, Zhao XJ, Li RA. 2004. A comparative study of soil fertility change of upland soil in Cixi County. Chinese Journal of Soil Science 35, 91-93.

Zong Y, Chen Z, Innes JB, Chen C, Wang Z, Wang H. 2007. Fire and flood management of coastal swamp enabled first rice paddy cultivation in east China. Nature 449, 459-62.

Chapter IV

Origin of subsoil carbon in a Chinese paddy soil chronosequence

Status: Published in Radiocarbon 55 (3-4), xxxx.

Abstract

Rice paddies are highly important agricultural soils in view of their relevance as major staple food provider in the world and their key role in the global carbon cycle, caused by special management practices. A soil chronosequence, consisting of paddy and upland soils, developed on reclaimed estuarine sediments in the Province of Zhejiang, China, was sampled to investigate the influence of duration of agricultural use (50 yrs to 2,000 yrs) on soil composition. The uniform composition of the parent material provides the unique opportunity to compare the effects of different land management practices (paddy and non-paddy) on soil carbon dynamics and the origin of organic carbon (OC) in top- and subsoils, using ^{14}C measurements by accelerator mass spectrometry (AMS). The total soil organic carbon (TOC) was split into chemically defined pools of different mobility, namely the acid and water soluble fulvic acids (FA), the alkali soluble humic acids (HA) and insoluble humin fraction. The more mobile HA and FA fractions contain significantly more ^{14}C than the corresponding TOC and humin, indicating a downward transport of OC in the subsoil. Plant roots with ^{14}C concentrations up to 128 % of the modern standard, found far below the plough pan, reveal plant roots and root exudates as other direct sources of subsoil OC in paddy soils.

Introduction

Rice paddy soils are the most important agricultural soils in the world because (i) Paddy soils provide the staple food for nearly half the world population (MacLean et al. 2002) and (ii) Paddy soils play an important role in the global carbon and methane cycle. Rice is the major crop in the tropics and sub-tropics, whereas China represents the predominant rice producer with about 30 % of the global rice production and 19 % of the total world rice paddy area (FAOSTAT 2010). In the context of mitigating the increase of the atmospheric greenhouse gases CO_2 and CH_4, paddy soils are considered of outstanding importance in view of the high soil organic carbon (SOC) level observed in paddy topsoils, their assumed high C sequestration potential (Pan et al. 2003; Xu et al. 2011), and the amenability of their properties to active management. The larger paddy topsoil SOC stocks, compared to upland soils, are caused by a large carbon input via straw incorporation and/or other organic additions (Tanji et al. 2003; Rui and Zhang 2010). Furthermore, the water logged conditions during flooded phases lead to decreased decomposition rates and enhance the accumulation of SOC (Huang and Sun 2006; Kögel-Knabner et al. 2010).

After the oceans, soils are the largest active pool within the global carbon cycle (Lal 2008). The SOC pool is two times the size of the atmospheric C pool and nearly three times the size of the biotic C pool (Lal 2004). The amount of organic carbon (OC) in the upper 100 cm in the world's soils is estimated to be about 1,550 Pg (1 Pg = 10^{15} g) (Batjes 1996). Since soils are the largest reservoir for C in the terrestrial ecosystem, they play a key role within the global carbon cycle, and SOC dynamics were examined in numerous studies of increasing organic complexity over the past decades (Scharpenseel et al. 1989; Trumbore et al. 1989; Becker-Heidmann and Scharpenseel 1992; Wang et al. 1996; Six et al. 2001; Baisden et al. 2002; Rethemeyer et al. 2005; Dreves et al. 2007; Flessa et al. 2008; Marschner et al. 2008; Laskar et al. 2012).

In many cases only the topsoil (ca. 0-30 cm) of the related soil profile is considered. Although those upper 30 cm contain less than 50 % of the SOC (Jobbagy and Jackson 2000), the organic carbon located in subsoil horizons was assumed to be insignificant within the system of SOC transport and stabilization. Land-use-change related changes in SOC stocks, for example, were assumed to be significant only in topsoils (O'Brien and

Stout 1978; Baisden et al. 2002). The main reason for this point of view is the assumption that subsoil carbon is inert and does not take part in the dynamic interactions between different soil compartments. This is based on very low annual inputs of fresh organic matter and the limited spatial accessibility of subsoil OC for microbial activities and oxygen within the soil profile (Christensen 2001). Furthermore, in view of low ^{14}C activity of subsoil horizons, it is assumed that, with increasing depth, SOC becomes more stabilized and shows longer residence times (Rumpel and Kögel-Knabner 2011).

In the course of the discussion about global warming and the potential of deep soil OC as a sink for CO_2, subsoil OC attracted more attention over the last decade, with more and more reports pointing out the role of subsoil OC within the dynamic system of SOC transport and stabilization (Trumbore 2000; Baisden and Parfitt 2007; Helfrich et al. 2011). Thus, subsoil OC seems to be less inert than commonly assumed, especially with the input of fresh OC in the subsoil priming microbial processes (Fontaine et al. 2007).

Suitable for investigating subsoil OC dynamics under paddy management are the large floodplains in the coastal zone of subtropical China. Paddy and non-paddy soils (upland soils not used for submerged rice cultivation) of different ages, developed on reclaimed estuarine sediments originating from the nearby Yangtze River, were sampled near Cixi in the Province of Zhejiang, China. Previous results of bulk soil samples documented the transport-induced development of TOC and ^{14}C depth gradients in the initially uniform upper 1 m of sediment, and demonstrated a replacement of old organic carbon by young OC by using the radioactive isotope ^{14}C as a tracer (Bräuer et al. 2013). Water is the most likely transport medium, so a simple OC partition in acid/water soluble, alkali/water soluble and water insoluble was chosen to further evaluate OC transport. This is the classical purification scheme of radiocarbon dating, where the insoluble, non-mobile fraction is generally chosen as the most reliable fraction for dating (e.g. Grootes et al. 2004), and closely resembles the classical separation in fulvic acids, humic acids and humin of soil sciences. It serves to demonstrate OC transport by, and dynamic exchange of OC between these fractions without the necessity to define specific processes and their relative importance (e.g. Kleber et al. 2007).

Elevated ^{14}C concentrations, connected with the atmospheric testing of nuclear weapons of the late 1950's and early 1960's, make it possible to demonstrate the presence of

(sub)recent plant remains in the subsoil and the potential of roots and their exudates for introducing fresh OC into deep soil horizons. Identification of rice DNA in root material at 1 m depth in a paddy soil further documents rice root penetration deep below the plough pan. We here use ^{14}C concentrations of plant remains and of SOC fractions, characterized by different stability and mobility, to reveal the pathways of dynamic relocation of SOC into the subsoil and show that, despite the decoupling between topsoil and subsoil regarding OC accumulation (Wissing et al. 2011), subsoil OC dynamics, is important for understanding the role of soils in the global carbon cycle.

Methods

Study sites and soil sampling

The study sites belong to one of the oldest paddy soil regions in the world (Cao et al. 2006). The soil samples were taken near the southern coast of Hangzhou Bay around Cixi, Zhejiang Province, China (Fig. 4.1). With a mean annual temperature of 16.3°C and a mean precipitation of 1,325 mm per year the climate is classified as subtropical with periodical monsoon rain (Cheng et al. 2009). Estuarine sediment, which originates from the Yangtze River, represents the parent material of the study sites. Over the past centuries protective dikes were built to establish arable land. This led to the development of differently aged soils formed on the same substrate under comparable conditions of climate, topography and vegetation – the development of a soil chronosequence (Harden 1982). This circumstance allows us to study the uptake and relocation of OC with atmospheric ^{14}C composition on comparable sites established at different times. More detailed information about the study area and the historical development of the differently aged soils is given by Cheng et al. (2009) and Kalbitz et al. (2013).

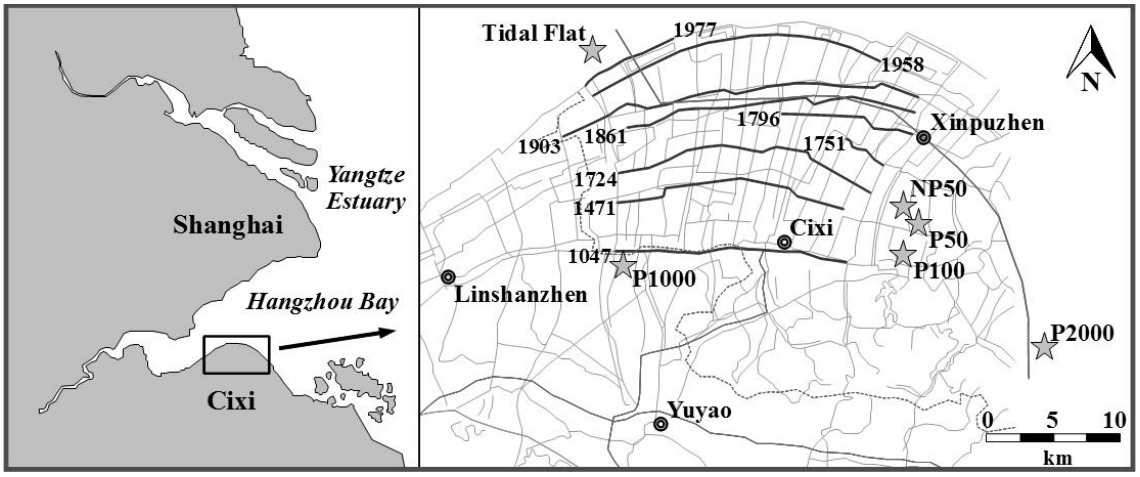

Figure 4.1: Geographical locations of the sampling sites at the south coast of Hangzhou Bay. To reclaim arable land protective dikes, partly indicated by heavy black lines, were built. Years of dike construction are given next to the dike lines. Stars represent the position of sampling points (P 50, NP 50, P 100, P 1,000, P 2,000-year old soil profiles and tidal flat).

Soil horizons were described by the FAO Guidelines for Soil Description (FAO 2006) and classified according to IUSS Working group WRB (2007). Paddy soil profiles were divided into topsoil and subsoil. Topsoils are represented by puddle layer and plough pan (A-horizons) and obtain average depths between 20 and 25 cm. The subsoils consist of several B-horizons. More detailed information regarding the soil profile description is given by Wissing et al. (2011). In addition to paddy (P) and non-paddy (NP) soils with different ages (50 yrs and 2,000 yrs), tidal flat samples (estuarine sediment) were taken. The latter represent the parent material from which soils developed in this region.

Sample preparation

All soil samples were air-dried and sieved through 2 mm mesh size to homogenize the material. Non soil-derived particles as well as identifiable plant residues were removed and kept for further studies.

Chemical Extraction

Soil samples were treated with 4 ml dilute (1 %) hydrochloric acid (HCl) per gram of soil to remove carbonates, and freeze dried without washing to determine their TOC content and TOC ^{14}C concentration. Furthermore, tidal flat, 50 years and 2,000 years old soil samples underwent chemical fractionation by acid-alkali-acid extraction (AAA). AAA in air is a standard method in radiocarbon dating to remove contaminating carbon from organic samples (charcoal, plant remains etc.) prior to ^{14}C measurements (Grootes et al. 2004). The application of AAA is similar to the classical humus fractionation procedure according to Stevenson (1994), resulting in three fractions: the acid soluble fulvic acid (FA), the alkali soluble humic acid (HA) and the insoluble humin fraction (alkali residue).

Dried soil samples were treated with diluted (1 %) HCl for > 10 hours to remove carbonates. The yellowish supernatant, containing acid-soluble compounds (FA), was separated. The pellet was washed with Milli-Q® water until pH > 4 to remove the hydrochloric acid and dissolved contaminants. Samples were then extracted with 1 % NaOH for 4 hours at 60°C. This yields an alkali-soluble fraction and a non-soluble residue (humin). Humic acids were precipitated from the alkaline solution by acidification with 37 % HCl down to a pH < 1 and washed till pH > 4 as above. In several cases the supernatant was kept to recover acid-soluble FA's. The insoluble residue (humin fraction) was washed with Milli-Q® water until pH < 10. To remove any atmospheric CO_2 introduced during the alkali treatment, the humin fraction was again treated with 1 % HCl and washed till pH > 4. All extracts, fulvic acids, humic acids and humin fractions were freeze-dried.

Macro-fossils (plant remains, roots)

To obtain identifiable macro-fossils water was added to large soil samples (ca. 5 kg) and plant remains were separated by elutriation and sieving (400 µm mesh size). The sieved material was inspected under a microscope and non-plant components (stones, shells etc.) were removed. Selected plant samples were subjected to the AAA treatment described above.

Isolation of genomic DNA and 18S rDNA analysis

To test whether rice plants roots reach below the plough pan, root material found at depth was tested for rice DNA by Dr. Nancy Weiland-Bräuer at the Institute of Microbiology, Christian-Albrechts Universität zu Kiel (CAU). Twenty samples of root material were used for genomic DNA extraction according to Doyle and Doyle (1987) with modifications. Plant parts (300 mg) were resuspended in CTAB buffer (140 mM sorbitol, 220 mM Tris[1], 22 mM EDTA[2], 800 mM NaCl, 1 % sarkosyl, 0.8 % CTAB[3], pH 8.0) and glass beads of 0.1 mm, 0.5 mm and 2.5 mm size were added prior to the mechanical cell disruption for 9 min. at 1,300 strokes/min (GenoGrinder®; BT&C/OPS Diagnostics, Bridgewater/USA). Chloroform extraction of the supernatant was performed followed by precipitation of the nucleic acids with isopropanol (0.7 vol) for 20 min. at room temperature and subsequent centrifugation for 1 h at 16,000 × *g* and 4°C. The DNA precipitate was washed twice with 70 % ethanol and resuspended in 15 µL Tris-EDTA buffer (10 mM Tris, 1 mM EDTA, pH 8.0).

18S rDNA gene fragments were amplified in a standard PCR (polymerase chain reaction) using 50 ng isolated genomic DNA, *GoTaq*® polymerase (Promega, Mannheim/Germany) and primer set 18S_FW (5'-AGGAATTGACGGAAGGGCAC-3') and 18S_RV (5'-GGACATCTAAGGGCATCACA-3') (Luan et al. 2005). Reaction mixtures were incubated in a PT-100 thermal cycler® (MJ Research Inc., Waltham/USA) at 94°C for 5 min., followed by 30 cycles at 94°C for 30 sec., 50°C for 45 sec., and 72°C for 30 sec. resulting in a 324 bp PCR fragment. DNA sequences of PCR products were determined completely by the sequencing facility at the Institute of Clinical Molecular Biology, CAU (IKM). Sequences were compared to available databases using BLAST (Basic Local Alignment Search Tool) network service (Altschul 1990) to determine their approximate phylogenetic affiliations.

Sample treatment for AMS

After freeze-drying, sample aliquots were transferred into pre-combusted (4 hours, 900°C) quartz tubes, evacuated, subsequently flame sealed, and combusted with CuO (450 mg) and silver wool (150 mg) at 900°C for 4 hours. The resulting CO_2 was reduced to graphite

with H_2 at 600°C over an iron catalyst. The ^{14}C measurements were made with the 3 Million Volt HVE Tandetron AMS (accelerator mass spectrometry) system at the Leibniz-Laboratory in Kiel (Germany), with a 1-σ precision of about 0.25 pMC (Nadeau et al. 1997, 1998).

Radiocarbon values are stated in percent modern carbon (pMC) and were calculated from the measured $^{14}C/^{12}C$ ratios of the sample and the oxalic acid standard according to Stuiver and Polach (1977).

Results and discussion

Depth gradients of ^{14}C in chemical soil organic matter (SOM) fractions

The ^{14}C concentrations of TOC (Bräuer et al. 2013) and the three corresponding chemical fractions humin, humic acid, and fulvic acid are given as function of depth for the 50 years old paddy (P50) and non-paddy soil (NP50) and the 2,000 years old paddy soil (P2000) in Figures 4.2a-c and Table 1, together with the values obtained for the sediment of the tidal flat. The results clearly show the age inhomogeneity of the TOC, with the insoluble humin fraction consistently older, and the more mobile humic acids younger than TOC. The measured fulvic acids have, with one exception, a higher ^{14}C concentration than the humic acids. In P50, the striking drop in ^{14}C concentration across the plough pan (horizon Ardp), already observed for TOC (Bräuer et al. 2013), is also seen in the chemical fractions (Figure 4.2a). The development of their ^{14}C concentrations with depth is very similar. The NP50 shows a more or less constant decrease in ^{14}C with depth for all SOC fractions, comparable to ^{14}C gradients reported by Scharpenseel et al. (1989) and Paul et al. (1997). Thus, the decoupling of topsoil from subsoil by plough pan development under rice paddy management clearly affects all SOC fractions in the subsoil and delays the buildup of the customary ^{14}C - or “age” -depth profile beyond 50 years. After 2,000 years such a profile is also found in the paddy subsoil (Fig. 4.2c).

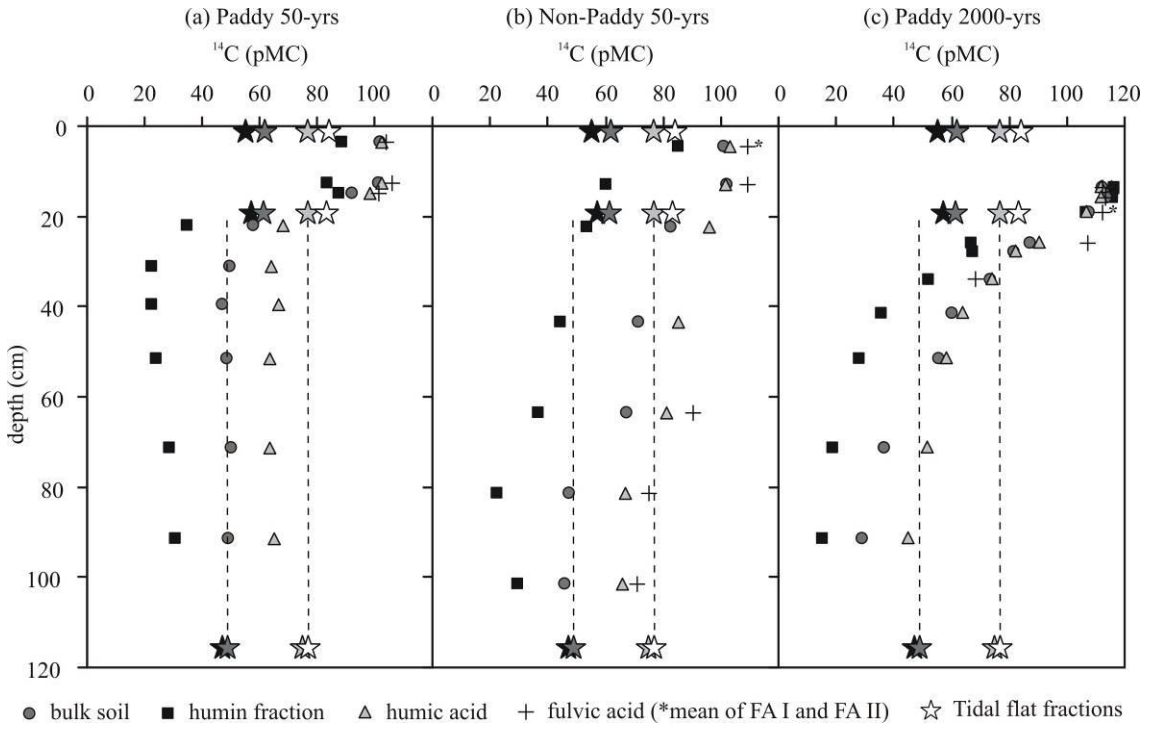

Figure 4.2: ^{14}C concentrations of bulk soil samples and the corresponding SOM fractions (humin, humic acid, fulvic acid) for P50, NP50 and P2000. The stars display ^{14}C concentrations of the parent material, represented by tidal flat samples from depths of 0-2 cm, 18-20 cm and 115-120 cm (black: humin fraction; dark grey: bulk soil; light grey: humic acid and white: fulvic acid). ^{14}C measurement uncertainties are smaller than the symbol sizes.

After 50 years of cultivation, bulk soil samples from the topsoil of both paddy and non-paddy gave ^{14}C contents above 100 pMC, close to the atmospheric $^{14}CO_2$ level (105 pMC) in 2008, the year of sampling (Levin et al. 2010; Graven et al. 2012). This indicates that, already after 50 years, a high proportion of the original OC of the tidal flat sediments, with about 61 pMC, had been replaced with OC derived from recent atmospheric photosynthesis products. Both, P50 and NP50 topsoils show comparable radiocarbon concentrations for all SOC fractions. The humin fraction, with ^{14}C values around 85 pMC, still clearly shows the influence of the original OC. The rapid ^{14}C increase in this relatively stable fraction may be due more to the increase in TOC and humin OC in the paddy topsoil than to replacement. All topsoil fractions of P2000 are characterized by ^{14}C values significantly higher than those of the P50 and NP50 sites (Table 4.1).

The high ^{14}C and TOC values can be assigned to the accumulation of plant-derived carbon during the last several decades. Interestingly, the humin fraction, which is assumed to be the most stable part of SOC, shows the highest modern ^{14}C concentrations within the uppermost 15 cm (116.4 pMC in horizon Alp). These values, which exceed the atmospheric radiocarbon level in 2008, indicate the contribution of OC from the last 40 to 50 years (average $^{14}CO_2$ = 116.6 pMC in 1989). The ^{14}C concentrations of the humic and fulvic acids in the P2000 topsoil, (slightly) below those of the TOC, though still well above the atmosphere of 2008, suggest these derive on average from more recent decomposition of organic material.

The observed decrease in ^{14}C in the humin fraction with increasing soil depth is commonly observed and has been interpreted in previous reports by Balesdent (1987), Pessenda et al. (2001), and Rethemeyer et al. (2005) as aging and a relative increase of recalcitrant organic compounds in the humin fraction (Rice 2001). Yet, in the case of this chronosequence, it documents the replacement of the original estuarine OC by younger components moving down the soil profile, presumably as DOC, and then becoming incorporated in the humin fraction. Right below the P2000 plough pan with 116 pMC the humin fraction shows 67 pMC, already indicating mostly aged, recalcitrant SOC with an apparent age of ca. 3,000 ^{14}C years, yet almost 20 pMC enriched in ^{14}C compared to the original estuarine sediments of the tidal flat.

The humin fraction shows ^{14}C contents lower than those of the initial tidal flat sediment at depth in all profiles (Fig. 3.2). The decrease is too large to be caused by natural decay, even in 2,000 years, which would reduce the 47.6 pMC of the deep tidal flat to 37.4 pMC. Instead, the low ^{14}C concentrations of the deep humin fractions may reflect the effect of a supply of fresh OC to a subsoil containing a mixture of organic material, in part old, reworked, and in part contemporaneous with the time of sedimentation (Bräuer et al. 2013). With measured ^{14}C concentrations in the deep tidal flat close to 50 pMC, the contemporaneous fraction must be at least 50 % of the bulk and humin OC. The values close to 23 pMC at 30 to 40 cm in P50, and around 80 cm in NP50, as well as the values below 20 pMC in P2000 below 70 cm (Table 4.1), indicate only 23 % or less ‘young’ OC remained in these humin fractions, which means that 65 % or more of the younger components of the estuarine OC mixture were preferentially degraded and lost. Interestingly, in P50, where the ploughpan still has blocked most of the downward

transport of OC, the minimum ^{14}C concentration is found closely below this ploughpan, while in NP50 and P2000 minimum concentrations are found at depth, near the groundwater table. This suggests a relatively rapid preferential degradation of younger OC stimulated by a supply of fresh OC ('priming') and a gradual buildup of more recalcitrant young OC. The ca. 50 pMC still found at depth in the tidal flat may then reflect absence of vegetation and anoxic conditions.

The extracted FA's differ in ^{14}C concentration from the humic acids and the humin, and show small, yet significant differences before and after alkali treatment. In the P2000 topsoil the ^{14}C of all FA's is above that of the 2008 atmosphere (105 pMC, Levin et al. 2010; Graven et al. 2012), in NP50 this is only true for FA II, while in P50 only one FA II exceeds the atmosphere. With the exception of the Bdg horizon at 26 cm in P2000, the FA's in the subsoil have a ^{14}C concentration below 100 pMC. In the P2000 topsoil, the ^{14}C in FA II is higher than in FA I at 13.5 and 16 cm depth (Table 4.1) and closer to the humin fraction from which it was separated. At 19 cm FA II has less ^{14}C than FA I and, thus, is again closer to the humin fraction. This apparent link between FA II and the humin fraction seems broken in the NP50 topsoil, where FA II shows a ^{14}C concentration well above that of the 2008 atmosphere, although all other fractions are below it. This seemingly erratic pattern may be ascribed to the diverse components of the organic mixture. The starting material was a mixture of old, reworked OC and young OC with a ^{14}C concentration, presumably, close to 100 pMC, to which plant material was added over the years with ^{14}C concentrations increasing irregularly from 98 pMC in 1954 to ca. 180 pMC in 1964 and then gradually dropping to 105 pMC in 2008 (Levin et al. 2010; Graven et al. 2012). This is reflected in the high pMC values of the humin fraction in the P2000 topsoil, indicating OC on average a few decades old with high bomb-^{14}C concentrations. The FA I fraction is fairly small (Fig. 4.3) and contains readily accessible and exchangeable components (Kleber et al. 2007) with a ^{14}C closer to the recent atmosphere.

Table 4.1: Organic carbon content and radiocarbon concentration given as percent modern carbon (pMC) of bulk soil samples and SOM fractions from four sampling sites with different times of duration (50 yrs; 2,000 yrs; recent tidal flat) and different types of land use (Paddy = lowland rice cultivation; Non-Paddy = upland crops; Tidal Flat).

				bulk soil			humin fraction			humic acid			fulvic acid (FA I)			fulvic acid (FA II)		
Sample ID	**Sample site**	**Depth** (cm)	**Horizon**	**^{14}C** (pMC)	±	**C_{org}** (%)	**^{14}C** (pMC)	±	**C_{org}** (%)	**^{14}C** (pMC)	±	**C_{org}** (%)	**^{14}C** (pMC)	±	**C_{org}** (%)	**^{14}C** (pMC)	±	**C_{org}** (%)
KIA 41465	paddy 50	3.5	Alp	101.99	0.43	1.20	88.72	0.27	0.43	102.71	0.29	57.30	N/A	N/A	N/A	103.99	0.31	1.89
KIA 39160		12.5	Arp	101.48	0.25	1.13	83.72	0.25	0.31	102.71	0.26	24.86	N/A	N/A	N/A	106.17	0.36	0.52
KIA 39161		15	Ardp	92.36	0.25	0.49	87.61	0.31	0.17	98.38	0.23	25.36	N/A	N/A	N/A	101.54	0.57	0.12
KIA 39162		22	Ardp	57.92	0.25	0.19	34.72	0.22	0.09	68.17	0.22	10.18	N/A	N/A	N/A	N/A	N/A	N/A
KIA 39163		31	Bwg1	49.81	0.25	0.17	22.42	0.18	0.07	64.06	0.23	8.31	N/A	N/A	N/A	N/A	N/A	N/A
KIA 39164		39.5	Bwg2	46.98	0.25	0.19	22.60	0.19	0.08	66.64	0.24	8.00	N/A	N/A	N/A	N/A	N/A	N/A
KIA 39165		51.5	Bwg3	48.87	0.25	0.15	24.34	0.23	0.07	63.50	0.28	9.48	N/A	N/A	N/A	N/A	N/A	N/A
KIA 39166		71.5	Blg	50.48	0.25	0.13	28.71	0.21	0.07	63.55	0.31	9.05	N/A	N/A	N/A	N/A	N/A	N/A
KIA 39167		91.5	Blg	49.42	0.25	0.15	30.70	0.21	0.09	65.26	0.30	9.85	N/A	N/A	N/A	N/A	N/A	N/A
KIA 41466	non-paddy 50	4.5	Ap	101.07	0.25	0.67	85.30	0.28	0.22	103.20	0.29	47.39	104.72	0.56	0.21	109.32	0.30	1.19
KIA 41467		13	ABw	102.06	0.25	0.54	60.23	0.28	0.11	101.85	0.34	36.52	N/A	N/A	N/A	109.42	0.30	0.97
KIA 39481		22.5	Bw	82.86	0.25	0.27	53.79	0.23	0.10	96.14	0.32	9.34	N/A	N/A	N/A	N/A	N/A	N/A
KIA 39482		43.5	BCg	71.39	0.25	0.18	44.26	0.54	0.08	85.30	0.35	13.50	N/A	N/A	N/A	N/A	N/A	N/A
KIA 39483		63.5	CBg	67.29	0.25	0.15	36.95	0.24	0.08	80.97	0.28	12.62	90.22	0.70	0.08	N/A	N/A	N/A
KIA 39484		81.5	CBlg	47.30	0.25	0.15	22.61	0.21	0.09	67.08	0.30	12.04	75.01	0.93	0.05	N/A	N/A	N/A
KIA 39485		101.5	CBlg	45.75	0.25	0.16	29.58	0.23	0.07	65.82	0.26	10.04	71.00	1.18	0.05	N/A	N/A	N/A
KIA 39171	paddy 2000	13.5	Alp	112.25	0.25	3.30	116.42	0.32	1.35	111.70	0.29	32.14	112.14	0.43	3.79	114.18	0.45	1.85
KIA 39986		16	Ar(d)p	113.67	0.25	3.01	116.01	0.31	1.46	111.96	0.35	8.32	113.48	0.38	2.70	114.61	0.29	1.55
KIA 39987		19	Ar(d)p	107.74	0.25	1.51	106.82	0.37	0.75	106.73	0.38	13.66	112.23	0.36	1.47	109.49	0.31	0.94
KIA 39988		26	Bdg	87.32	0.25	0.40	67.05	0.34	0.09	90.14	0.32	8.73	107.11	0.66	0.26	N/A	N/A	N/A
KIA 39989		28	2Ahgb	81.73	0.25	0.43	67.24	0.26	0.10	82.14	0.32	6.33	N/A	N/A	N/A	N/A	N/A	N/A
KIA 39990		34	2Ahgb	73.54	0.25	0.35	52.32	0.24	0.10	74.21	0.35	6.38	68.09	0.44	0.21	N/A	N/A	N/A
KIA 39991		41.5	2Bg1	60.18	0.25	0.24	35.59	0.21	0.09	63.77	0.34	6.63	N/A	N/A	N/A	N/A	N/A	N/A
KIA 39992		51.5	2Bg2	55.85	0.25	0.20	28.03	0.20	0.08	58.43	0.27	6.06	N/A	N/A	N/A	N/A	N/A	N/A
KIA 39993		71.5	2Blg	36.70	0.25	0.13	18.74	0.23	0.06	51.35	0.28	5.64	N/A	N/A	N/A	N/A	N/A	N/A
KIA 39994		91.5	2Blg	29.08	0.25	0.06	15.20	0.25	0.05	44.87	0.57	2.73	N/A	N/A	N/A	N/A	N/A	N/A
KIA 39997	Tidal flat	1	N/A	61.78	0.25	0.33	55.12	0.21	0.10	76.62	0.24	19.49	N/A	N/A	N/A	84.12	0.31	0.25
KIA 39998		19	N/A	61.32	0.25	0.31	57.00	0.22	0.12	76.69	0.25	22.94	N/A	N/A	N/A	83.29	0.33	0.17
KIA 39913		117.5	N/A	48.74	0.25	0.18	47.66	0.32	0.12	76.05	0.30	11.61	75.01	1.03	0.04	N/A	N/A	N/A

FA I: fulvic acid after first acid treatment and carbonate removal
FA II: fulvic acid after alkali treatment and humic acid precipitation

Relative importance of mobile fractions

The relative contributions of the SOC fractions to the TOC are given in Figure 4.3. As described under Methods, the humin fraction is what remains after acid-alkali-acid extraction. The humic acid fraction is precipitated from the alkali extract with acid and washed until free of acid and soluble organic compounds. Quantification of the humic acids and the humins generally yields calculated fulvic acid (FA) contents as the difference with TOC (Figure 4.3). Direct recovery of the complete fulvic acid fraction is difficult, since it requires collection of all water used in the various washings. In a number of cases, fulvic acids were recovered by freeze-drying the first acid extract (FA I) and the acid supernatant after precipitation of the humic acid fraction from the alkali extract (FA II).

For practical reasons the subsequent, ever more diluted washings were not included. The isolated fulvic acids thus represent only a fraction of the TOC not accounted for by the humin and humic acid fractions (10 to 50 % for FA I plus FA II, Figure 4.3). The missing material was assigned to the fulvic acid fraction, although it may include some fine colloidal material, which chemically does not belong to the fulvic acids. Interestingly, FA II generally contains more OC than FA I. While slightly acidic water can mobilize only a small fraction of the available SOC, as generally observed, the four hours of alkaline extraction at 60°C apparently loosens chemically bound compounds (e.g. Kleber et al. 2007), many of them belonging to the fulvic acid fraction, that were resisting the acidic solution.

With an average contribution of close to 50 % of the TOC, the so-defined FA's constitute the main SOC fraction in each profile. The average contribution of the humic acid fraction is less than 20 % for all soil profiles, while the humin fraction represents ca. 30 % of the TOC. The importance of the insoluble humin fraction increases with increasing depth (Figure 4.3), up to 47 % of TOC at depth in P50 and 67 % in P2000, but only 36 % in NP50. Since both TOC and the humin fraction decrease strongly with depth, especially from plough pan to subsoil (e.g. Table 4.1, TOC from ca. 1.2 % C in the P50 topsoil to 0.14 % C at depth, from 3.3 % C in the P2000 topsoil to ca.0.1 % at depth), this relative increase reflects a very strong decrease in the more mobile fractions, especially in the FA's, in the subsoil. The TOC in the deeper subsoil is more or less the same in all three profiles (P50, NP50 and P2000) and similar to, or slightly lower than that in the deep tidal

flat. The same is true for the three humin fractions, which are, however, reduced relative to the tidal flat. The carbon mass balance thus provides the picture of strongly decreasing mobile components and little change in the subsoil that led to the neglect of subsoil processes.

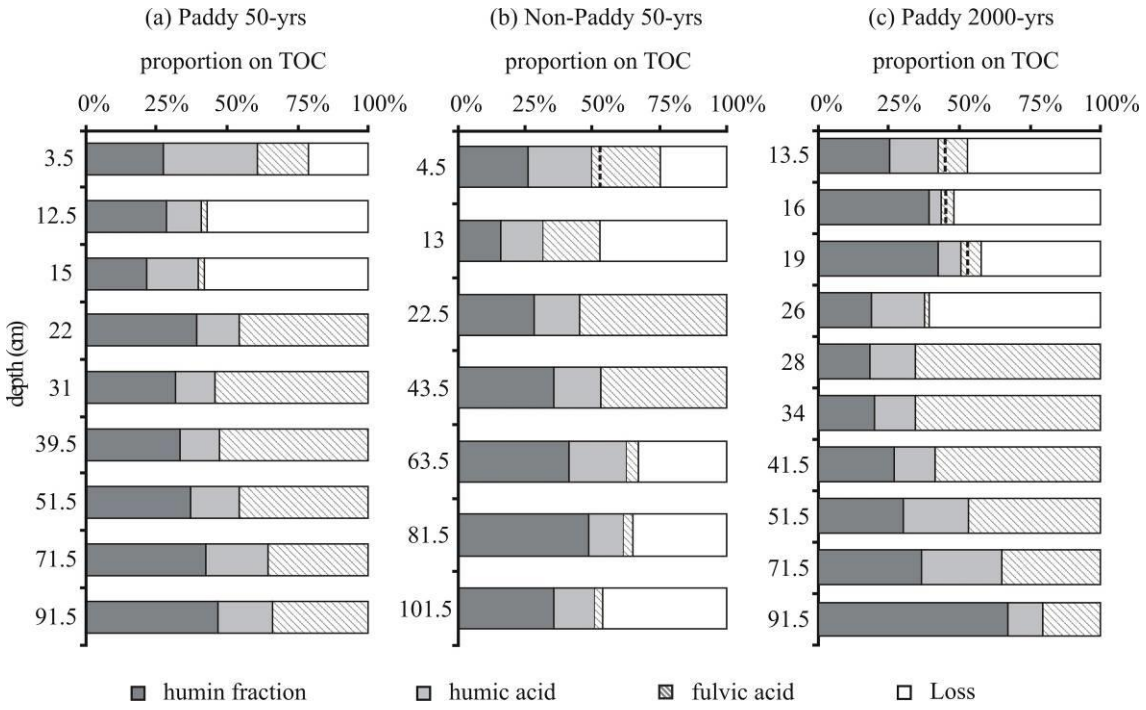

Figure 4.3: The proportions of single SOM fractions on the total organic carbon (TOC) given in percent. Quantification of humic acids and humin fraction yields fulvic acids (FA) as difference with TOC. The FA of samples without a stated loss was calculated from the TOC, humin and HA fraction amounts and not isolated. The mass balance for samples, from which FA's were extracted for ^{14}C measurement, is incomplete due to material loss during wet chemistry sample preparation. In cases where both FA fractions, before (FA I) and after alkali treatment (FA II), were recovered FA II always delivers proportions on TOC at least two times (max. 6x) higher than FA I.

The buildup of ^{14}C concentration profiles in the originally homogeneous, ^{14}C-depleted sediment of the subsoil documents, however, the downward transport of SOC, presumably as dissolved organic carbon (DOC), with infiltrating water. FA's are of major importance for this transport of OC through the soil profile as indicated by their high proportion, especially within the transition zone from plough pan to subsoil. Maie et al. (2004) reported chemical characteristics of FA's leached from the plough layer of a paddy soil,

where the FA fraction was up to 56 % of the OC. The liberation of FA's by alkali extraction and the parallel behavior of the ^{14}C-depth curves for humins, humic acids, and fulvic acids (Figure 4.2) suggest a dynamic exchange between these three SOC fractions and a likely role of the mobile FA and HA fractions as main driver for the described refreshment of SOC pools below plough pan level by organic matter with younger ^{14}C signature.

Plant remains - another pathway of OC transport into subsoil

In addition to visual methods, molecular biological methods were applied to identify plant remains found deep in soil profiles. This is particularly useful when only parts of plants are available. The characterization is based on isolation of genomic plant DNA and subsequent amplification of the 18S rDNA fragment with specific primers in a PCR. Plant remains recovered by wet sieving from all depths of the soil profiles were differentiated by morphological means. Most of these plant-derived macrofossils were found in the topsoil of each profile. The assemblage consists of seeds, spelts and grains of several species like millet, wheat, barley or rice. Furthermore, straw, rice hulls, roots and charcoals were found. Collecting such plant remains below the plough pan was more difficult due to their rare occurrence. Most of the plant remains found in deep soil horizons could be identified visually only as roots or rather root remains and root mats. Thus, classification into a species by visual means was not possible. DNA extraction and analysis identified one out of twenty root samples as rice (*Oryza sativa*) indicating rice root penetration below the plough pan to a surprising depth of 97-100 cm (Table 4.2).

Rice is often described as a shallow-rooting crop with roots mostly located above the plough pan, which restricts deep-rooting growth (Wade et al. 1999). Yet, Mishra et al. (1997) reported a maximum rooting depth between 55 cm and 65 cm, depending on water table conditions. The rooting depth is assumed to be influenced by the prevalent water regime, so dry-land varieties are characterized by deeper rooting depths, while submerged rice plant varieties tend to be shallow-rooted (Yoshida and Hasegawa 1982). Soil cracks that develop when the soil dries out facilitate root penetration below the plough pan. Thus, the presence of roots, including those of rice, is not totally unexpected and indicates that young carbon may be inserted directly into the subsoil as root material and root exudates.

Table 4.2: Radiocarbon and organic carbon contents of plant remains (roots and root mats) selected from deep subsoil horizons of different aged paddy soils. The table includes also ^{14}C data of plant remains of 100 yrs and 1,000 yrs old paddy soils. No data are available for the P2000 soil profile. The presented data belong to the samples which were used for DNA analysis.

Sample ID	**Sample site**	**Horizon**	**sampled depth** (cm)	**^{14}C** (pMC)	±	**C_{org}** (%)
KIA 39164	Paddy 50	Bwg2	38-41	112.08	0.47	52.34
KIA 39166	Paddy 50	Blg	70-73	119.57	1.03	48.44
KIA 40291	Paddy 100	Bwlg1	72-75	110.08	0.46	37.11
KIA 40292*	Paddy 100	Bwlg2	97-100	127.57	0.75	41.88
KIA 40324	Paddy 1000	3Bl	107-110	118.34	0.33	49.28

* This is the only sample, which could be identified as rice (*Oryza sativa*).

Although the roots formed a root mat, it cannot be excluded that plant and root remains were relocated down by bioturbation, since canals and holes of up to several mm diameter as well as living earthworms as indicators for bioturbation activity were observed during sampling across the entire soil profile. Recent studies identified such macropore systems as flow paths and therefore revealed crack and root channels as well as earthworm burrows as responsible for water loss and solute leaching (Janssen and Lennartz 2008; Lennartz et al. 2009).

Conclusions

Soil profiles from a chronosequence of plots under paddy and non-paddy management formed on the same uniform ^{14}C depleted estuarine sediments reveal the rapid development of ^{14}C and TOC gradients in the subsoil as a result of organic carbon mobility and relocation. Processes of subsoil "OC-refreshing" indicated by radiocarbon concentrations are:

1. Direct input of fresh (modern) SOC into deep subsoil by plant roots and their exudates. This process is evident by roots and root remains, including rice roots identified by their DNA signature, with modern ^{14}C signature found far below the plough pan in deep soil horizons.

2. Relocation and transport of young OC through the plough pan via mobile SOC fractions (humic acids and fulvic acids). Due to their high proportion on total organic carbon, we assume fulvic acids to be the main driver for the input of OC through the plough pan into the subsoil.

3. Downward movement of plant remains into the subsoil through animal activity and soil cracking.

Despite this input of fresh organic material, OC concentrations in the subsoil remain largely constant over the chronosequence, while the ^{14}C concentration increases. The composition of subsoil OC down to the 1 m depth of this investigation is thus determined by a dynamic equilibrium between the import of fresh OC, mineralization, and export into groundwater and deeper subsoil.

Acknowledgement

We thank the German Research Foundation (DFG) for funding this project as part of the Research Unit 995 “Biogeochemistry of Paddy Soil Evolution”. The authors also gratefully acknowledge the support of Prof. Z.-H. Cao (Institute of Soil Science, Chinese Academy of Sciences, Nanjing), who provided the chance to work on the described soil chronosequence and the assistance in the analyses of the team of the Leibniz-Laboratory. Furthermore, we thank Dr. Nancy Weiland-Bräuer (Institute of Microbiology, CAU Kiel) for her support during sample DNA preparation and sequencing, and a reviewer for constructive comments.

References

Altschul S, Gish W, Miller W, Myers E, Lipman D. 1990. Basic local alignment search tool. Journal of Molecular Biology 215 (3), 403-410.

Balesdent J. 1987. The turnover of soil organic fractions estimated by radiocarbon dating. The Science of the Total Environment 62, 405-408.

Baisden WT, Amundson R, Brenner DL, Cook AC, Kendall C, Harden JW. 2002. A multiisotope C and N modeling analysis of soil organic matter turnover and transport as a function of soil depth in a California annual grassland soil chronosequence. Global Biochemical Cycles 16 (4), 8210-8226.

Baisden WT, Parfitt RL. 2007. Bomb ^{14}C enrichment indicates decadal C pool in deep soil. Biogeochemistry 85, 59-68.

Batjes, NH. 1996. Total carbon and nitrogen in the soils of the world. European Journal of Soil Science 47, 151-163.

Becker-Heidmann P, Scharpenseel HW. 1992. Studies of soil organic matter dynamics using natural carbon isotopes. The Science of the Total Environment 117/118, 305-312.

Bräuer T, Grootes PM, Nadeau MJ, Andersen N. 2013. Downward carbon transport in a 2000-year rice paddy soil chronosequence traced by radiocarbon measurements. Nuclear Instruments and Methods in Physics Research B 294, 584-587.

Cao ZH, Ding JL, Hu ZY, Knicker H, Kögel-Knabner I, Yang LZ, Yin R, Lin XG, Dong YH. 2006. Ancient paddy soils from the Neolithic age in China's Yangtze River Delta. Naturwissenschaften 93 (5), 232-236.

Cheng YQ, Yang LZ, Cao ZH, Yin S, 2009. Chronosequential changes of selected pedogenic properties in paddy soils as compared with non-paddy soils. Geoderma 151, 31-41.

Christensen BT. 2001. Physical fractionation of soil and structural and functional complexity in organic matter turnover. European Journal of Soil Science 52, 345-353.

Dai J, Ran W, Xing B, Gu M, Wang L. 2006. Characterization of fulvic acid fractions obtained by sequential extractions with pH buffers, water, and ethanol from paddy soils. Geoderma 135, 284-295.

Doyle JJ, Doyle JL. 1987. A rapid DNA isolation procedure for small quantities of fresh leaf tissue. Phytochemistry Bulletin 19, 11-15.

Dreves A, Andersen N, Grootes PM, Nadeau M-J, Garbe-Schönberg CD. 2007. Colloidal matter in water extracts from forest soils. Environmental Chemistry 4 (6), 424-429.

FAO. 2006. Guidelines for soil description. FAO: Rome. 97 p.

FAOSTAT (Food and Agricultural Organization of the United Nations). 2010. Online, URL: http://faostat.fao.org/

Flessa H, Amelung W, Helfrich M, Wiesenberg GLB, Gleixner G, Brodowski S, Rethemeyer J, Kramer C, Grootes PM. 2008. Storage and stability of organic matter and fossil carbon in a Luvisol and Phaeozem with continuous maize cropping: A synthesis. Journal of Plant Nutrition & Soil Science 171, 36-51.

Fontaine S, Barot S, Barre P, Bdioui N, Mary B, Rumpel C. 2007. Stability of organic carbon in deep soil layers controlled by fresh carbon supply. Nature 450, 277-280.

Graven HD, Guilderson TP, Keeling RF. 2012. Observations of radiocarbon in CO_2 at seven global sampling sites in the Scripps flask network: Analysis of spatial gradients and seasonal cycles. Journal of Geophysical Research 117: D02303, doi:10.1029/2011JD016535.

Grootes PM, Nadeau MJ, Rieck A. 2004. ^{14}C-AMS at the Leibniz-Labor: radiometric dating and isotope research. Nuclear Instruments and Methods in Physics Research B 223/224, 55-61.

Harden JW. 1982. A quantitative index of soil development from field descriptions: Examples from a chronosequence in central California. Geoderma 28, 1-28.

Helfrich M, Flessa H, Ludwig B. 2010. Modelling carbon dynamics in subsoils using simple models. Journal of Plant Nutrition and Soil Science 173 (5), 671-677.

Huang Y, Sun W. 2006. Changes in topsoil organic carbon of croplands in mainland China over the last two decades. Chinese Science Bulletin 51 (15), 1785-1803.

IUSS Working Group WRB. 2007. World reference base for soil resources. World Soil Resources Reports, Vol. 103. FAO: Rome. 145 p.

Janssen M, Lennartz B. 2008. Characterization of Preferential Flow Pathways through Paddy Bunds with Dye Tracer Tests. Soil Science Society of America Journal 72 (6), 1756-1766.

Jobbagy EG, Jackson RB. 2000. The vertical distribution of soil organic carbon and its relation to climate and vegetation. Ecological Applications 10 (2), 423-436.

Kalbitz K, Kaiser K, Fiedler S, Kölbl A, Amelung W, Bräuer T, Cao ZH, Don A, Grootes PM, Jahn R, Schwark L, Vogelsang V, Wissing L, Kögel-Knabner I. 2013. The carbon count of 2,000 years of rice cultivation. Global Change Biology, accepted.

Kögel-Knabner I, Amelung W, Cao ZH, Fiedler S, Frenzel P, Jahn R, Kalbitz K, Kölbl A, Schloter M. 2010. Biogeochemistry of paddy soils. Geoderma 157, 1-14.

Lal R. 2004. Soil Carbon Sequestration Impacts on Global Climate Change and Food Security. Science 304, 1623-1626.

Lal R. 2008. Carbon sequestration. Philosophical Transactions of the Royal Society B 363, 815-830.

Laskar AH, Yadava MG, Ramesh R. 2012. Radiocarbon and stable isotopes in two soil profiles from northeast India. Radiocarbon 54 (1), 81-89.

Lennartz B, Horn R, Duttmann R, Gerke HH, Tippkötter R, Eickhorst T, Janssen I, Janssen M, Rüth B, Sander T, Shi X, Sumfleth K, Taubner H, Zhang B. 2009. Ecological safe management of terraced rice paddy landscapes. Soil & Tillage Research 102, 179-192.

Levin I, Naegler T, Kromer B, Diehl M, Francey RJ, Gomez-Pelaez AJ, Steele LP, Wagenbach D, Weller R, Worthy DE. 2010. Observations and modeling of the global distribution and long-term trend of atmospheric $^{14}CO_2$. Tellus 62 B, 26-46.

Luan YX, Mallatt JM, Xie RD, Yang YM, Yin WY. 2005. The phylogenetic positions of three basal-hexapod groups (Protura, Diplura, and Collembola) based on ribosomal RNA gene sequences. Molecular Biology and Evolution 22, 1579-1592.

MacLean JL, Dawe DC, Hardy B, Hettel GP. 2002. Rice Almanac: Source Book for the Most Important Economic Activity on Earth. Wallingford: CABI Publishing. 270 p.

Maie N, Watanabe A, Kimura M. 2004. Chemical characteristics and potential source of fulvic acids leached from the plow layer of paddy soil. Geoderma 120, 309-323.

Marschner B, Brodowski S, Dreves A, Gleixner G, Gude A, Grootes PM, Hamer U, Heim A, Jandl G, Ji R, Kaiser K, Kalbitz K, Kramer C, Leinweber P, Rethemeyer J, Schaeffer A, Schmidt MWI, Schwark L, Wiesenberg GLB. 2008. How relevant is recalcitrance for the stabilization of organic matter in soils? Journal of Plant Nutrition & Soil Science 171 (1), 91-110.

Mishra HS, Rathore TR, Pant RC. 1997. Root growth, water potential, and yield of irrigated rice. Irrigation Science 17, 69-75.

Nadeau MJ, Schleicher M, Grootes PM, Erlenkeuser H, Gottdang A, Mous DJW, Sarnthein JM, Willkomm H. 1997. The Leibniz-Labor AMS facility at the Christian-Albrechts University, Kiel, Germany. Nuclear Instruments and Methods in Physics Research B 123, 22-30.

Nadeau MJ, Grootes PM, Schleicher M, Hasselberg P, Rieck A, Bitterling M. 1998. Sample troughput and data quality at the Leibniz-Labor AMS facility. Radiocarbon 40 (1), 239-245.

O'Brien BJ, Stout JD. 1978. Movement and turnover of soil organic matter as indicated by carbon isotope measurements. Soil Biology and Biochemistry 10 (4), 309-317.

Pan G, Li L, Wu L, Zhang X. 2003. Storage and sequestration potential of topsoil organic carbon in China's paddy soils. Global Change Biology 10, 79-92.

Paul EA, Follett RF, Leavitt SW, Halvorson A, Petersen GA, Lyon DJ. 1997. Radiocarbon dating for determination of soil organic matter pool sizes and dynamics. Soil Science Society of America Journal 61, 1058-1067.

Pessenda LCR, Gouveia SEM, Aravena R. 2001. Radiocarbon dating of total soil organic matter and humin fraction and its comparison with 14C ages of fossil charcoal. Radiocarbon 43, 595-601.

Rethemeyer J, Kramer C, Gleixner G, John B, Yamashita T, Flessa H, Andersen N, Nadeau MJ, Grootes PM. 2005. Transformation of organic matter in agricultural soils: radiocarbon concentration versus soil depth. Geoderma 128, 94-105.

Rice JA. 2001. Humin. Soil Science 166 (11), 848-857.

Rui W, Zhang W. 2010. Effect size and duration of recommended management practices on carbon sequestration in paddy field in Yangtze Delta Plain of China: A meta-analysis. Agriculture, Ecosystems and Environment 135, 199-205.

Rumpel C, Kögel-Knabner I. 2011. Deep soil organic matter - a key but poorly understood component of terrestrial C cycle. Plant and Soil 338 (1-2), 143-158.

Scharpenseel HW, Becker-Heidmann P, Neue HU, Tsutsuki K. 1989. Bomb-carbon, ^{14}C-dating and ^{13}C-measurements as tracers of organic matter dynamics as well as of morphogenetic and turbation processes. The Science of the Total Environment 81/82, 99-110.

Six J, Guggenberger G, Paustian K, Haumaier L, Elliott ET, Zech W, 2001. Sources and composition of soil organic matter fractions between and within soil aggregates. European Journal of Soil Science 52, 607-618.

Stevenson FJ. 1994. Humus Chemistry - Genesis, composition, reactions. John Wiley: New York. 512p.

Stuiver M, Polach HA. 1977. Discussion: reporting of ^{14}C data. Radiocarbon 19, 355-363.

Tanji KK, Gao S, Scardaci SC, Chow AT. 2003. Characterizing redox status of paddy soils with incorporated rice straw. Geoderma 114 (3-4), 333-353.

Trumbore SE, Vogel JS, Southon JR. 1989. AMS ^{14}C measurements of fractionated soil organic matter: An approach to deciphering the soil carbon cycle. Radiocarbon 31 (3), 644-654.

Trumbore SE. 2000. Age of soil organic matter and soil respiration: radiocarbon constraints on belowground C dynamics. Ecological Applications 10 (2), 399-411.

Wade LJ, Fukai S, Samson BK, Ali A, Mazid MA. 1999. Rainfed lowland rice: physical environment and cultivar requirements. Field Crop Research 64, 3-12.

Wang Y, Amundson R. 1996. Radiocarbon Dating of Soil Organic Matter. Quaternary Research 45, 282-288.

Wissing L, Kölbl A, Vogelsang V, Fu JR, Cao ZH, Kögel-Knabner I. 2011. Organic carbon accumulation in a 2000-year chronosequence of paddy soil evolution. Catena 87, 376-385.

Xu S, Shi X, Zhao Y, Yu D, Li C, Wang S, Tan M, Sun W. 2011. Carbon sequestration potential of recommended management practices for paddy soils of China, 1980-2050. Geoderma 166, 206-213.

Yoshida S, Hasegawa S. 1982. The rice root system: its development and function. In: Drought resistance in crops with emphasis on rice. IRRI: Manila. 97-114.

[1] Tris: tris(hydroxymethyl)aminomethane

[2] EDTA: Ethylenediaminetetraacetic acid

[3] CTAB: Cetrimonium bromide

Chapter V

Modeling soil organic carbon dynamics in paddy soils of different ages

Status: in preparation.

Abstract

We investigated the dynamics of soil organic matter (SOM) along a chronosequence of paddy soils in Eastern China that developed on reclaimed marsh sediments during the past 2,000 years. To estimate turnover times and pool sizes of organic matter, we used a time-dependent steady-state box model and radiocarbon data of soil samples collected to at least 1 m depth. The model yielded two SOM pools. The more labile pool gave turnover times ranging from 1.5 to 21 years depending on the soil depth. The stable C pool is characterized by residence times ranging from 150 to 2,000 years. The wide range of the calculated values is caused by (i) the different depth intervals within the soil profile and (ii) the age of the paddy soil site. Thus, the oldest soils reveal the lowest decomposition rates and topsoils are characterized by the shortest turnover times. However, the calculated pool sizes as well as the residence times are strongly affected by the choice of model parameters. This is evident from repeated calculations with different starting values resulting in varying results for C pool sizes and residence times.

Introduction

Due to its influence on soil physical properties and plant nutrient supply, soil organic matter (SOM) is linked to soil fertility. According to this, the importance of organic manures for maintaining or improving the fertility of soils has been recognized since the first days of agriculture (Allison 1973). Guidelines for farmers about crop and soil management were developed, based on the results of experimental studies conducted since the middle of the last century (Henin and Dupuis 1945; Springer and Lehner 1952; Kortleven 1963; Sauerbeck and Gonzalez 1977). However, SOM content of soils tends towards an equilibrium value that is characteristic for the environmental conditions to which that system is exposed (Powlson and Olk 2000). For example, a soil under continuous flooded rice (rice–rice) accumulates carbon at a higher rate than under a rice–wheat rotation that is aerobic for part of the time (Shibu et al. 2006).

In the last two decades, more and more attention has been paid to the sustainability and the effects of crop management practices on resource quality of the rice-based production systems in tropical and subtropical Asia (Cassman and Pingali 1995; Dawe et al. 2000; Dobermann et al. 2000; Aggarwal et al. 2000; Arora et al. 2006; Fageria et al. 2011; Schulz et al. 2011). One of the major findings, provided by long-term experiments under intensive rice-cropping systems, is the disclosure of ‘soil-exhaustion’, indicated by declining or stagnating yields (Dawe et al. 2000; Narang and Virmani 2001; Ladha et al. 2003). Especially, a quantitative and qualitative reduction of SOM, leading to a depletion of soil fertility, is supposed to be the main driver for the observed decrease in yield (Ram 1998, 2000; Dawe et al. 2003). At this point SOM models can be important tools for the investigation of long-term effects of intensive cultivation on soil C dynamics. Such models describe the influence of environmental conditions, as well as the relations between the various components. Subject to the condition that a suitable calibration and validation is available, models can be used to explore soil organic matter dynamics and to examine the possibilities for modification of SOM content through various intervention measures in the system.

In addition to its importance for soil fertility, soil organic carbon (SOC) is the largest active C pool within the global carbon budget (Lal 2008). More than 50 % of the organic carbon stored in soils worldwide is located in subsoil horizons (Jobbagy and Jackson

2000). Estimates of the global total organic carbon in the upper meter of the world's soils converge to an amount of ca. 1,500 Pg (1 Pg = 1 Gt = 10^{15} g) (Batjes 1996). Additionally 800 Pg of organic carbon are stored at a depth between one and three meters below surface (Jobbagy and Jackson 2000). Despite this knowledge, the majority of the existing C-dynamic investigations examine only the organic carbon stock of the topsoil horizons (upper 30 cm) (Parton et al. 1987; Jenkinson et al. 1992).

Several aspects which are responsible for SOC studies mostly investigating the topsoil horizons during the last decades are discussed in detail by Rumpel et al. (2012). Briefly, organic carbon located in subsoil horizons was assumed to be functionally inert and insignificant within the system of SOC transport and stabilization, due to its chemical composition, a strong adsorption to mineral surfaces, very low annual inputs of fresh organic matter and reduced microbial activity (Taylor et al. 2002; Fierer et al. 2003, von Lützow et al. 2008). Furthermore, increasing mean residence times (MRT) with increasing soil depth, reaching values of several thousand years, suggest a higher level of stabilization of deep SOC compared to OC in topsoil horizons (Rumpel and Kögel-Knabner 2011). However, the recent past generated studies directing more attention to SOC of deep soil horizons, since subsoil OC seems to be less inert than commonly assumed and contains more components that turn over on timescales of decades. (Trumbore 2000; Baisden and Parfitt 2007; Sanderman et al. 2008; Helfrich et al. 2010; Schimel et al. 2011).

The experience of several decades in measuring radiocarbon of soils and SOC fractions led to an increased understanding of the changing global carbon cycle in general (O'Brien and Stout 1978; Goh et al. 1976; Scharpenseel et al. 1989; Trumbore et al. 1989; Becker-Heidmann and Scharpenseel 1992; Wang et al. 1996; Gaudinski et al. 2000; Baisden et al. 2002; Bruun et al. 2005; Kondo et al. 2010). Yet, only little is known about SOC dynamics occurring in deep soil layers due to methodical and technical issues. Namely, SOC consists of a wide variety of compounds with different origins and apparent ages (mean residence times) ranging from years to millennia. Consequently, its average ^{14}C concentration is determined by the mixing ratio and ^{14}C contents of its components. To handle this problem, fractionation schemes (physical and chemical) were developed to separate SOC into discrete pools with intrinsic turnover times (Baisden and Amundson 2003; Trumbore 2009). Since the use of such separation methods turned out to be less satisfying than assumed, the use of distinct C pools separated mathematically became favored in recent

years (Krull et al. 2003; Trumbore 2009). Trumbore (1993) described ^{14}C time series measurements as an appropriate tool to quantify SOC turnover rates, since turnover rates up to thousands of years are detected by radioactive decay as well as turnover rates in the order of years due to highly elevated ^{14}C concentrations in the atmosphere after nuclear weapons tests over the years 1954 to 1962. Furthermore, Baisden et al. (2011) demonstrated the ability of ^{14}C time series measurements in association with modeling to quantify conceptual SOC pools without the need of physical or chemical separation of SOC fractions.

Several studies addressed the estimation of turnover rates and investigated SOC dynamics (Elzein and Balesdent 1995; Baisden et al. 2002; Castanha et al. 2008). However, the authors are aware of only a few studies that examine SOC dynamics in subsoil horizons (Parton et al 1998; Jenkinson and Coleman 2008). These elaborate models, which often include dissolved organic matter (DOM), require considerable analytical data, including C concentrations, C stocks and specific C pools, obtained by physical and chemical fractionation (Tipping et al. 2012). Often, these data are not available. Thus, it remains uncertain how a complex model of subsoil C dynamics can be calibrated and validated with the limited information available (Helfrich et al. 2010).

According to this, we used ^{14}C data, obtained from paddy soils of various ages, in a simple two-pool model to estimate residence times for a fast and slow cycling SOC pool. We simulated the carbon dynamics of the entire soil profiles down to 1 m depth and compared measured and modeled SOC pools. The calculations were conducted in multiple approaches to investigate the sensitivity of the model towards changes in assumptions. Furthermore, running the model several times with different initial values made it possible to assess the reliability of estimated turnover rates and the contribution of calculated C pools to total organic carbon (TOC) by comparison with previous findings, obtained by radiocarbon analysis of different chemically isolated SOC fractions (Bräuer et al. 2013b).

Methods

Site description and soil sampling

To satisfy the need of food supply of the rapidly expanding human population, huge paddy field areas developed, governed by a unique water regime for rice cultivation (Timsina and Connor 2001). Irrigated rice-based cropping systems, with up to three rice crops produced each year at the same field, are the predominant agricultural land use in the lowland areas in subtropical to warm-temperate climate zones in Southeast Asia (Cassman and Pingali 1995). About 30 % of world total rice production is provided by China (FAOSTAT 2011). Further, the total Chinese cropland area comprises 20 % of paddy fields, whereat this fifth part contains about 30 % of the topsoil soil organic carbon stocks of China's croplands (Zhao et al. 1997).

Paddy soils are assumed to have a greater potential for SOC sequestration than upland soils in the same climate zone due to specific management practices (Pan et al. 2003; Liu et al. 2006; Xu et al. 2011; Zhang et al. 2012). The paddy soil development is attributed to periodical phases of submergence, which indicate the paddy ecosystem as a temporary man-made aquatic habitat (Rui and Zhang 2010). Paddy soils are characterized by high SOC levels, which have been repeatedly observed for paddy soils in China (Pan et al. 2003; Li et al. 2010). The enlarged SOC stocks, compared to non-paddy soils, are caused by high rates of organic amendments, carbon inputs via straw incorporation (Tanji et al. 2003), and retarded decomposition rates, respectively (Huang and Sun 2006; Kögel-Knabner et al. 2010).

The study sites are located around Cixi (30° 10′ N, 121° 14′ E), approximately 180 km south of Shanghai and 150 km east of Hangzhou, within the warm temperate zone of the East Asian monsoon region. The mean annual temperature amounts 16.3°C and the mean precipitation of 1,325 mm per year is massed with nearly 75 % during the rice paddy flooding season from April to October (Cheng et al. 2009; Zou et al. 2011). More detailed information about the study area and the historical development of the differently aged soils is given by Su and Wang (1989), Cheng et al. (2009) and Kalbitz et al. (2013).

During the past centuries new farmland was created through consecutive land reclamation by protective dikes in the Zhejiang Province, PR China. These land reclamation efforts provide a unique chronosequence of soil formation under agricultural use. Parts of the land were used for paddy rice, other parts for a variety of non-irrigated crops. Thus, we are able to study the uptake and relocation of OC over time by using the atmospheric ^{14}C input and to examine the dynamics of paddy soil development in direct comparison to soils not used for lowland rice cultivation. (Bräuer et al. 2013a).

In a joint sampling campaign in June 2008, soil profiles of the chronosequence were excavated and horizontally described according to FAO (2006) and classified according to IUSS Working group WRB (2007). One soil profile was situated at the tidal flat, consisting of estuarine sediment. These deposits represent the parent material and, consequently, day zero of paddy soil development. The other seven profiles represent different stages of the chronosequence, ranging from 50 to 2,000 years of rice cultivation (P50-P2000).

Sample treatment and analysis

Soil samples were air-dried and sieved through 2 mm mesh size to homogenize the material. Non soil-derived particles as well as identifiable plant residues were removed and kept for further studies. Bulk soil samples were treated with 4 ml dilute (1 %) hydrochloric acid (HCl) per gram of soil to remove carbonates, and freeze dried without washing to determine their TOC content and ^{14}C concentration.

After freeze-drying, sample aliquots were transferred into pre-combusted (4 hours, 900°C) quartz tubes, evacuated, subsequently flame sealed, and combusted with copper oxide (CuO) (450 mg) and silver wool (150 mg) at 900°C for 4 hours. The resulting CO_2 was reduced to graphite with hydrogen (H_2) at 600°C over an iron catalyst. The ^{14}C measurements were made with the 3 Million Volt HVE Tandetron AMS (accelerator mass spectrometry) system at the Leibniz-Laboratory in Kiel (Germany), with a 1-σ precision of about 0.25 pMC (Nadeau et al. 1997, 1998).

Radiocarbon values are stated in percent modern carbon (pMC):

$$\text{pMC (percent Modern Carbon)} = \frac{A_{sn}}{A_{abs}} * 100,$$

where A_{sn} is the ^{14}C activity in the sample (i.e. the measured $^{14}C/^{12}C$ ratio) normalized to $\delta^{13}C$ = -25‰ and A_{abs} is the absolute ^{14}C activity in the international isotopic standard (NBS oxalic acid) according to Stuiver and Polach (1977).

Modeling

One of the criteria for accurate radiocarbon dating of a sample is that the system has to be closed with respect to ^{14}C (Wang et al. 1996). Soils which form over long periods of time represent open systems with respect to carbon and are in apparent violation of this criterion. Obviously, the standard C dating models are not applicable to soils. However, existing models describe the variation in organic carbon with time for a soil or any of its horizons under the assumption that organic matter decomposition is the only mechanism for carbon loss in soils (Wang and Hsieh 2002).

Considering the description of SOM dynamics, existing SOM models can be classified on the basis of the type of quantitative description. One can distinguish analytical models and simulation models. In analytical models, SOM is considered to be a single homogenous pool with a characteristic relative decomposition rate (k), that is either constant or changes with time (Henin and Dupuis 1945; Kortleven 1963; Kolenbrander 1969; Janssen 1984; Yang 1996).

In contrast, simulation models consider SOM as a heterogeneous mixture represented by a number of functional pools. Decomposition of components in this mixture occurs at different relative rates. The application of such a process-based modeling approach to simulate SOM dynamics was initiated by Parnas in 1975 (Parnas 1975). Most of the current multi-component models (e.g., ANIMO, DAISY, SUNDIAL, RothC, CANDY, and CENTURY) are based on a similar structure with a variable number of pools of fresh organic matter (residues), old (more stable) organic matter and microbial biomass.

The decomposition rate constants of these different pools have generally been derived from fitting the models to measured data (Paustian 1994). Here, we pursued the approach of simulation models. A rice-based cropping system, which is characterized by a puddle and flooded soil during part of the year, needs at least two layers to represent a paddy soil profile. Thus, models like RothC and CENTURY, which are related to a single compartment concept assuming a uniform layer to a depth of 20 cm, are not able to simulate such a system. DNDC, which can be applied to wetland ecosystems, is inappropriate as well, since a fixed number of soil compartments (10 layers of 5 cm each) make the model more comprehensive. Further, a number of soil characteristics for different soil depths, which are required by DNDC, may not be measured routinely.

We calculated the SOC turnover times using measured ^{14}C values of bulk soil samples from paddy soils of a 2,000 yr chronosequence. The used ^{14}C time series consists of 2 points, (i) the ^{14}C content of the soil sample at the beginning of agricultural use, estimated from tidal flat samples representing the parent material as the starting point of the time series and (ii) the measured ^{14}C content of the soil sample in the year of sampling representing the endpoint of the time series. SOC turnover times were estimated using a simple first-order decomposition model, which we developed according to a time-dependent steady-state box model described elsewhere (e.g. Wang et al. 1996; Castanha et al. 2008). However, two improvements were made to examine SOC dynamics under paddy management.

In contrast to the existing approach, our model provides SOC pools as a function of depth, i.e. turnover rates were estimated for every single genetic horizon across the entire soil profile. The consideration of different depth intervals is an improvement for the application of the existing models, which are usually working only with single topsoil layers. To consider different depth levels, a new parameter was implemented to simulate SOC turnover down to 1 m depth: *r*, which moves organic carbon down the profile also referred to as the downward transport rate.

Furthermore, we improved the simple steady-state box model in regard to the assumption that a soil horizon can be modeled as a time-dependent box and SOM decomposes homogeneous as one component. For this purpose, the total SOC was divided into two

pools of different stabilities and another parameter was implemented: *p*, which describes the interaction between the two SOC pools.

We assume two SOC pools: *P1* (labile) and *P2* (stable), whereat each pool comes with a first-order decomposition rate, a downward transport rate and a pool - pool interaction rate, which represents the exchange between the pools. Beginning in the year of agricultural use (e.g. paddy management), the model incorporates input of organic carbon to the SOC pools into the uppermost soil horizon with a ^{14}C signature equal to that of the atmosphere, taken from atmospheric $^{14}CO_2$ data (Levin et al. 2010). The below-surface SOC pools gain C input from each other and from the horizon above (cf. Figure 5.1).

For each year (*y*) the carbon stock (*C*) is calculated as follows:

$$C_{y(P1)} = C_{y\text{-}1(P1)}\,(1\text{-}(k + r + p)) + (C_{y\text{-}1(P2)} \cdot p) + (I \cdot I_{\%(P1)}).$$

The radiocarbon content can be expressed according to the following equation:

$$^{14}C_{y(P1)} = \left(\frac{C_{y-1(P1)}\left(1-\left(k+r+p\right)\right)}{C_{y(P1)}}\ {}^{14}C_{y-1(P1)} + \frac{C_{y-1(P2)} \cdot p}{C_{y(P1)}}\ {}^{14}C_{y-1(P2)} + \frac{(I \cdot I_{\%(P1)})}{C_{y(P1)}}\ {}^{14}C_{Atm} \right) \cdot \left(1-\lambda\right)$$

where, *C* is the carbon stock of a soil fraction (kg m^{-2}); ^{14}C is the ^{14}C concentration of a soil fraction (pMC); *k* is the decomposition constant; *r* is the downward transport rate; *p* is the pool - pool interaction rate; *I* is the annual carbon input (kg m^{-2}); $I_{\%(P1)}$ is the proportion of *P1* on the Input; $^{14}C_{Atm}$ is the ^{14}C value of the atmosphere (Levin et al. 2010); and λ is the radioactive decay constant ($1.21 \cdot 10^{-4}$).

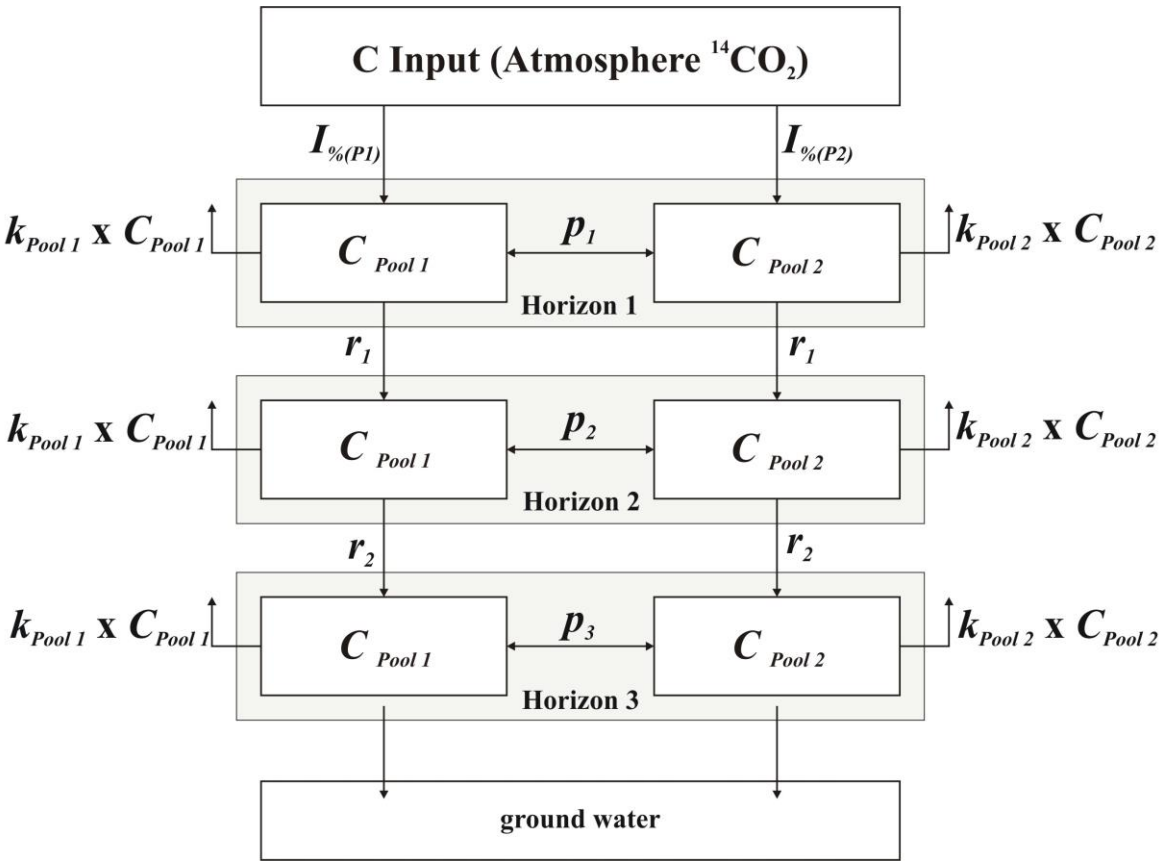

Figure 5.1: Structure of OC decomposition and relocation model.

The model assumes that the single SOC pools are homogenous regarding the contained C and that the material is in steady state. The numerically starting point of our model is the respective year, in which the reclaimed marsh was converted to arable land and paddy management started. We further assume the time period between diking-in and beginning of tillage as negligible. Cui et al. (2012) and Iost et al. (2007) suggest a rapid desalinization of soils in this region immediately after reclamation. Thus the ^{14}C concentration of the parent material, of about 50 pMC, is a suitable value as starting point for our model. Further assumptions are: (1) since the parent material was deposited after passing the Yangtze delta and the contained OC is assumed to be old reworked carbon originating from the Chinese inland, the major part of OC located in the original sediment was accounted to the more stable SOC pool (*P2*). Given that *P2* comprises 95 % of the entire OC stock with a ^{14}C signature of 48 pMC, *P1* contains the remaining 5 % with a

calculated ^{14}C concentration of 98 pMC. (2) The assignation of the annual OC input to the uppermost soil horizon, derived from photosynthesis, turned out in favor of the more labile and mobile SOC pool, Pool 1 ($I_{\%(P1)}$ = 0.95). (3) The OC input to the topsoil was assumed to be constant with time. (4) The downward transport rate *r* is assumed to be higher in the uppermost horizon (0.1 for *P1* and 0.005 for *P2*) compared to subsoil layers and decreases to a constant value below the topsoil (0.01 for *P1* and 0.001 for *P2*). Furthermore, *r* is assumed to be higher in the labile SOC pool (*P1*) than in the stable pool (*P2*).

To check the applied two-pool model (model A) regarding the impact of certain model parameters the calculations were carried out repeatedly with a modified downward transport rate *r*, which led to an altered decomposition constant *k* (model B) and a readjustment of the initial C stocks of the tidal flat (model C). Thus, model C is determined by initial SOC pools, each containing 50 % of the entire OC stock. A summary of the used model parameters and the revealed residence times is given in Table 5.1. Table 5.5 gave the amounts of OC transferred 'vertical' from horizon to horizon and 'lateral' between SOC pools, calculated according to the applied *r* and *p* values.

Table 5.1: Parameter and mean residence times of applied models

	Model parameter	**Model A**		**Model B**		**Model C**	
		Pool 1	**Pool 2**	**Pool 1**	**Pool 2**	**Pool 1**	**Pool 2**
topsoil	starting ^{14}C of tidal flat (pMC)	98	47.47	98	47.47	98	2
	starting content on SOC (%)	5	95	5	95	50	50
	I (kg m^{-2} $year^{-1}$)	0.4		0.4		0.4	
	I%	95	5	95	5	95	5
	MRT (years)	2	200	1.5	2,000	3-7	150-300
	r	$r_1 > r_2$		$r_1 > r_2$		$r_1 > r_2$	
	p	$p_1 = p_2$		$p_1 = p_2$		$p_1 = p_2$	
	λ (decay)	$1.21 \cdot 10^{-4}$		$1.21 \cdot 10^{-4}$		$1.21 \cdot 10^{-4}$	
subsoil	starting ^{14}C of tidal flat (pMC)	98	47.47	98	47.47	98	2
	starting content on SOC (%)	5	95	5	95	50	50
	MRT (years)	5	500	1.5	2,000	7-21	300
	r	$r_1 > r_2$		$r_1 = r_2$		$r_1 > r_2$	
	p	$p_1 = p_2$		$p_1 = p_2$		$p_1 > p_2$	
	λ (decay)	$1.21 \cdot 10^{-4}$		$1.21 \cdot 10^{-4}$		$1.21 \cdot 10^{-4}$	

Model calibration

The data set of the 50-year old paddy site (P50) was used to calibrate the models. The decomposition constant, *k*, or its reciprocal, the turnover time or mean residence time is obtained by matching the modeled and the measured ^{14}C values for the year of soil sampling. The number of adjustable parameters was three (the decomposition rate *k*, the downward transport rate *r*, and the pool-pool interaction rate *p*). The calculations were implemented in Microsoft® Excel® with an annual time step. The value of *k* was obtained by fitting the modeled and the measured data using the optimization tool 'solver'. The optimized fit minimizes the sum of squared errors between the modeled and measured values. However, regarding the optimization process, it cannot be excluded that only a local minimum was found. Table 5.2 shows the obtained decomposition rates.

Table 5.2: Calibration results (decomposition rates) for model A, B and C.

Model		***k* Pool 1**	***k* Pool 2**
A	topsoil	$5 \cdot 10^{-1}$	$5 \cdot 10^{-3}$
	subsoil	$2 \cdot 10^{-1}$	$2 \cdot 10^{-3}$
B	topsoil	$6.7 \cdot 10^{-1}$	$1 \cdot 10^{-3}$
	subsoil	$6.7 \cdot 10^{-1}$	$1 \cdot 10^{-3}$
C	topsoil	$1.4 \cdot 10^{-1}$	$7 \cdot 10^{-3}$
	subsoil	$4.8 \cdot 10^{-2}$	$3 \cdot 10^{-3}$

Model validation

The validation of the models was performed with the data sets of the older paddy sites (P100 - P2000) using the parameter values obtained by the calibration. Since soils are natural, open systems and results obtained by models are always ambiguous, validation of numerical models of natural systems is impossible. Thus, models are representations, useful for guiding further study but not susceptible to proof (Oreskes et al. 1994). To evaluate the performance of the applied models, the model efficiency *EF* was calculated as follows (Smith et al. 1997).

$$EF = \frac{\sum_{i=1}^{n}(M_i - M)^2 - \sum_{i=1}^{n}(P_i - M_i)^2}{\sum_{i=1}^{n}(M_i - M)^2};$$

whereat M_i is the measured value, P_i is the modeled value, and M is the mean of the measured data. *EF* compares the efficiency of the chosen model to the efficiency of describing the data as the mean of the observations. Values of *EF* range from -∞ to 1. A positive *EF* indicates that the simulated values describe the trend in the measured data better than the mean of the observations. For an ideal fit, *EF* equals 1. The calculated model efficiency values for the calibration and the validation are given in Table 5.3.

Table 5.3: Model efficiency in predicting TOC (EF_{TOC}) and ^{14}C (EF_{14C}) for the calibration (P50 site) and validation (P100 and older) of the applied models.

	Model A		**Model B**		**Model C**	
Site	EF_{TOC}	EF_{14C}	EF_{TOC}	EF_{14C}	EF_{TOC}	EF_{14C}
P50	0.98	0.99	0.99	0.98	0.99	0.98
P100	0.98	0.63	0.95	0.85	0.95	0.93
P300	0.33	0.77	0.54	0.29	0.25	0.00
P700	-0.30	0.81	0.66	-0.32	-0.49	-1.20
P1000	-1.94	0.54	-1.02	-1.19	-1.57	-3.30
P2000	0.62	0.57	0.86	-0.19	0.49	-0.97
NP50	-7.49	-0.15	-8.34	0.11	-19.48	-3.58

Results

Model A

The calibration of model A using the P50 data set provided a nearly perfect fit between measured and modeled values for both, TOC (*EF* = 0.98) as well as ^{14}C (*EF* = 0.99) (Figure 5.2a and 5.3a). Regarding the topsoil, the calculation yields a labile SOC pool (*P1*) having a MRT of 2 years comprising 35 % of total SOC. The remaining 65 % of SOC are assigned to a 200 year-old pool (*P2*). The same residence times are discovered for the plough pan horizon, whereat *P1* contains merely 12 % of total SOC. Below the plough pan (17 cm) down to a depth of 1 m *P1* is characterized by a residence time of 5 years and *P2* shows a MRT of 500 years. Between 20 and 50 cm *P1* contains only 1 % SOC, and below this depth the labile pool totally disappears.

According to the nearly perfect fit of the 50 year-old paddy data and due to considerations regarding comparability, the emerged decomposition rate *k* was applied to paddy soil data sets of all ages. Therefore, the validation of model A was performed by using paddy soil datasets comprising more than 50 years of paddy management (P100 - P2000). The proportion of both SOC pools, *P1* and *P2*, stays more or less the same for all paddy sites with about 30 % of TOC in topsoils and a negligible percentage in subsoils for *P1*. Whereas the modeled values deliver nice fits to the paddy soil data with 100 (EF_{TOC} = 0.98; EF_{14C} = 0.63) and 300 (EF_{TOC} = 0.33; EF_{14C} = 0.77) years of cultivation history (cf. Figure 5.2b-c and 5.3b-c), the older paddy soils start to get more problematic (P700 - P2000).

Since the 300 year-old paddy soil shows a surprising high measured total organic carbon content in the topsoil (3.56 % TOC), the simulated OC content is lower than the observed OC value. This led to an underestimation of the calculated OC content of the A-horizon due to a topsoil decomposition rate too large to deliver a concordant fitting (Figure 5.2c). With increasing depth the underestimation of the modeled OC stocks continuous. Although, the decomposition rate *k* was reduced for subsoil samples it is still too large to represent the observed OC values. Exceedingly large deviations occur for 700; 1,000 and 2,000 year-old paddy soils (Figure 5.2d-f). We assume fossil and buried A-horizons (P700:

45 - 69cm and 106 - 116cm; P1000: 21 - 40cm and 80 - 93cm; P2000: 27 - 35cm) to be responsible for the observed mismatches and the resulting low *EF* values. These horizons, partly enriched in OC, are not reproducible with the applied parameters used in our simple model. Concerning the 700 year-old paddy soil the estimation of ^{14}C values (*EF* = 0.81) seems to be more robust regarding the choice of decomposition rates in comparison to OC stocks (*EF* = -0.30) (Figure 5.3d). Despite the large underestimation of OC, the ratio between labile and stable SOC pool seems to be estimated quite well. Here, with exception of the deep fossil A-horizon (106 - 116cm) the calculated ^{14}C concentrations fit fairly nice to the measured data.

Modeled ^{14}C contents of the P2000 data set are consistently too high below the plough pan, while the OC values estimated as too low as mentioned before. The overestimation of ^{14}C appears in a different light after considering the extremely low ^{14}C values observed in the deep soil. The given duration time of 2,000 years would reduce the measured 48.7 pMC of the deep tidal flat to 38.3 pMC by natural decay. Actually, 29.1 pMC were measured and, therefore, the decrease is too large to be explained by this cause alone. The additional decrease in ^{14}C may be caused by fresh OC supply into the subsoil (Bräuer et al. 2013b). A stimulation of OC decomposition due to enhanced microbial processes after the supply of fresh organic carbon into the deep subsoil was reported repeatedly (Dalenberg and Jager 1989; Kuzyakov et al. 2000; Fontaine et al. 2007). Furthermore, it shows the heterogeneous nature of the stable SOC pool.

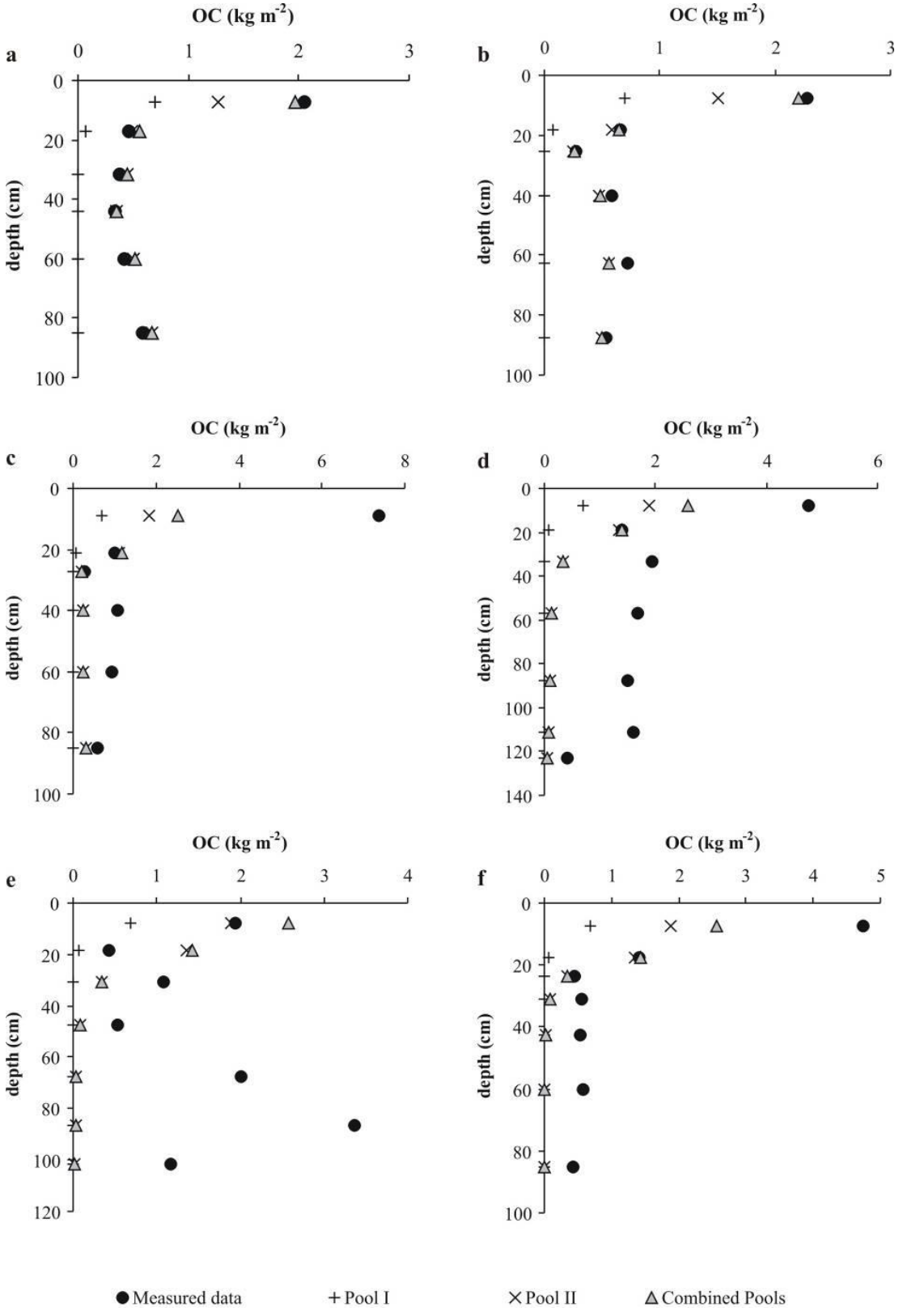

Figure 5.2: Model A: Organic carbon contents of 6 paddy soils with different times of duration; a (50 years); b (100 years); c (300 years); d (700 years); e (1,000 years) and f (2,000 years). Black dots depict measured OC values, straight crosses represent modeled values of *P1*, diagonal crosses represent modeled values of *P2* and grey triangles gave the combination of *P1* and *P2*.

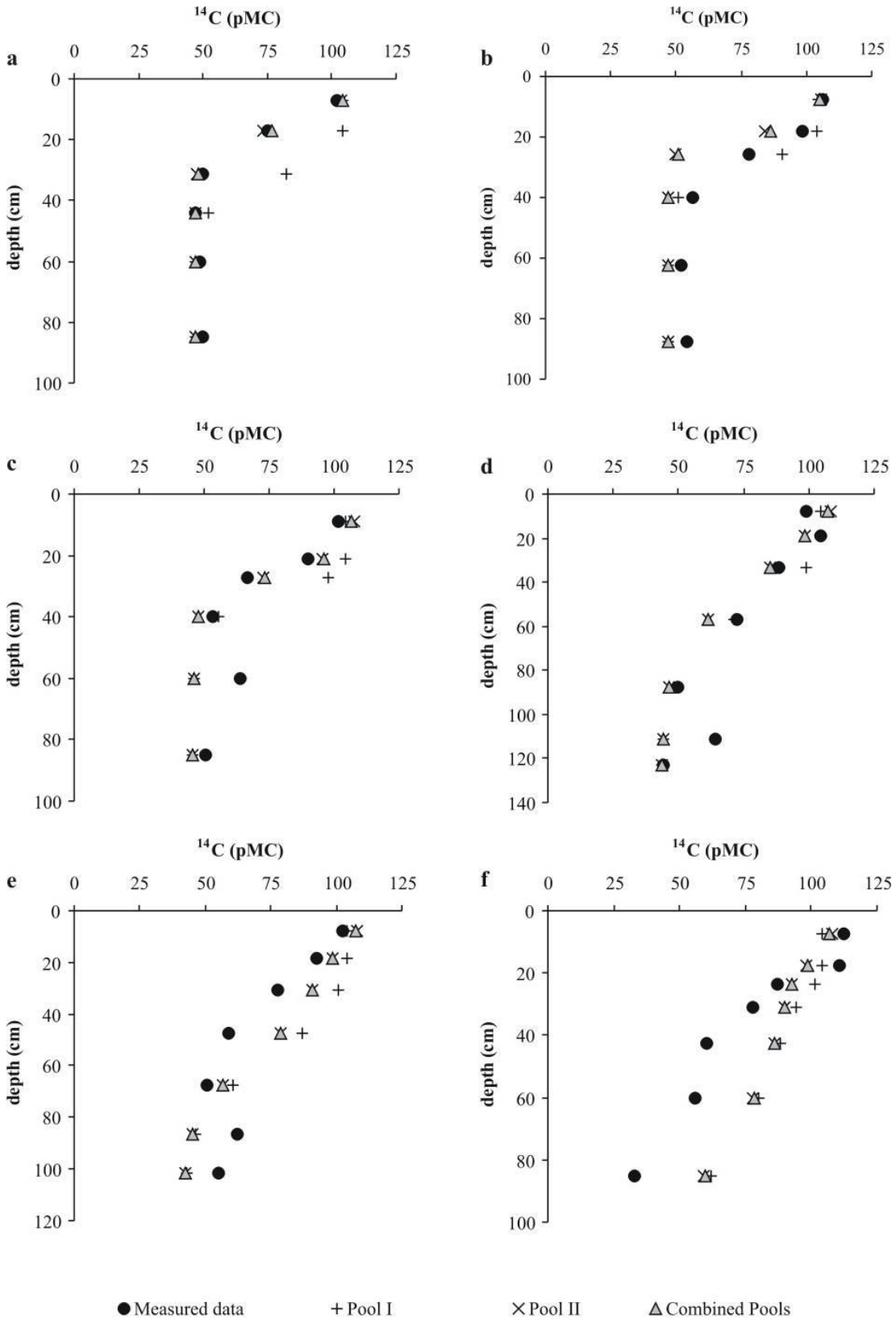

Figure 5.3: Model A: ^{14}C contents of 6 paddy soils with different times of duration; a (50 years); b (100 years); c (300 years); d (700 years); e (1,000 years) and f (2,000 years). Black dots depict measured OC values, straight crosses represent modeled values of *P1*, diagonal crosses represent modeled values of *P2* and grey triangles gave the combination of *P1* and *P2*.

Model B

Model B is characterized by an equalization of the downward transport rate *r* for *P1* and *P2*. Hence, both SOC pools differ solely in the decomposition rate. The matching of the calculated values to the measured values of the P50 site results in constant residence times for both, topsoil and subsoil samples. The best model fit gave a residence time of 1.5 years for *P1* and 2,000 years for *P2* (Figure 5.4a and 5.5a). Regarding the topsoil, merely 15 % of SOC belongs to *P1*. After decreasing to a content of 3 % within the plough pan, *P1* totally disappears below it. The results of model A and B regarding the 50 year-old paddy soil are nearly identical. The 100 years-old soil gave a satisfying fit as well, whereat the ^{14}C calculation seems to be better compared to model A (cf. Table 5.3). The equal *r* for both SOC pools causes a better fitting of OC values in the subsoil for 300 and 700 year-old profiles (Fig. 5.4c-d). However, the modeled ^{14}C concentrations of soils equal to or older than 700 years show a larger deviation than the results brought by model A (Fig. 5.5d-f).

Due to the model-inherent assumption that the soil profiles developed on estuarine sediments, containing mainly old reworked carbon originating from the Chinese inland and the following distribution of the entire SOC stock (*P1*: 5 %; *P2*: 95 %), the observed predominance of the more stable SOC pool *P2* is not surprising. Model A comprises an average SOC content of ca. 30 % for *P1* in the topsoil, while model B gave about 20 %. For subsoil horizons it is regardless from which model approach the SOC contents were emerged. The labile pool disappears totally below the plough pan in both, model A and model B. In conclusion, the labile pool is more or less meaningless for the ^{14}C calculation of subsoil samples and of minor significance for topsoil samples (cf. Figure 5.6). This conclusion is owed to the development history of the presented soil profiles on the estuarine sediment and the major contribution of the initial OC stock to the stable C pool *P2*.

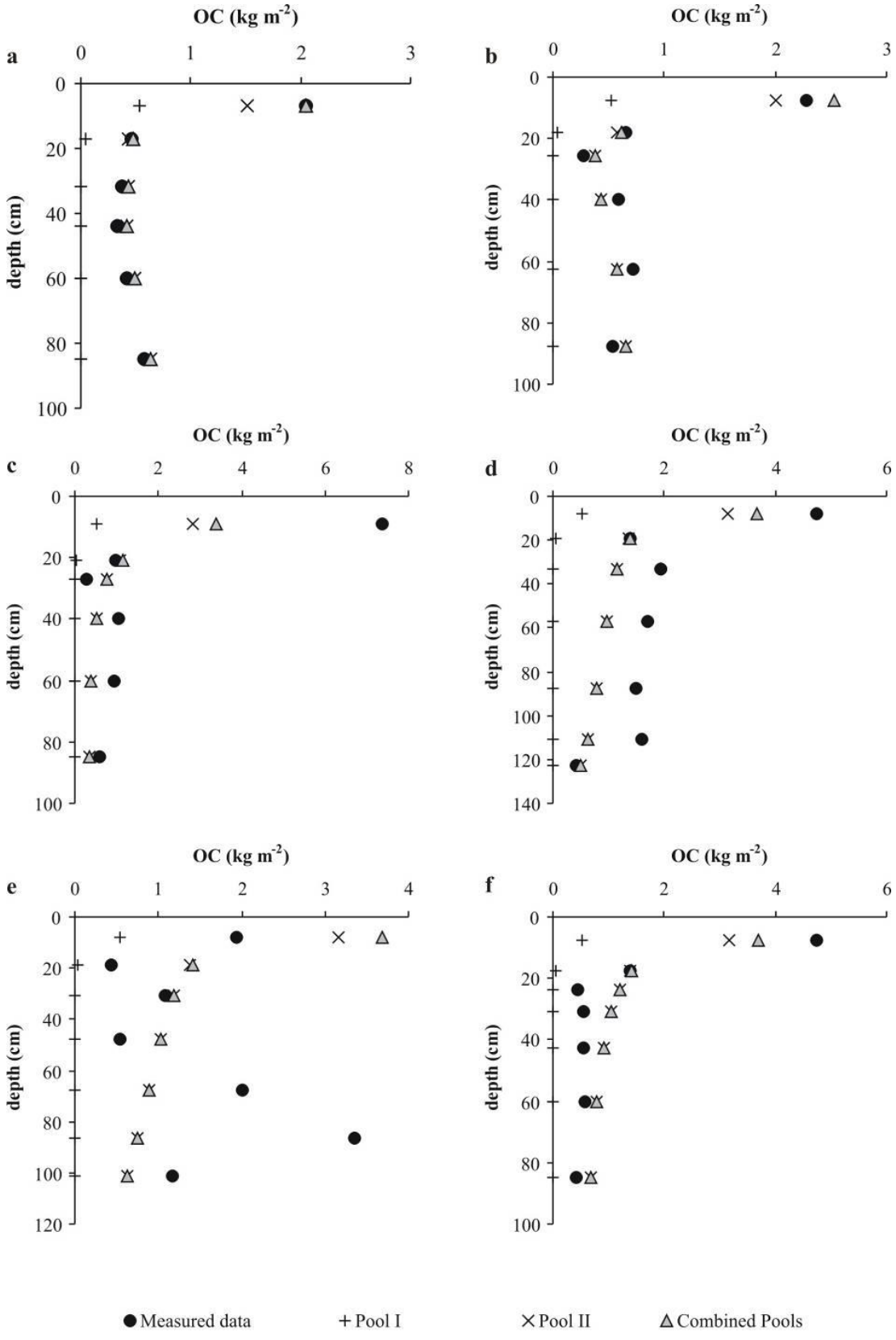

Figure 5.4: Model B Organic carbon contents of 6 paddy soils with different times of duration; a (50 years); b (100 years); c (300 years); d (700 years); e (1,000 years) and f (2,000 years). Black dots depict measured OC values, straight crosses represent modeled values of *P1*, diagonal crosses represent modeled values of *P2* and grey triangles gave the combination of *P1* and *P2*.

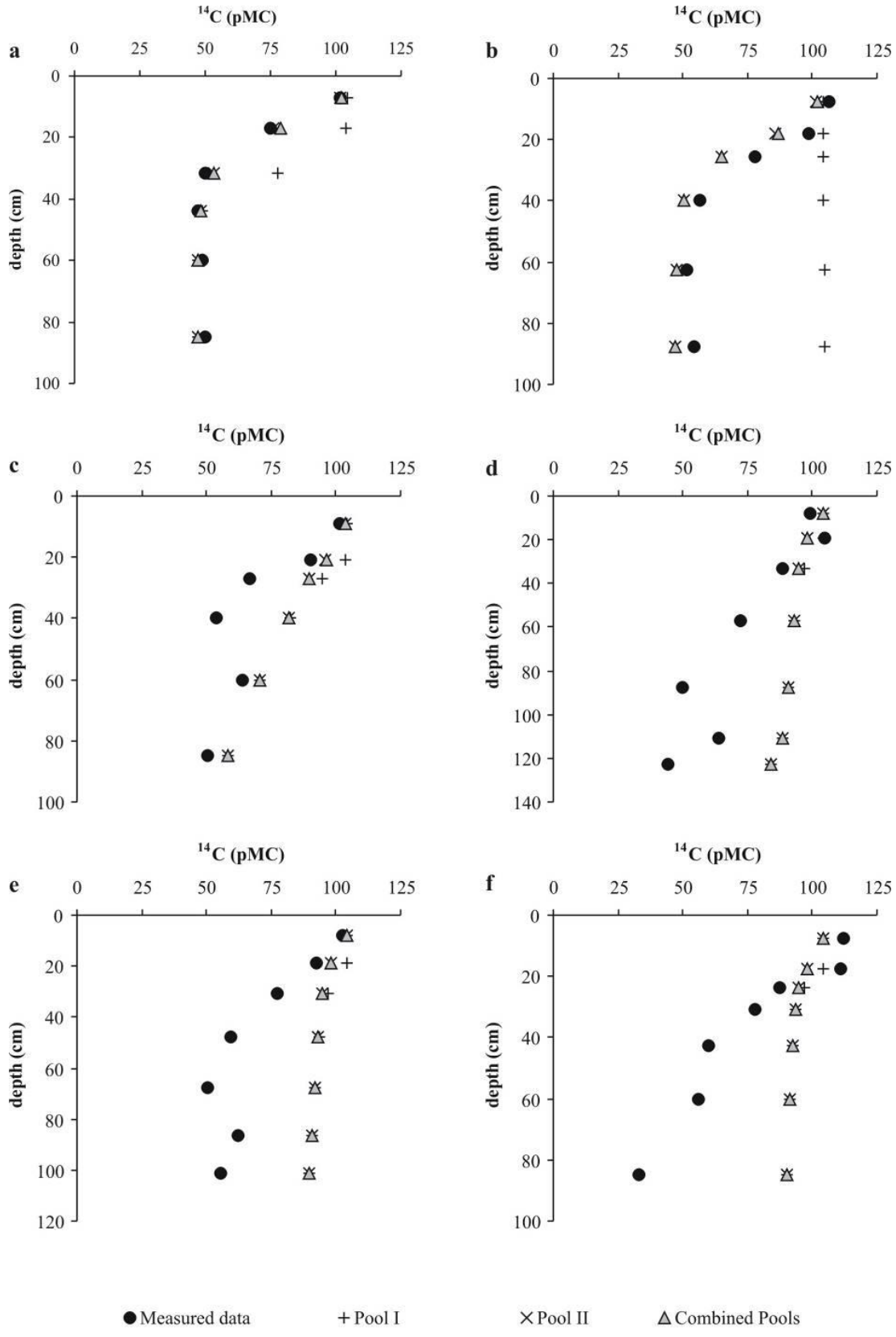

Figure 5.5: Model B ^{14}C contents of 6 paddy soils with different times of duration; a (50 years); b (100 years); c (300 years); d (700 years); e (1,000 years) and f (2,000 years). Black dots depict measured OC values, straight crosses represent modeled values of *P1*, diagonal crosses represent modeled values of *P2* and grey triangles gave the combination of *P1* and *P2*.

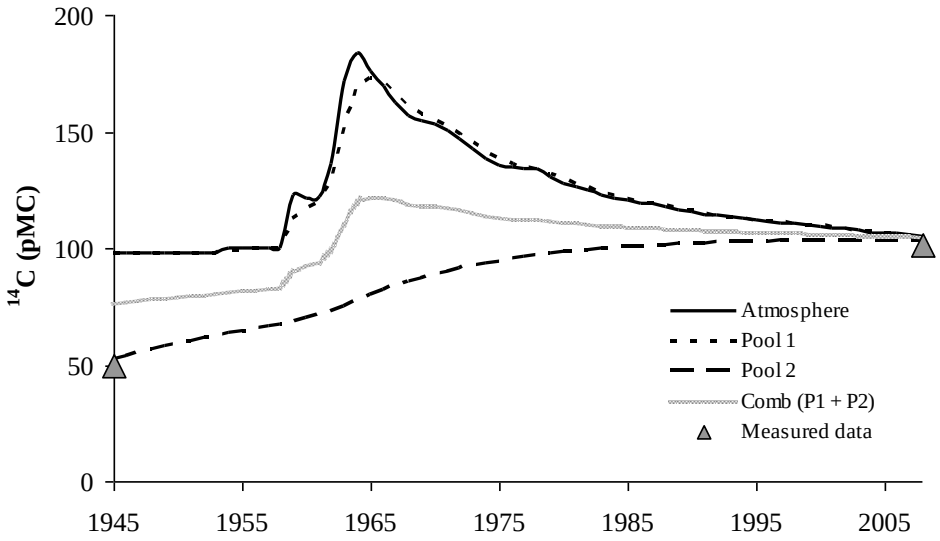

Figure 5.6: ^{14}C values of topsoil samples from a tidal flat (1945) and a paddy soil after land reclamation followed by 50 years of paddy management (2008). The nice fit of observed (measurement) and simulated (Pool 2) values disclose the predominance of stabilized SOC in model A and B.

Model C

The predominance of a stable SOC pool as revealed by the calculations of model A and model B is in contradiction with previous results (Bräuer et al. 2013b). Due to its high proportion on total organic carbon, we previously proposed a highly mobile and fast cycling SOC fraction (fulvic acids) to be the main driver for the input of OC through the plough pan into the subsoil. For this reason, we conducted model C which provides SOC pools with the same proportion on the starting TOC stock. Thereby, the quantitative influence of the slow cycling C pool on the calculated pool sizes could be reduced. Results of model C are depicted in Figure 5.7a-f and 5.8a-f. Again, the best fit between calculation and measurement is delivered by the youngest paddy soils (Figures 5.7a-b; 5.8a-b).

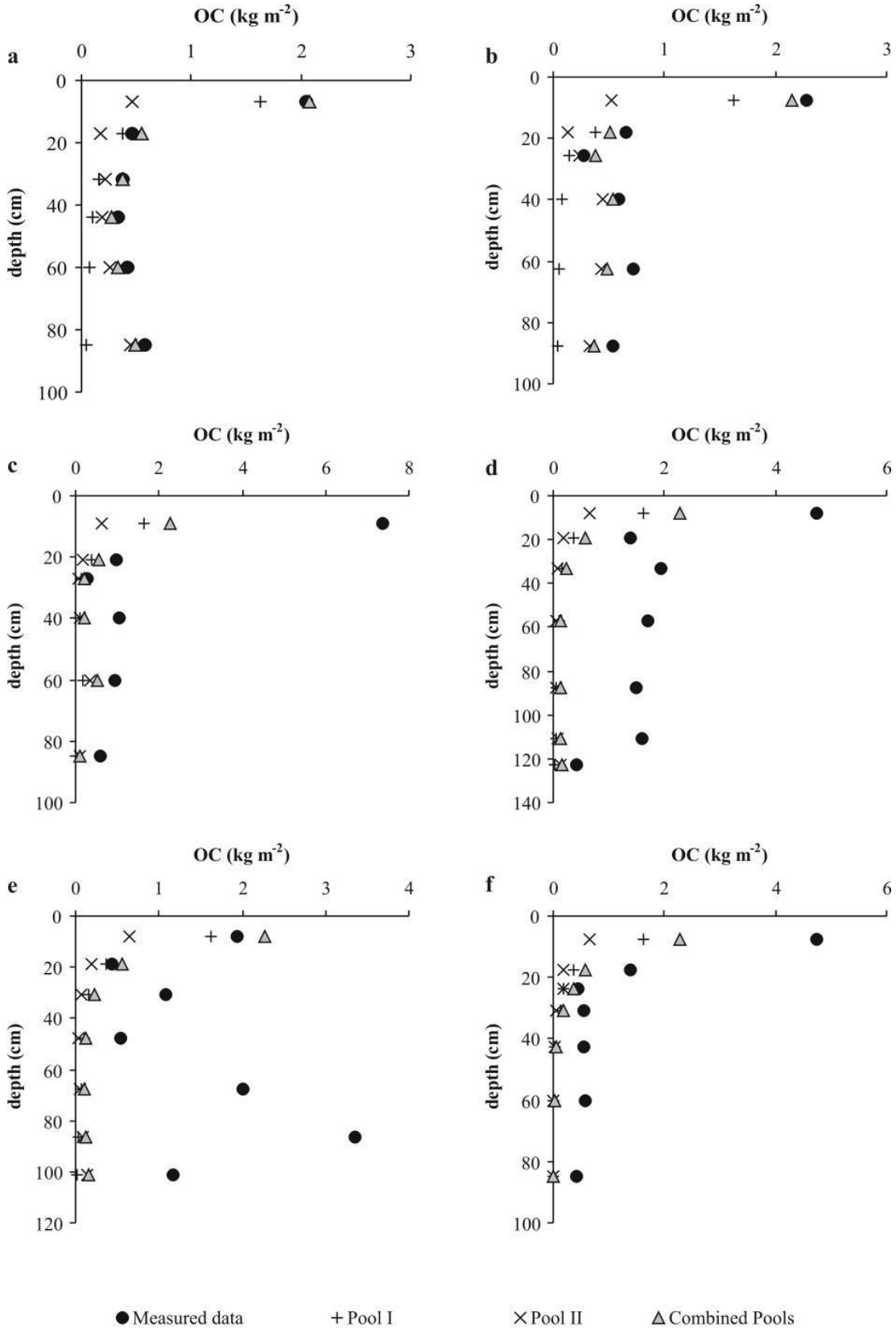

Figure 5.7: Model C Organic carbon contents of paddy soils with different times of duration; a (50 years); b (100 years); c (300 years); d (700 years); e (1,000 years) and f (2,000 years). Black dots depict measured OC values, straight crosses represent modeled values of *P1*, diagonal crosses represent modeled values of *P2* and grey triangles gave the combination of *P1* and *P2*.

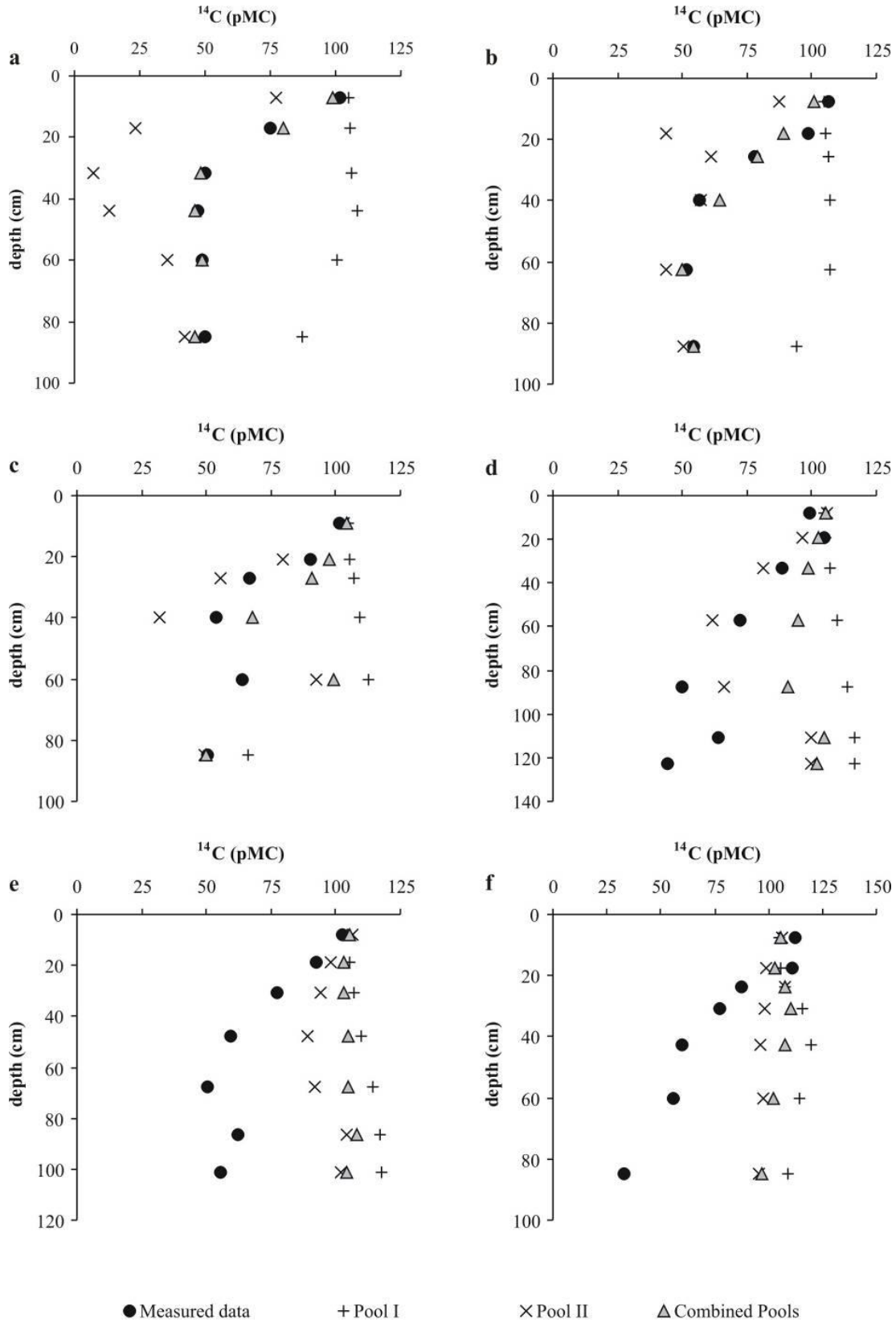

Figure 5.8: Model C ^{14}C contents of 6 paddy soils with different times of duration; a (50 years); b (100 years); c (300 years); d (700 years); e (1,000 years) and f (2,000 years). Black dots depict measured OC values, straight crosses represent modeled values of *P1*, diagonal crosses represent modeled values of *P2* and grey triangles gave the combination of *P1* and *P2*.

After calibration, the residence times of *P1* for the 50-year old paddy soil range from 3 to 7 years in the topsoil (Table 5.1). The labile C pool comprises an average content on TOC of 73 %. The remaining SOC of *P2* is characterized by a MRT between 150 and 300 years. In the subsoil horizons, the calculated turnover rates are decreasing. *P1* shows MRT's between 7 and 21 years, and *P2* gave a residence time of 300 years. The labile C pool contains 34.6 % of the total SOC.

In comparison to model A and B, the validation of model C by using the P100 dataset delivers the best fit between simulation and observation (EF_{TOC} = 0.95; EF_{14C} = 0.93). In accordance with the previous model approaches, A and B, the model efficiency is decreasing to negative values for paddy sites older than 300 years. The fossil A-horizons still disturb a data fitting as good as for the young paddy soils.

To obtain the very good calibration of model C, in addition to the decomposition rate *k*, another parameter had to be adjusted, the pool - pool interaction rate *p*. Regarding model A and B, *p* was chosen equal for both SOC pools, *P1* and *P2*. Model C required an increased flux of OC from *P1* to *P2* for genetic soil horizons below the plough pan. Thus, the stable pool is growing at the expense of the labile C pool. The OC gain of *P2* from *P1* exceeds the flux by a factor of max. 10. The much higher C flux from *P1* to *P2* does not imply a large quantitative net OC gain for the stable pool, since the initial *p* value was very low (cf. model A and B). However, the applied modification of *p* is not only a necessary adjusting of the model; it is linked to natural processes occurring in soils. Changing redox conditions abet the development of Fe-Mn concretions, which on thermodynamic considerations are classified as very stable and, thus, contribute to SOM stabilization (Schwertmann and Fitzpatrick 1992). Results of ^{14}C measurements indicate a stabilization of SOM by inclusion in Fe-Mn concretions. Such a process can be considered as an example for the growth of a stabilized SOC pool by C uptake from a less stable pool (Dreves 2008; Elberling et al. 2013). The concretions, which were separated from different paddy soils (cf. Figure 5.9) amount up to 4 % by soil weight and were found in all subsoil horizons with larger contents directly below the plough pans (cf. Figure 5.10). The ^{14}C concentration of the OC in concretions is always lower than that of the surrounding bulk soil, which shows that in the long run OC is stabilized by inclusion in concretions (cf. Table 5.4).

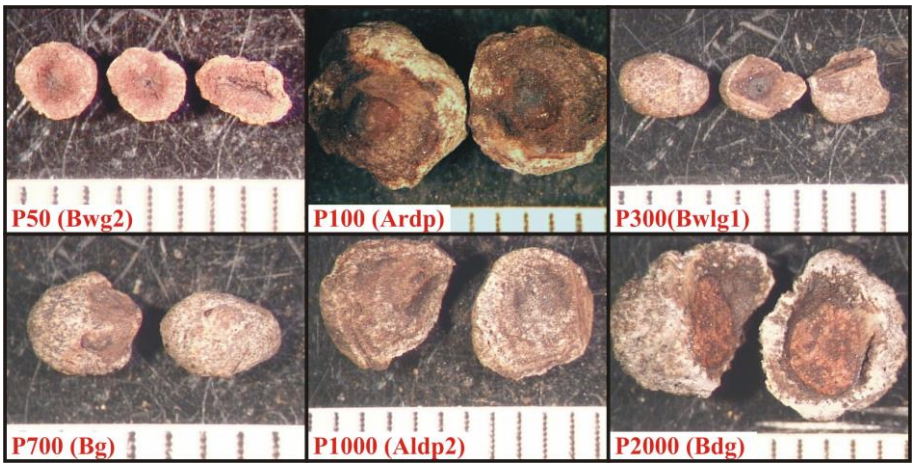

Figure 5.9: Photographs of concretions separated from paddy soils. Scale is given in mm.

Table 5.4: ^{14}C and TOC values of Fe-Mn concretions and the surrounding bulk soil. Concretions were separated from bulk soil by wet sieving over a 400 µm sieve of large (~ 5 kg) soil samples.

Site	**Depth** cm	**$^{14}C_{bulk\ soil}$** pMC	**$OC_{bulk\ soil}$** %	**$^{14}C_{Fe\text{-}Mn\ concr.}$** pMC	**$OC_{Fe\text{-}Mn\ concr.}$** %	**Ø $_{Fe\text{-}Mn\ concr.}$** mm
P100	21-30	78.00	0.20	66.82	0.20	2-3
P100	50-75	48.94	0.18	43.96	0.17	3-5
P300	24-30	66.63	0.28	63.29	0.16	2-3
P300	70-100	50.54	0.14	46.89	0.1	2-4
P1000	21-40	87.27	0.43	75.83	0.35	4-6

Table 5.5: Average amounts of OC moved downwards, calculated according to the downward transport rate *r* and average amounts of OC exchanged between Pool 1 and Pool 2, calculated according to the pool - pool interaction rate *p* for the 50-year old and 2,000-year old paddy site. Values are given in g m^{-2} yr^{-1}.

		OC according to *r				****OC according to *p***			
		P50		**P2000**		**P50**		**P2000**	
Model		**Pool 1**	**Pool 2**	**Pool 1**	**Pool 2**	**Pool 1**	**Pool 2**	**Pool 1**	**Pool 2**
A	topsoil	35.00	6.00	34.50	9.40	0.70	1.00	0.69	1.80
	subsoil	0.40	0.80	0.40	0.84	0.04	0.80	0.04	0.84
B	topsoil	26.50	7.60	26.50	15.80	0.53	1.52	0.53	3.16
	subsoil	0.40	8.40	0.40	8.40	0.04	0.80	0.04	0.83
C	topsoil	163.00	0.46	163.00	0.65	1.63	0.46	1.63	0.65
	subsoil	40.00	0.54	44.00	0.44	22.00	2.70	22.00	2.55

*Values indicate the flux to the underlying horizon
**Values stated in the column of Pool 1 indicate the flux to Pool 2 and vice versa.

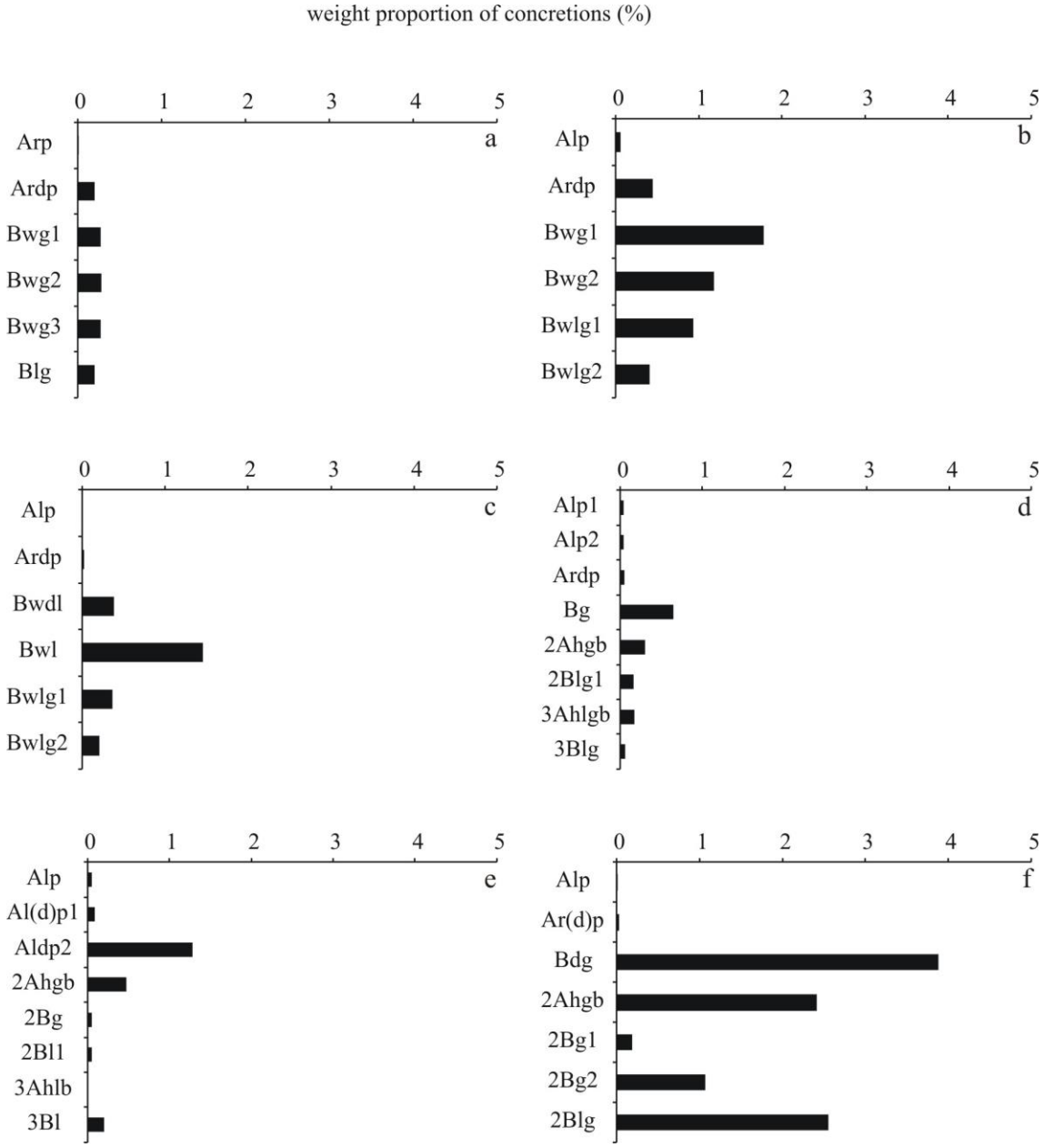

Figure 5.10: Weight proportion of concretions from different paddy sites; a (Paddy 50), b (Paddy 100), c (Paddy 300), d (Paddy 700), e (Paddy 1000), f (Paddy 2000)

Discussion

Results of the described calculations reveal an increasing complexity with increasing time of duration. The fittings between modeling and measurement become more insufficient the longer the period of time is which has to be comprised by the model. Although the decomposition of SOC is a complex process, the applied models were capable of simulating satisfactorily the C dynamics under paddy management for at least the first 300 years of rice cultivation as can be seen by high positive model efficiencies. For paddy sites older than 300 years the model efficiency decreases strongly and the presented simulations are not able to predict observed conditions.

The decomposition rate constants decreased with soil depth (Table 5.2), which is consistent with the common finding that C turnover decreases with increasing soil depth (Flessa et al. 2008; Rumpel et al. 2002). Furthermore, they are comparable with decomposition rate constants observed for other paddy soils. For example, the decomposition rate constants of a puddle layer of a Japanese rice field determined by Lu et al. (2003) ranged from $5.83 \cdot 10^{-1}$ to $7.23 \cdot 10^{-1}$. A comparison with results of other multi-compartment SOM models need to be treated with caution, since most of the existing models are adjusted for ecosystems in temperate climate. However, depending on the number of C pools and their composition, complex models like DAISY, RothC, CENTURY or DNDC deliver decomposition rate constants in a range comparable to the SOC pools in our calculations.

In addition, the model was run with a dataset, which originates from a 50-year old non-paddy site (cf. Table 5.3). Results of the efficiency calculation reveal the applied model parameters as highly inappropriate to simulate the carbon dynamics for upland soils, especially for TOC. The largest deviation appears for topsoil horizons, where the calculated TOC exceeds the observed data by an average factor of 4. Thus, a calibration of the model with a non-paddy dataset delivered significant differences regarding mean residence times of SOC in paddy and non-paddy soils. The matching of measured and calculated values reveals much lower MRT's for *P2* of the non-paddy topsoil (4-7 years) and higher MRT's for *P1* of the non-paddy subsoil (up to 170 years). This indicates significant differences between paddy and non-paddy soils regarding their SOC dynamics,

which can be attributed to the different management practices, which result in distinct soil characteristics.

In this context, one of the most critical points in using a steady-state model is the lack of knowledge regarding the C input history and the assumption of equal carbon input rates (Baisden and Canessa 2013). The applied amounts of OC input in our model were adapted according to values reported by Bronson et al. (1998) and Kimura et al. (2004), which can be assumed to be reasonable for the last decades. But for a period of 2,000 years of paddy management doubts about the reliability of those data are appropriate. In our model, it becomes even more difficult due to the need of the initial partitioning of SOC into two C pools. There is no proper way to estimate the proportion of the annual carbon input on SOC fractions and even more for conceptual SOC pools (Bruun et al. 2005). However, we decided to account the major part of OC input to the more mobile fraction (*P1*). Regarding the consistence of estimated residence times down to at least 1m depth, the paddy management causes differences between soil horizons above and below the plough pan. The apparent decoupling of the topsoil from the subsoil, caused by plough pan formation, is evident by increased MRT's for the deep SOC.

At this point it is not clear what is more crucial for the non-satisfying simulation of the older paddy sites, the duration of paddy management or the disturbed soil profile formation by buried A-horizons. Likely, both factors have to be considered. The influence of time is evident by increased topsoil OC contents with increasing age, which lead to an altered OC supply for the subsoil. Furthermore, the effect of fossil A-horizons is evident by high OC and ^{14}C contents in the subsoil.

Another crucial point that always has to be considered for the comparison of different soil profiles and sampling sites, respectively, is the spatial variability. Several studies pointed out the importance of the spatial-dependence of diverse soil properties. Sumfleth and Duttmann (2008) demonstrated the ability of terrain variables to improve the prediction of soil properties in a Chinese paddy soil landscapes. Accordingly, soil properties like topsoil carbon, nitrogen and silt content showed a significant correlation with different terrain variables. Regression analyses revealed the relative elevation and the distance to nearest flow path as the best predictors for total carbon and nitrogen content of A-horizons. Their findings are in accordance with large scale studies by Liu et al. (2004, 2007) dealing with

the spatial variability of organic matter and nutrients in paddy field landscapes located in Zhejiang Province at the north shore of Hangzhou Bay. The results of this studies indicated that the soil variability increased with the increase in study scale. Although a strong influence of relief parameters can be assumed to be insignificant due to the naturally flat characteristic of our study aera, the spatial variability of soil properties has to be considered in the context of the disability of our model to produce good fittings for the older paddy soils. Thereby, it should be suggested that the 50-year and 100-year old sites, which gave nice fittings, are located very close to each other (cf. Figure 2.1), in sharp contrast to the older paddy sites (300 yrs and older).

By comparing the nearly identical data fits of model A and model B for the P50 site which however, deliver at the same time strongly differing residence times for the stable pool, the question concerning the reliability of conceptual SOC pools arises. Most critical point is the disability to isolate and quantify such conceptual SOC pools (Bruun et al. 2010). Depending on the model parameter which is in focus of the investigation, calculated turnover rates and pool sizes can differ significantly. The differences regarding C pool sizes emerged by model A and model B are negligible, since both approaches result in soil profiles dominated by *P2*. Therefore, the modification of the downward transport rate seems to be of minor influence for C pool sizes. In contrast, the residence times for *P2* of subsoil samples are differing by a factor of 10.

Especially, the C pool size is of importance because estimated residence times are fairly meaningless if the SOC pool, where they belong to, does not exist (cf. model A and B). Thus, we suppose model C as the most appropriate approach to calculate residence times since the obtained pool sizes are in accordance with results, which indicate a fast cycling and more mobile fraction of SOM to be responsible for OC supply to the depth (Bräuer et al. 2013b). Thus, the mobile SOM fraction was determined with an average contribution of close to 50 % of the TOC and decreasing values with increasing depth. This is concordant with the contribution of *P1*, with percentages up to 60 % in the topsoil and average contribution of 31 % to subsoil TOC. Further, results of model C suggest a significant proportion of material not originating from Yangtze River on the deposited sediments, which represent the parent material. Thus, the influence of marine deposits, with higher ^{14}C signatures than the terrestrial material delivered by rivers, has to be accounted.

This becomes even more obvious by taking a look at the exchange rates between soil horizons (*r*) and SOC pools (*p*). Due to the modified composition of the original sediment (more material with higher ^{14}C concentrations), *r* and *p* applied for model C are significant different compared to those of model A and B. Since the stable pool has to gain material from the labile pool to fit measured and simulated values, the young material, which is moving from *P1* to *P2*, has to be provided by an increased transport of fresh SOC from above. Therefore, the increased C fluxes of model C can be explained.

Kalbitz et al. (2013) reported a significant loss of organic carbon in paddy subsoils during the first 50 years after land embankment (330 - 550 kg OC ha^{-1} a^{-1}) and again at later stages of soil development when the organic carbon accrual in the surface soil approached a steady-state level, i.e., after 700 years. Taking account of our calculations, we can confirm the loss of OC in paddy subsoils, especially for the 50-year old site. Model C revealed a loss of ca. 18 % OC within 50 years of rice cultivation (1962: 0.61 kg m^{-2}, 2012. 0.5 kg m^{-2}). Moreover, we can attribute nearly the entire OC loss to the fast cycling SOC pool *P1*, providing that an appropriate content of the original sediment can be accounted to younger material (cf. model C).

However, each of the three models gave mean residence times for *P1* in the order of years. Thus, *P1* can be described as a fast cycling SOC pool including fresh plant material and root exudates. Amundson (2001) defines stabilized C pools as pools with decadal turnover times and passive (inert) C pools as pools with millennial MRT's. Since *P2* comprises both, a stabilized and a passive nature, we assume *P2*, with MRT's between 150 and 2,000 years, as a slow cycling SOC pool. The estimated turnover rates of *P1* reveal the investigated paddy soils as man-made wetlands with significant proportion on a fast cycling SOC pool with residence times in the order of years. Though, the importance of this labile C pool is decreasing with increasing soil depth.

Conclusions

Bulk soil samples related to soil profiles from a chronosequence under paddy management formed on the same uniform ^{14}C depleted estuarine sediments were used to calculate mean residence times of two conceptual C pools. Most relevant findings are:

- The applied simple first-order decomposition models are appropriate tools to describe SOC dynamics in paddy top- and subsoils for the first few hundred years of rice cultivation.
- To obtain high model efficiencies, the models required the implementation of two parameters, *r* and *p*, which take account of different depth levels and the interaction between different SOC pools.
- Calculations of mean residence times and OC stocks confirm the observed loss of OC in paddy subsoils, especially at the beginning of paddy soil development.
- Depending on the depth, the fast cycling SOC pool is characterized by residence times between 1.5 and 21 years, while the stable SOC pool reveals residence times from 150 to 2,000 years.

However, even the simple models applied here suffered from a lack of data. Especially, the insufficient simulation of the older paddy sites could be improved by more detailed information about the carbon input and supply over the last centuries.

Acknowledgement

We thank the German Research Foundation (DFG) for funding this project as part of the Research Unit 995 “Biogeochemistry of Paddy Soil Evolution”. The authors also gratefully acknowledge the support of Prof. Z.-H. Cao (Institute of Soil Science, Chinese Academy of Sciences, Nanjing), who provided the chance to work on the described soil chronosequence and the assistance in the analyses of the team of the Leibniz-Laboratory.

References

Aggarwal PK, Bandhoyapadhyay SK, Pathak H, Kalra N, Chander S, Kumar S. 2000. Analyses of yield trends of the rice–wheat system in north- western India. Outlook Agric. 29, 259-268.

Allison FE. 1973. Soil Organic Matter and Its Role in Crop Production. Elsevier Science, New York.

Amundson R. 2001. The Carbon Budget in Soils. Annual Review of Earth and Planetary Sciences 29, 535-562.

Arora VK, Gajri PR, Uppal HS. 2006. Puddling, irrigation, and transplanting- time effects on productivity of rice-wheat system on a sandy loam soil of Punjab, India. Soil & Tillage Research 85(1-2), 212-220.

Baisden WT, Amundson R, Brenner DL, Cook AC, Kendall C, Harden JW. 2002. A multiisotope C and N modeling analysis of soil organic matter turnover and transport as a function of soil depth in a California annual grassland soil chronosequence. Global Biogeochemical Cycles 16 (4). doi:10.1029/2001GB001823

Baisden WT, Amundson R. 2003. An analytical approach to ecosystem biogechemistry modeling. Ecological Applications 13 (3), 649-663.

Baisden WT, Parfitt RL. 2007. Bomb ^{14}C enrichment indicates decadal C pool in deep soil? Biogeochemistry 85 (1), 59-68. doi:10.1007/s10533-007-9101-7

Baisden WT, Parfitt RL, Ross C, Schipper L, Canessa S. 2011. Evaluating 50 years of time-series soil radiocarbon data: towards routine calculation of robust C residence times. Biogeochemistry. doi:10.1007/s10533-011-9675-y

Baisden WT, Canessa S. 2013. Using 50 years of soil radiocarbon data to identify optimal approaches for estimating soil carbon residence times. Nuclear Instruments and Methods in Physics Research Section B: Beam Interactions with Materials and Atoms 294, 588-592.

Batjes NH. 1996. Total carbon and nitrogen in the soils of the world. European Journal of Soil Science 47, 151-163.

Becker-Heidmann P, Scharpenseel HW. 1992. Studies of soil organic matter dynamics using natural carbon isotopes. Science of the Total Environment 117-118, 305-312.

Bräuer T, Grootes PM, Nadeau MJ, Andersen N. 2013a. Downward carbon transport in a 2000-year rice paddy soil chronosequence traced by radiocarbon measurements. Nuclear Instruments and Methods in Physics Research Section B: Beam Interactions with Materials and Atoms 294, 584-587.

Bräuer T, Grootes PM, Nadeau MJ. 2013b. Origin of subsoil carbon in Chinese paddy soil chronosequence. Radiocarbon 55 (3-4), xxx.

Bronson KF, Cassman KG, Wassmann R, Olk DC, van Noordwijk M, Garrity DP. 1998. Soil carbon dynamics in different cropping systems in principal ecoregions of Asia. In: Lal R, Kimble JM, Follett RF, Stewart BA. (editors). Management of carbon sequestration in soil. Boca Raton, Fla. (USA): CRC Press. p 35-57.

Bruun S, Ågren GI, Christensen BT, Jensen LS. 2010. Measuring and modeling continuous quality distributions of soil organic matter. Biogeosciences 7 (1), 27-41.

Bruun S, Six J, Jensen LS, Paustian K. 2005. Estimating turnover of soil organic carbon fractions based on radiocarbon measurements. Radiocarbon 47 (1), 99-113.

Cassman KG, Pingali PL. 1995. Extrapolating trends from long-term experiments to farmer's fields: the case of irrigated rice systems in Asia. In: Barnett V, Payne R., Steiner R. (Eds.), Agricultural Sustainability. Economic, Environmental and Statistical Considerations. John Wiley and Sons, Chichester, pp. 63–84.

Castanha C, Trumbore S, Amundson R. 2008. Methods of separating soil carbon pools affect the chemistry and turnover time of isolated fractions. Radiocarbon 50 (1), 83-97.

Cheng YQ, Yang LZ, Cao ZH, Ci E, Yin S. 2009. Chronosequential changes of selected pedogenic properties in paddy soils as compared with non-paddy soils. Geoderma 151 (1-2), 31-41.

Cui J, Liu C, Li Z, Wang L, Chen X, Ye Z, Fang C. 2012. Long-term changes in topsoil chemical properties under centuries of cultivation after reclamation of coastal wetlands in the Yangtze Estuary, China. Soil and Tillage Research 123, 50-60.

Dalenberg J, Jager G. 1989. Priming effect of some organic additions to ^{14}C-labelled soil. Soil Biology and Biochemistry 21 (3), 443-448.

Dawe D, Dobermann A, Moya P, Abdulrachman S, Singh B, Lal P, Li SY, Lin B, Panaullah G, Sariam O, Singh Y, Swarup A, Tan PS, Zhen XQ. 2000. How widespread are yield declines in long-term rice experiments in Asia? Field Crops Res. 66, 175-193.

Dawe D, Dobermann A, Ladha JK,Yadav RL, Bao L, Gupta RK, Lal P, Panaullah G, Sariam O, Singh Y, Swarup A, Zhen QX. 2003. Do organic amendments improve yield trends and profitability in intensive rice systems? Field Crops Res. 83, 191-213.

Dobermann A, Dawe D, Roetter RP, Cassman KG. 2000. Reversal of rice yield decline in a long-term continuous cropping experiment. Agron. J. 92, 633-643.

Dreves A. 2008. C-Dynamik in Böden unter forst- und landwirtschaftlicher Nutzung - Untersuchungen mittels Radiokohlenstoff (^{14}C-AMS), Thesis CAU Kiel, p.191.

Elberling B, Breuning-Madsen H, Knicker H. 2013. Carbon sequestration in iron-nodules in moist semi-deciduous tropical forest soil. Geoderma 200-201, 202-207.

Elzein A, Balesdent J. 1995. Mechanistic Simulation of Vertical Distribution of Carbon Concentrations and Residence Times in Soils. Soil Science Society of America Journal 59, 1328-1335

Fageria NK, Carvalhom GD, Santos AB, Ferreira EPB, Knupp AM. 2011. Chemistry of Lowland Rice Soils and Nutrient Availability. Communications in Soil Science and Plant Analysis, 42(16), 1913-1933.

FAO. 2006. Guidelines for soil description. FAO: Rome. 97 p.

FAOSTAT (Food and Agricultural Organization of the United Nations). 2011. Online, URL: http://faostat.fao.org/

Fierer N, Allen AS, Schimel JP, Holden PA. 2003. Controls on microbial CO2 production: a comparison of surface and subsurface soil horizons. Global Change Biology 9, 1322-1332.

Flessa H, Amelung W, Helfrich M, Wiesenberg GLB, Gleixner G, Brodowski S, Rethemeyer J, Kramer C, Grootes PM. 2008. Storage and stability of organic matter and fossil carbon in a Luvisol and Phaeozem with continuous maize cropping: A synthesis. J. Plant Nutr. Soil Sci. 171, 36–51.

Fontaine S, Barot S, Barré P, Bdioui N, Mary B, Rumpel C. 2007. Stability of organic carbon in deep soil layers controlled by fresh carbon supply. Nature 450, 277-280.

Gaudinski JB, Trumbore SE, Davidson EA, Zheng S. 2000. Soil carbon cycling in a temperate forest : radiocarbon-based estimates of residence times, sequestration rates and partitioning of fluxes. Biogeochemistry 51, 33-69.

Goh KM, Rafter TA, Stout JD, Walker TW. 1976. The accumulation of soil organic matter and its carbon isotope content in a chronosequence of soils developed on aeolian sand in New Zealand. Journal of Soil Science 27, 89-100.

Helfrich M, Flessa H, Ludwig B. 2010. Modeling carbon dynamics in subsoils using simple models. Journal of Plant Nutrition and Soil Science 173 (5), 671-677.

Henin S, Dupuis M. 1945. Essai de bilan de la matière organique du sol. Ann. Agron. 15, 17–29.

Huang Y, Sun W. 2006. Changes in topsoil organic carbon of croplands in mainland China over the last two decades. Chinese Science Bulletin 51 (15), 1785-1803.

Iost S, Landgraf D, Makeschin F. 2007. Chemical soil properties of reclaimed marsh soil from Zhejiang Province P.R. China. Geoderma 142, 245-250.

IUSS Working Group WRB. 2007. World reference base for soil resources. World Soil Resources Reports, Vol. 103. FAO: Rome. 145 p.

Janssen BH. 1984. A simple method for calculating decomposition and accumulation of ‘young’ soil organic matter. Plant Soil 76, 297-304.

Jenkinson DS, Harkness D, Vance ED, Adams D, Harrison AF. 1992. Calculating net primary production and annual input of organic matter to soil from the amount and radiocarbon content of soil organic matter. Soil Biology and Biochemistry 24, 295-308.

Jenkinson DS, Coleman K. 2008. The turnover of organic carbon in subsoils. Part 2. Modelling carbon turnover. European Journal of Soil Science 59, 400-413.

Jobbagy EG, Jackson RB. 2000. The vertical distribution of soil organic carbon and its relation to climate and vegetation. Ecological Applications 10 (2), 423-436.

Kalbitz K, Kaiser K, Fiedler S, Kölbl A, Amelung W, Bräuer T, Cao ZH, Don A, Grootes PM, Jahn R, Schwark L, Vogelsang V, Wissing L, Kögel-Knabner I. 2013. The carbon count of 2,000 years of rice cultivation. Global Change Biology, accepted.

Kimura M, Murase J, Lu Y. 2004. Carbon cycling in rice field ecosystems in the context of input, decomposition and translocation of organic materials and the fates of their end products (CO_2 and CH_4). Soil Biology and Biochemistry 36, 1399-1416.

Kögel-Knabner I, Amelung W, Cao Z, Fiedler S, Frenzel P, Jahn R, Kalbitz K, Kölbl A, Schloter, M. 2010. Biogeochemistry of paddy soils. Geoderma 157, 1-14.

Kolenbrander GJ. 1969. De bepaling van de waarde van verschillende soorten organische stof ten aanzien van hun effect op het humusgehalte bij bouwland. Inst. Bodemvruchtb., Haren.

Kondo M, Uchida M, Shibata Y. 2010. Radiocarbon-based residence time estimates of soil organic carbon in a temperate forest: Case study for the density fractionation for Japanese volcanic ash soil. Nuclear Instruments and Methods in Physics Research Section B: Beam Interactions with Materials and Atoms 268 (7-8), 1073-1076.

Kortleven H. 1963. Quantitative aspects of humus accumulation and decomposition. Versl. Landbk. Onderz., vol. 69.1. Pudoc, Wageningen.

Krull ES, Baldock J, Skjemstad JO. 2003. Importance of mechanisms and processes of the stabilisation of soil organic matter for modelling carbon turnover. Functional Plant Biology 30 (2), 207-222.

Kuzyakov Y, Friedel JK, Stahr K. 2000. Review of mechanisms and quantification of priming effects. Soil Biology and Biochemistry 32, 1485-1498.

Ladha JK, Dawe D, Pathak H, Padre AT, Yadav RL, Singh B, Singh Y, Singh Y, Singh P, Kundu AL, Sakal AR, Ram N, Regmi AP, Gami SK, Bhandari AL, Amin R, Yadav CR, Bhattarai EM, Das S, Aggarwal HP, Gupta RK, Hobbs PR. 2003. How extensive are yield declines in long-term rice–wheat experiments in Asia? Field Crops Res. 81, 159-180.

Lal R. 2008. Carbon sequestration. Philosophical transactions of the Royal Society of London. Series B, Biological sciences 363 (1492), 815-30.

Levin I, Naegler T, Kromer B, Diehl M, Francey RJ, Gomez-Pelaez AJ, Steele LP. 2010. Observations and modelling of the global distribution and long-term trend of atmospheric $^{14}CO_2$. Tellus B 62 (1), 26-46.

Li Z, Liu M, Wu X, Han F, Zhang T. 2010. Effects of long-term chemical fertilization and organic amendments on dynamics of soil organic C and total N in paddy soil derived from barren land in subtropical China. Soil and Tillage Research 106, 268-274.

Liu X, Xu J, Zhang M, Zhou B. 2004. Effects of Land Management Change on Spatial Variability of Organic Matter and Nutrients in Paddy Field: A Case Study of Pinghu, China. Environmental Management 34 (5), 691-700.

Liu QH, Shi XZ, Weindorf DC, Yu DS, Zhao YC, Sun WX, Wang HJ. 2006. Soil organic carbon storage of paddy soils in China using the 1:1,000,000 soil database and their implications for C sequestration. Global Biogeochemical Cycles 20 (3), n/a-n/a. doi:10.1029/2006GB002731

Liu X, Zhao K, Xu J, Zhang M, Si B, Wang F. 2007. Spatial variability of soil organic matter and nutrients in paddy fields at various scales in southeast China. Environmental Geology 53, 1139-1147.

Lu Y, Watanabe A, Kimura M. 2003. Carbon dynamics of rhizodeposits, root- and shoot-residues in a rice soil. Soil Biology and Biochemistry 35, 1223-1230.

Nadeau MJ, Schleicher M, Grootes PM, Erlenkeuser H, Gottdang A, Mous DJW, Sarnthein JM. 1997. The Leibniz-Labor AMS facility at the Christian-Albrechts University, Kiel, Germany. Nuclear Instruments and Methods in Physics Research Section B: Beam Interactions with Materials and Atoms 123, 22-30.

Nadeau MJ, Grootes PM, Schleicher M, Hasselberg P, Rieck A, Bitterling M. 1998. Sample throughput and data quality at the Leibniz-Labor AMS facility. Radiocarbon 40 (1), 239-245.

Narang RS, Virmani SM. 2001. Rice–wheat Cropping Systems of the Indo- Gangetic Plain of India. Consortium Paper Series, vol. 11. Rice–wheat Consortium for the Indo-Gangetic Plains, New Delhi.

O´Brien BJ, Stout JD. 1978. Movement and turnover of soil organic matter as indicated by carbon isotope measurements. Soil Biology and Biochemistry 10, 309-317.

Oreskes N. Shrader-Frechette K, Belitz K. 1994. Verification, validation, and confirmation of numerical models in the earth sciences. Science 263, 641-646.

Pan G, Li L, Wu L, Zhang X. 2003. Storage and sequestration potential of topsoil organic carbon in China's paddy soils. Global Change Biology 10, 79-92.

Parnas H. 1975. Model for decomposition of organic material by microorgan- isms. Soil Biol. Biochem. 7, 161-169.

Parton WJ, Schimel DS, Cole CV, Ojima DS. 1987. Analysis of factors controlling soil organic matter levels in Great Plains grasslands. Soil Science Society of America Journal 51 (5), 1173-1179.

Parton WJ, Hartman M, Ojima D, Schimel D. 1998. DAYCENT and its land surface submodel: description and testing. Global and Planetary Change 19, 35-48.

Paustian K. 1994. Modelling soil biology and biochemical processes for sustainable agriculture research. In: Pankhurst, C.E., Doube, D.M., Gupta, V.V.S.R., Grace, P.R. (Eds.), Soil Biota: Management in Sustainable Farming Systems. CSIRO, Canberra, pp. 182-193.

Powlson DS, Olk DC. 2000. Long-term soil organic matter dynamics. In: Kirk, G.J.D., Olk, D.C. (Eds.), Carbon and Nitrogen Dynamics in Flooded Soils. Proceedings of the workshop on Carbon and Nitrogen Dynamics in Flooded Soils. International Rice Research Institute, Los Banõs, pp. 49-63.

Ram N. 1998. Effect of continuous fertilizer use on soil fertility and productivity of a mollisol. In: Swarup, A., Reddy, D.D., Prasad, R.N. (Eds.), Long-term Soil Fertility Management Through Integrated Plant Nutrient Supply. Indian Institute of Soil Science, Bhopal, pp. 229-237.

Ram N. 2000. Long-term effects of fertilizers on rice-wheat-cowpea productivity and soil properties in a Mollisol. In: Abrol, I.P., Bronson, K. F., Duxbury, J.M., Gupta, R.K. (Eds.), Long-term soil fertility experiments with rice-wheat rotations in South Asia. Rice-Wheat Consortium Paper Series 6. Rice-Wheat Consortium for the Indo-Gangetic Plains, New Delhi, India, pp. 50-55.

Rui W, Zhang W. 2010. Effect size and duration of recommended management practices on carbon sequestration in paddy field in Yangtze Delta Plain of China: A meta-analysis. Agriculture, Ecosystems & Environment 135 (3), 199-205.

Rumpel C, Kögel-Knabner I, Bruhn F. 2002. Vertical distribution, age, and chemical composition of organic, carbon in two forest soils of different pedogenesis. Org. Geochem. 33, 1131-1142.

Rumpel C, Kögel-Knabner I. 2011. Deep soil organic matter - a key but poorly understood component of terrestrial C cycle. Plant and Soil 338 (1-2), 143-158.

Rumpel C, Chabbi A, Marschner B. 2012. Carbon storage and sequestration in subsoil horizons: Knowledge, gaps and potentials. In: Lal R, Lorenz K, Hüttl RF, Schneider BU, von Braun J. (editors). Recarbonization of the Biosphere: Ecosystems and the Global Carbon Cycle. Springer Dordrecht, Heidelberg, New York, London. p. 444-464.

Sanderman J, Amundson R. 2008. A comparative study of dissolved organic carbon transport and stabilization in California forest and grassland soils. Biogeochemistry 89 (3), 309-327.

Sauerbeck DR, Gonzalez MA. 1977. Field decomposition of carbon-14-labelled plant residues in various soils of the Federal Republic of Germany and Costa Rica. Soil Organic

Matter Studies. Proceedings of a Symposium Organized by IAEA, FAO and Agrochimica, Braunschweig, vol. I, pp. 159-170.

Scharpenseel HW, Becker-Heidmann P, Neue HU, Tsutsuki K. 1989. Bomb-carbon, ^{14}C-dating and ^{13}C-measurements as tracers of organic matter dynamics as well as of morphogenetic and turbation processes. Science of the Total Environment 81/82, 99-110.

Schimel JP, Wetterstedt JÅM, Holden P, Trumbore SE. 2011. Drying/rewetting cycles mobilize old C from deep soils from a California annual grassland. Soil Biology and Biochemistry 43 (5), 1101-1103.

Schulz E, Breulmann M, Boettger T, Wang KR, Neue HU. 2011. Effect of organic matter input on functional pools of soil organic carbon in a long-term double rice crop experiment in China. European Journal of Soil Science 62, 134-143.

Schwertmann U, Fitzpatrick RW. 1992. Iron minerals in surface environments. In: Skinner, HCW, Fitzpatrick RW. (Eds.). Biomineralization processes of iron and manganese; modern and ancient environments. Cremlingen-Destedt: Catena. pp. 7-30.

Shibu ME, Leffelaar P, Van Keulen H, Aggarwal PK. 2006. Quantitative description of soil organic matter dynamics—A review of approaches with reference to rice-based cropping systems. Geoderma 137, 1–18.

Smith P. Smith JU, Powlson DS, McGill WB, Arah JRM, Chertov OG, Coleman K, Franko U, Frolking S, Jenkinson DS, Jensen LS, Kelly RH, Klein-Gunnewiek H, Komarov AS, Li C, Molina JAE, Mueller T, Parton WJ, Thornley JHM, Whitmore AP. 1997. A comparison of the performance of nine soil organic matter models using datasets from seven long-term experiments. Geoderma 81, 153-225.

Springer U, Lehner AZ. 1952. Organic matter decomposition and humus formation in the aerobic decomposition of agricultural and silvicultural important organic materials I: Zeits. Pflanzenernähr. Düng. Bodenk 58, 193-231.

Stuiver M, Polach HA. 1977. Discussion Reporting of ^{14}C data. Radiocarbon 19 (3), 355-363.

Su J, Wang K. 1989. Changjiang river plume and suspended sediment transport in Hangzhou Bay. Continental Shelf Research 9 (1), 93-111.

Sumfleth K, Duttmann R. 2008. Prediction of soil property distribution in paddy soil landscapes using terrain data and satellite information as indicators. Ecological Indicators 8, 485-501.

Tanji KK, Gao S, Scardaci SC, Chow AT. 2003. Characterizing redox status of paddy soils with incorporated rice straw. Geoderma 114 (3-4), 333-353.

Taylor JP, Wilson B, Mills MS, Burns RG. 2002. Comparison of microbial numbers and enzymatic activities in surface soils and subsoils using various techniques. Soil Biology and Biochemistry 34, 387-401.

Timsina J, Connor D. 2001. Productivity and management of rice-wheat cropping systems: issues and challenges. Field Crops Research 69, 93-132.

Tipping E, Chamberlain PM, Fröberg M, Hanson PJ, Jardine PM. 2012. Simulation of carbon cycling, including dissolved organic carbon transport, in forest soil locally enriched with ^{14}C. Biogeochemistry 108, 91-107.

Trumbore SE, Vogel JS, Southon JR. 1989. AMS ^{14}C measurements of fractionated soil organic matter: an approach to deciphering the soil carbon cycle. Radiocarbon 31 (3), 644-654.

Trumbore SE 1993. Compaison of carbon dynamics in tropical and temperate soils using radiocarbon measurements. Global Biogeochemical Cycles 7 (2), 275-290.

Trumbore SE 2000. Age of soil organic matter and soil respiration: radiocarbon constraints on belowground C dynamics. Ecological Applications 10 (2), 399-411.

Trumbore SE 2009. Radiocarbon and Soil Carbon Dynamics. Annual Review of Earth and Planetary Sciences 37 (1), 47-66.

von Lützow M, Kögel-Knabner I, Ludwig B, Matzner E, Flessa H, Ekschmitt K, Guggenberger G, Marschner B, Kalbitz K. 2008. Stabilization mechanisms of organic matter in four temperate soils: Development and application of a conceptual model. Journal of Plant Nutrition and Soil Science 171, 111-124.

Wang Y, Amundson R, Trumbore S. 1996. Radiocarbon dating of soil organic matter. Quaternary Research 45 (3), 282-288.

Wang Y, Hsieh YP. 2002. Uncertainties and novel prospects in the study of the soil carbon dynamics. Chemosphere 49, 791-804.

Xu S, Shi X, Zhao Y, Yu D, Li C, Wang S, Tan M. 2011. Carbon sequestration potential of recommended management practices for paddy soils of China, 1980-2050. Geoderma 166 (1), 206-213.

Yang HS. 1996. Modelling organic matter mineralization and exploring options for organic matter management in arable farming in Northern China. PhD. thesis, Wageningen Agricultural University, Wageningen.

Zhang W, Xu M, Wang X, Huang Q, Nie J, Li Z, Li S. 2012. Effects of organic amendments on soil carbon sequestration in paddy fields of subtropical China. Journal of Soils and Sediments 12 (4), 457-470.

Zhao QG, Li Z, Xia YF. 1997. Organic carbon storage in soils of southeast China. Nutrient Cycling in Agroecosystems 49, 229-234.

Zou P, Fu J, Cao ZH. 2011. Chronosequence of paddy soils and phosphorus sorption-desorption properties. Journal of Soils and Sediments 11 (2), 249-259.

Chapter VI

Synthesis

Soil organic matter (SOM) has an essential impact on all physical and chemical soil properties and plays a key role regarding both, the agricultural productivity of soils and the global carbon cycle. In acting as a source as well as a sink of atmospheric CO_2, soils are assumed to influence the climate sustainably. Therefore, a detailed understanding of carbon dynamics in soils is crucial. In this context paddy soils are of special interest due to their high SOC sequestration potential. According to IUSS Working Group WRB (2007), paddy soils belong to the group of Anthrosols, which comprise soils that has been formed or heavily modified due to long-term human activity. The required inundated conditions can be obtained by several ways: (i) rain water, (ii) irrigation, (iii) lifting of the groundwater table, and (iv) managed flooding by rivers, which burst its banks. The paddy soils described in this thesis belong to the second group, since they are cultivated as irrigated lowland rice fields. The water is retained by field-surrounding bunds and the percolation of water is hindered by puddling. After a few days of water saturation CO_2, H_2S, N_2O and CH_4 are formed and released due to the domination of anoxic conditions in the topsoil. Mn^{4+} and Fe^{3+} become reduced as well as SO_4^{2-} and NO_{3-}. The redox potential declines strongly, which is linked to a pH increase. After drainage such processes taking place vice versa: pH-values are sinking, Fe and Mn get oxidized and precipitate on the surface of soil cracks. In contrast to the uppermost horizon, the paddy subsoil is hardly affected by the redox potential decline during flooding, so that the zone below the topsoil becomes enriched in Fe and Mn oxides. Such an accumulation of concretions could be observed (cf. Chapter V) for the paddy soils discussed in the preceding chapters.

This study was designed to investigate to what extent low land rice paddy management effects soil organic carbon dynamics with particular attention paid to subsoil carbon. The main emphasis was placed on the development of ^{14}C and TOC gradients depending on the time of duration and the differences between paddy and non-paddy soils caused by diverse management practices. The rapid accumulation of Yangzte River sediments, mainly consisting of eroded terrestrial material (Wang et al. 2008), has led to a fairly

homogeneous estuarine sediment with ca. 0.3 % TOC and a radiocarbon concentration of ca. 50 pMC on which soil development at the various sites of the chronosequence started. The 'old', in ^{14}C depleted signature of the tidal flat provided the unique opportunity to study the uptake and transport of OC with atmospheric ^{14}C composition.

Evolution of TOC and ^{14}C depth gradients

The ^{14}C concentrations of TOC in the soils of the chronosequence indicate a rapid transformation of the original sediment. The uppermost topsoil horizons of both, paddy and non-paddy, show a replacement within decades of the carbon from the parent material with organic carbon derived from the recent atmosphere. Already after 50 years of tillage the influence on the depth distribution of SOM caused by management practices associated with the cultivation of irrigated low land rice is distinguishable.

Non-paddy soils show high ^{14}C values in topsoil horizons and a nearly constant decrease with increasing soil depth down to the lowest ^{14}C values in the subsoil. The observed radiocarbon concentrations range from 103.27 pMC (modern) in the Ap (NP700) to 45.75 pMC (6281 years BP) in the deepest subsoil horizon of the NP50 (Table A1). All non-paddy soils show a strong correlation between the measured ^{14}C activity and the content of total organic carbon in the soil horizons (Figure A2). This indicates that young carbon is located in horizons with high carbon concentrations. Thus, non-paddy soil shows the customary 'age' -depth profile, as reported frequently (Scharpenseel et al. 1989; Paul et al. 1997; Rumpel et al. 2002; Eusterhues et al. 2003; Krull and Skjemstad 2003; Rumpel and Kögel-Knabner 2011; Laskar et al. 2012). Furthermore, the perception of decreasing ^{14}C contents with increasing depth could be confirmed by radiocarbon measurements of additional samples, which were taken in March, 2010. The first profile was excavated behind a dike, which was constructed in 1977. Therefore, soil profile formation takes places since ca. 30 years. The area is equipped with ponds for fish and crab farming. The second sample set was taken on a wheat field, which was also located behind the '1977'-dike but closer to the next older dike (constr. 1958). Results of both additional non-paddy profiles are given in figure A3. he reasons for the repeatedly described decrease of ^{14}C concentrations with depth are still not completely understood (Trumbore 2009). It is assumed that carbon compounds with long residence times, which are found in subsoil horizons in high concentrations, are responsible for high radiocarbon ages of deep soil

organic matter (Rumpel and Kögel-Knabner 2011). However, even recently synthesized, chemically labile carbon compounds can be characterized by high ^{14}C ages, due to the re-use and recycling of old, stabilized SOC in subsoils by microbial biomass (Rethemeyer et al. 2005). Furthermore, the supply of young carbon derived from plant litter into the subsoil is limited and led to a higher contribution of carbon resisting decomposition due to recalcitrance or adsorption to the mineral phase compared to topsoil horizons (Sollins et al. 1996). Due to the soil profile development on a sedimentary parent material, the explanation for low ^{14}C activity in subsoils given by Paul et al. (2001) and Helfrich et al. (2007) has to be accounted for our paddy and non-paddy soils as well. Both studies found high ^{14}C ages for resistant SOC in loess derived parent materials. Thus, a low ^{14}C activity could be attributed to the influence of SOC that was not formed *in situ*, but originally associated with the parent material. Therefore the contribution of old, reworked, maybe geogenic carbon (dead carbon) to the TOC has to be considered for the development of the observed ^{14}C depth gradients with low radiocarbon values (avg. over all profiles: 5,900 years BP) at the lowest depth in the soil profiles of our study area.

The ^{14}C depth profile of the contemporaneous paddy soil is strongly affected by the management-induced establishment of a dense, slightly permeable layer - the plough pan. The plough pan has a high mechanical strength and low hydraulic conductivity and therefore, controls the water regime of the underlying horizons (Chen and Liu 2002). Consequently, the downward transport and relocation of SOM through the plough pan is strongly diminished. This results in an observed ^{14}C depth gradient of the youngest paddy soil which is designated by a bisection of the radiocarbon content within several centimeters (Table A1). The radiocarbon content above the plough pan amounts 101.48 pMC and nine cm below, beneath the plough pan, the bulk soil contains 49.81 pMC. This large shift in ^{14}C within a relative small depth range decreases with increasing time of duration until it disappears completely. The assumption of a plough pan development which is well advanced within the first decades of paddy soil evolution is also indicated by the bulk density profiles (Wissing et al. 2011). Bulk densities between 0.9 - 1.2 g cm^{-3} were found in all puddled topsoil horizons. The highest bulk densities were measured in the plow pan (1.4 - 1.6 g cm^{-3}). Within the subsoil horizons the bulk densities slightly decrease, whereat the obtained values do not show a chronological trend. In contrast, the non-paddy soils are characterized by a more homogeneous distribution of bulk density with values ranging from 1.3 - 1.5 g cm^{-3}. However, results from Janssen and Lennartz

(2007) also indicate that the maturing process of the plough pan may take several decades. They reported infiltration rates from a plough pan of a loamy paddy soil, which decreased 35-fold after 20 years of cultivation and 175-fold after 100 years of cultivation.

According to the finding of a ^{14}C-documented plough pan formation of this study, OC contents higher in paddy topsoils than in non-paddy topsoils were quantified. This is in accordance with earlier results, as reported by Kögel-Knabner et al. (2010). It is still subject of discussion whether the increased SOC contents are caused by high organic matter input or by retarded decomposition rates (Neue et al. 1997; Kirk and Olk 2000; Tanji et al. 2003). However, topsoil OC stocks increase with slight variations with increasing time of duration. Aside from the plots including fossil A-horizons, all paddy soils show a correlation between the measured ^{14}C activity and the content of total organic carbon in the soil horizons as strong as the non-paddy soils (Figure A1).

The described plough pan formation leads to an apparent decoupling between topsoil and subsoil. Especially the subsoil horizons located below the plough pan will be discussed in the following. In general, subsoil horizons attracted more attention during the last years (Rumpel and Kögel-Knabner 2011; Rumpel et al. 2012). The increased accumulation of OC in paddy topsoils does not inevitably lead to a higher OC content in the paddy subsoil, even after 2,000 years of rice cultivation. Results for subsoil samples of paddy soils reveal increasing ^{14}C concentrations at constant or decreasing OC values. This vertical gradients, connected to the plough pan, document the replacement of original estuarine organic carbon by organic matter transported from above. Thus, the observed characteristic vertical distribution of SOC develops with paddy soil evolution and the presented age-depth profiles are the result of post-depositional transport processes. This finding emphasizes the importance of vertical OC relocation regarding the development of soil profiles on uniform sediments and the SOC dynamics under paddy management. However, ^{14}C depth gradients of the older paddy soils which start to match to those of the non-paddy soils indicate an increased penetration of OC with higher ^{14}C values. This confirms the findings of Sander and Gerke (2007), who demonstrated the occurrence of preferential flow in paddy rice fields. They conducted a dye tracer experiment on two rice fields located in the Sunjian watershed in the southeast China (Jiangxi province). The experiment demonstrated that the puddling and thus, plough pan formation did not completely destroy the connectivity of pathways in the plough pan. This is in accordance with ^{14}C results of this study, which

suggest a disturbed but not totally prevented penetration of fresh OC into the paddy subsoil horizons. ^{14}C and TOC results of different aged paddy soils suggest well mixed topsoils and a reduced OC transport through the low-permeability plough pan. Thus, the specific paddy management (e.g. puddling) seems to play a key role in the formation of OC depth profiles and ^{14}C depth profiles reflect a dynamic equilibrium between OC import, export, and stabilization on a time scale of decades.

Origin of subsoil OC

In a next step this study aimed to abolish the lack of knowledge regarding the components of SOC which are responsible for the observed organic carbon replacement in paddy subsoils. In general, four different sources of organic matter input into subsoils are widely recognized: plant roots, root exudates, dissolved organic carbon (DOC) and bioturbation. The input of plant-derived organic carbon into the soil can be distinguished. The first source of the carbon input into soils comprises all organic carbon released by living roots. Organic substances like water-soluble exudates, secretions, lysates, mucilages and sloughed-off cells are discharged continuously during the life of plants and are referred to as rhizodeposits (Lu et al. 2003). After plant death, root and shoot remains represent the second source of C input and contribute to the accumulation of soil organic matter in subsoils (Kuzyakov and Domanski 2000). The high potential to be stabilized in soils indicates the importance of roots for SOC sequestration (Rasse et al. 2006). The longevity of roots was determined with a mean age up to 18 years (Gaudinski et al. 2001). Despite the importance of roots as a subsoil C source, our knowledge on the carbon input by roots into soils is still incomplete due to uncertainties regarding the measurement of total root C input caused by low concentrations of root-derived organic substances in soils and fast decomposition of organic substances released from roots by microorganisms (Kuzyakov and Domanski 2000). However, Kleja et al. (2008) estimated roots and DOC equally important for OC supply into soils of a northern hardwood forest.

Organic matter as constituent of DOC has been identified as crucial for the translocation of pollutants, metals and nutrients in soils (Kaiser and Kalbitz 2012). Furthermore, DOC is considered to be the main source of deep SOC, especially under humid climate conditions (Kaiser and Guggenebrger 2000). Results reported by Baisden et al. (2002) indicate DOC transport as an important process in annual grassland ecosystems. The frequently observed

negative correlation between DOC concentrations and soil depth is attributed to the retention in the mineral soil by adsorption (Qualls and Haines 1992; Kaiser and Zech 1997). Strahm et al. (2009) disclosed the potential influence of land-use and management on DOC fluxes. Regarding paddy soils, especially soil cracks can be considered as important part of the macropore system, which facilitates water flow (Wopereis et al. 1994). Cracks may develop in the surface of paddy fields due to continuous drying after drainage and harvesting (Liu et al. 2003). The fourth C source for subsoils is the downward movement of SOM through bioturbation. Arthropods, earthworms, ants, termites and tree roots are efficient in forming voids in form of burrows, nests, chambers and root channels (Paton et al. 1995; Lavelle et al. 1997). The input of SOC in subsoils via such biopores is affected directly as well as indirectly by bioturbation (Wilkinson et al. 2009). Litter sequestration into nests, borrows etc. and animal waste disposal in form of dead tissues represent direct inputs. Indirect inputs of SOC into subsoils may occur by redistribution of SOC and subsurface mixing and burial. In addition there may be translocation of particulate organic matter and transport of clay-bound organic matter in certain soil types considered as fifth C input source (Rumpel and Kögel-Knabner 2011). Particulate organic matter such like black carbon seems to migrate easily into deeper soil horizons (Dai et al. 2006; Rumpel et al. 2009). Bioturbation can enhance the migration of such particles.

The relative importance of the different OC input sources is dependent on climatic parameters, soil inherent processes, vegetation types and land-use. In subsoil horizons, environmental conditions are supposed to be different from those in topsoil horizons, and SOC storage may be driven by specific processes (von Lützow et al. 2006). To reveal the most important SOC source for paddy subsoils the entire SOC pool was chemically fractionated into SOM fractions of different mobility, whereat the fulvic acid fraction, which is assumed to be the most mobile fraction among the three groups of humic substances, was revealed as the main driver for the input of organic matter into the subsoil. Since fulvic acids are the major component of dissolved organic matter (Stevenson 1994; Maie et al. 2004), the relocation of organic matter through the plough pan via mobile SOC fractions transported by percolating water is assumed to be a major process of subsoil ‘OC-refreshing’ in paddy soils. This is approved due to the high content of mobile SOC fractions on the total organic carbon in the investigated paddy soils (cf. Chapter IV).

A necessary precondition for the downward movement of DOC is the existence of an efficient system of preferential flow paths. The occurrence of such a network of cracks and biopores in paddy soils far below the compacted plough pan was described by Sander and Gerke (2007). The dye tracer experiments, already mentioned above, reveal losses of water and dissolved chemicals through the plough pan despite repeated soil structure destruction and soil compaction by puddling. It was shown that water movement occurs through preferential flow paths that are strongly correlated with the observed cracks and biopores (Lennartz et al. 2009). These earlier results, together with the ^{14}C data obtained in this study indicate puddling as a management procedure that does not necessarily prevent preferential flow in paddy fields and does not completely destroy the hydraulic continuity of macropores in the plow pan. Thus, preferential flow has to be considered as a relevant factor for water, nutrient and carbon cycling in paddy soils. Further indicators for the importance of DOC, in context of subsoil OC supply, are the large DOC concentrations and fluxes found in paddy soils. Katoh et al. (2004) gave fluxes of DOC in the field during a 98-day study between 320 and 630 kg DOC ha^{-1} a^{-1}. This percolation from the puddle layer into the subsoil exceeds the large fluxes from Oa horizons of forest soils (100-400 kg C ha^{-1} a^{-1}) under temperate climate (Michalzik et al. 2001). Also Maie et al. (2004) described the main part of subsoil organic matter in paddy soils as leached dissolved organic matter originating from the plough pan (200 kg C ha^{-1} in approx. 4 month). The long periods with anaerobic conditions in the A horizon are supposed to be the reason for these large DOC fluxes in paddy soils. Thus, the less efficient decomposition of organic matter under anaerobic conditions favors the enrichment of water-soluble metabolites as organic anions like acetate, formate, propionate and lactate (Ponnamperuma 1972; Moore and Dalva 2001; Fiedler and Kalbitz 2003; Sahrawat 2004).

In addition to the supply of fresh OC to paddy subsoils by DOC this study disclose another pathway for organic matter into paddy subsoils via direct input of OC by plant roots and their exudates. Root exudates are of significant importance for the OC supply of subsoils (Vranova et al. 2013). More than 40 % of the net carbon fixed during photosynthesis can be released into the rhizosphere including root respiration (Singh et al. 2004; Dennis et al. 2010). Roots and plant remains with modern radiocarbon signatures were discovered far below the plough pan. DNA analysis of root samples revealed even rice (*Oryza sativa*) as a contributor to this OC supply. To our knowledge, this is the first attempt to identify plant remains, found in deep paddy subsoil horizons, by DNA extraction and 18S rDNA

analysis. Unfortunately we're not able to determine the pathway by which the plant remains reached the observed depths, either direct growing/rooting or vertical relocation by dropping into macropores. Likely, both processes take part in the subsoil OC supply. Biopores, which were observed in the field, and cracks that form when the soils run dry facilitate root penetration below the plough pan. The same macropore system could be responsible for the downward movement of dead plant material following gravity. Thus, the presence of roots in deep subsoil horizons, including those of rice, indicates that young carbon may be inserted directly into the subsoil as root material/root exudates and is a result of both, dynamic (cracks and root channels) and relative static (earthworm burrows) macropore development.

Despite the described input of fresh organic matter into deep subsoil horizons, organic carbon concentrations in the subsoil remain largely constant or slightly decrease across the chronosequence. At the same time the ^{14}C contents increase. According to this the composition of subsoil organic carbon down to 1 m depth of the investigated paddy soils is determined by a dynamic equilibrium between the import of fresh organic matter, mineralization, and export into groundwater and deeper subsoils. This finding is in contradiction to reports by Zhang and He (2004) and Li et al. (2005) which described an accumulation of organic carbon in paddy subsoils. However, the same authors suggest, now in accordance with our results, the subsoil OC to be transported from above as dissolved organic carbon. It shows that the spatially heterogeneous distribution of fresh organic carbon seems to be one of the most important factors in determining SOM dynamics. Therefore, pedological processes like preferential flow and bioturbation, which influence the OC distribution in soils has to be considered for the investigation of SOC dynamics. In accordance with previous studies we revealed dissolved organic matter and root biomass as main sources of subsoil organic matter.

Estimation of SOC turnover rates

In chapter V the vertical distribution of C and ^{14}C was estimated by modeling transport mechanisms of SOM. To investigate SOM dynamics in subsoils, applied models need to address the downward movement of C and its stability in deep soil layers (Rumpel and

Kögel-Knabner 2011). Numerous studies revealed radiocarbon to be an appropriate tracer for SOM turnover investigations (O'Brien and Stout 1978; Goh et al. 1976; Scharpenseel et al. 1989; Trumbore et al. 1989; Elzein and Balesdent 1995; Gaudinski et al. 2000; Baisden et al. 2002; Bruun et al. 2005; Castanha et al. 2008; Sanderman and Amundson 2008; Kondo et al. 2010; Schimel et al. 2011; Baisden and Canessa 2013).

Radiocarbon concentrations of total organic carbon indicate a rapid turnover, especially in paddy topsoils (Scharpenseel et al. 1996). This conclusion is confirmed by a recovered fast cycling SOC pool. Depending on the applied model parameters and the sampling depth, the mean residence times of this labile C pool range between 1.5 and 21 years. Thus, calculations of turnover rates, using different parameters and initial values, reveal fairly comparable residence times for both, the labile and the stable SOC pool. However, significant variations regarding the modeled C pool sizes were found. Estimations of C turnover rates, using an abundant initial proportion of parent material highly depleted in ^{14}C (model A and B), reveal the exceedingly importance of a stable SOC pool with residence times of at least 200 years. With regards to the subsoil horizon, the absolutely predominant C pool comprises merely slow cycling carbon. This is in accord with the conclusion made by Brovkin et al. (2008), who attributed most of soil organic carbon to a millennial time scale. Only in paddy topsoils, the labile SOC pool reaches noteworthy percentages up to 35 %. In this context the age of the investigated paddy soil influences the size of the fast cycling C pool, since the labile pool is represented more strongly in the younger paddy topsoils. Turnover rates and mainly SOC pool sizes, ascertained by model A and B, suggest the predominance of a slow cycling SOC pool caused by the pre-existing parent material, which contains mainly old reworked carbon. This 'overprinting' effect can not be compensated by the revealed input of fresh organic matter described in chapter IV.

Modification of the assumed tidal flat composition regarding the ^{14}C signature, now with a decreased content of ^{14}C-depleted material (c.f. model C), results in an increased significance of the more active SOC pool. The proportion of the fast cycling C pool exceeds 50 % in all topsoil, and yet below the plough pan the labile pool comprises more than a third of TOC. In consideration of previous results (cf. chapter IV) the estimations generated by model C are assumed to be the most reliable depiction of the intrinsic composition and distribution of SOC in paddy soils. Thus, calculations conducted by

model C reinforce the idea of rapid C cycling in paddy soils due to high 'bomb-^{14}C' inputs to larger depths and low C residence times (Scharpenseel et al. 1996).

To obtain SOC pool sizes estimated by model A and B comparable to SOC pools delivered by model C, we assume the OC input into the topsoil as the pivotal parameter. An increased carbon input, considered for model A and B, may affect the size of its labile SOC pool and abolish the predominance of the slow cycling stabilized SOC pool caused by the parent material composition. Consequently, model A and B could be able to produce results in accordance with model C regarding the SOC pool sizes. Nevertheless, model C seems to be more reliable since there are no evidences for an increased OC input. Thus, we assume an initial sediment composition with significant proportions of marine deposits as more likely than a strong increase in OC supply to the topsoil.

Baisden et al. (2011) estimated C turnover rates for a New Zealand silt loam soil under pasture. The authors assume the modeled active C pool to be negligible due to its relative small size and the large size of a pool with decadal turnover rates. In contrast to that, the fast cycling SOC discovered in the investigated paddy soils has to be considered for calculating residence times, due to the appreciable size of the labile SOC pool in paddy topsoils, as well as in subsoils, and the lack of a moderate stabilized C pool. In summary, the results presented in chapter III to V suggest a dynamic balance of OC fluxes, rather than a long-term stabilization of SOC.

Conclusions

- Differences in soil profile formation caused by paddy and non-paddy management are most distinct in the first decades of rice cultivation.

- Rice paddy management affects SOC distribution and dynamics for both, topsoils and subsoils. Topsoils are characterized by increased OC contents compared to non-paddy soils. In spite of a reduced transport of OC through the plough pan subsoils are characterized by a ^{14}C-documented replacement of 'old' carbon by 'modern' carbon over time.

- The development of a dense plough pan does not lead to a decoupling between topsoil and subsoil. Results reveal a time dependence regarding SOC dynamics.

- The observed TOC and ^{14}C gradients are the result of OC mobility and relocation.

- Two processes of paddy subsoil 'OC-refreshing' could be identified: (i) Relocation and transport of young OC through the plough pan via mobile SOC fractions (humic acids and fulvic acids). Due to their high proportion on total organic carbon, we assume fulvic acids to be the main driver for the input of OC into the subsoil. (ii) Input of fresh (modern) OC into deep subsoil horizons by plant roots and their exudates, either by direct rooting into depth or by downward movement of plant remains into the subsoil through animal activity and soil cracking This process is evident by roots and root remains, including rice roots identified by their DNA signature, with modern ^{14}C signature found far below the plough pan in deep soil horizons.

- Total SOC of the entire soil profiles could be divided into two conceptual C pools by means of mean residence time calculations.

- Due to the implementation of two parameters (r and p), which take account of different depth levels and the interaction between different SOC pools, the applied simple first-order decomposition models turned out to be appropriate tools to describe SOC dynamics in paddy topsoils as well as subsoils for the first few hundred years of rice cultivation.

- Depending on the depth, the fast cycling SOC pool is characterized by residence times between 1.5 and 21 years, while the stable SOC pool reveals residence times from 150 to 2,000 years.

- Results of this study reveal increased OC contents for paddy topsoils and slightly decreased OC contents for paddy subsoils. This suggests a dynamic balance of OC fluxes, rather than a long-term stabilization of SOC.

Outlook

Future studies should investigate further mechanisms of SOM transformation and stabilization to get a deeper insight into the carbon dynamics of paddy soils. For this purpose specific SOM compounds (e.g. organo-mineral complexes, lipids and amino acids) should be used for radiocarbon dating. The comparison with ^{14}C data of macrofossils will reveal the vertical mobility of the various compounds within the soil profile. Radiocarbon concentrations of several meaningful soil organic matter pools could be used as a measure of their role in the dynamic SOC cycling.

To obtain a better understanding of the general chronology of paddy soil profiles, macrofossils (charcoal, grains, shells etc.) should be identified and measured. This will help to determine a real age of a soil horizon and will expand our knowledge of vertical transport of macro remains.

Since the mechanisms which are responsible for the transport of organic matter into subsoil horizons and the processes leading to retarded decomposition of organic matter in subsoil horizons are still understood only in parts, more studies should be carried out to quantify SOM input into subsoils (roots growth, DOC perculation and bioturbation). More accurate measurements of deep C inputs and deep C losses are needed to design subsoil C models. Moreover, pedological characteristics has to be related to the factors which govern the decomposition of subsoil SOM.

Considering the outstanding importance of rice as a staple food provider and the worldwide distribution of rice cultivation, we suggest the investigation of paddy soil formation on different substrates as essential for a comprehensive understanding of SOC dynamics and the biogeochemistry of soils under paddy management. Thus, the study of paddy soils developed on different parent materials under different hydrological and climatic conditions could help to distinguish between the influence of soil type and climate and the affect of management practices.

References

Baisden WT, Amundson R, Brenner DL, Cook AC, Kendall C, Harden JW. 2002. A multiisotope C and N modeling analysis of soil organic matter turnover and transport as a function of soil depth in a California annual grassland soil chronosequence. Global Biogeochemical Cycles 16 (4). doi:10.1029/2001GB001823

Baisden WT, Parfitt RL, Ross C, Schipper L, Canessa S, 2011. Evaluating 50 years of time-series soil radiocarbon data: towards routine calculation of robust C residence times. Biogeochemistry. doi:10.1007/s10533-011- 9675-y.

Baisden WT, Canessa S. 2013. Using 50 years of soil radiocarbon data to identify optimal approaches for estimating soil carbon residence times. Nuclear Instruments and Methods in Physics Research Section B: Beam Interactions with Materials and Atoms 294, 588-592.

Brovkin V, Cherkinsky A, Goryachkin S. 2008. Estimating soil carbon turnover using radiocarbon data: A case-study for European Russia. Ecological Modelling 216, 178-187.

Bruun S, Six J, Jensen LS, Paustian K. 2005. Estimating turnover of soil organic carbon fractions based on radiocarbon measurements. Radiocarbon 47 (1), 99-113.

Castanha C, Trumbore S, Amundson R. 2008. Methods of separating soil carbon pools affect the chemistry and turnover time of isolated fractions. Radiocarbon 50 (1), 83-97.

Chen S, Liu CW. 2002. Analysis of water movement in paddy rice fields (I) experimental studies. Journal of Hydrology 260, 206-215.

Dai J, Ran W, Xing B, Gu M, Wang L. 2006. Characterization of fulvic acid fractions obtained by sequential extractions with pH buffers, water, and ethanol from paddy soils. Geoderma 135, 284-295.

Dennis PG, Miller AJ, Hirsch PR. 2010. Are root exudates more important than other source of rhizodeposits in structuring rhizosphere bacterial communities? FEMS Microbiol. Ecol. 72, 313–327.

Elzein A, Balesdent J. 1995. Mechanistic Simulation of Vertical Distribution of Carbon Concentrations and Residence Times in Soils. Soil Science Society of America Journal 59, 1328-1335.

Eusterhues K, Rumpel C, Kleber M, Kögel-Knabner I. 2003. Stabilisation of soil organic matter by interactions with minerals as revealed by mineral dissolution and oxidative degradation. Organic Geochemistry 34, 1591-1600.

Fiedler S, Kalbitz K. 2003. Concentrations and properties of dissolved organic matter in forest soils as affected by the redox regime. Soil Sci. 168, 793-801.

Gaudinski JB, Trumbore SE, Davidson EA, Zheng S. 2000. Soil carbon cycling in a temperate forest : radiocarbon-based estimates of residence times, sequestration rates and partitioning of fluxes. Biogeochemistry 51, 33-69.

Gaudinski JB, Trumbore SE, Davidson EA, Cook AC, Markewitz D, Richter DD. 2001. The age of fine-root carbon in three forests of the eastern United States measured by radiocarbon. Oecologia 129, 420-429.

Goh KM, Rafter TA, Stout JD, Walker TW. 1976. The accumulation of soil organic matter and its carbon isotope content in a chronosequence of soils developed on aeolian sand in New Zealand. Journal of Soil Science 27, 89-100.

Helfrich M, Flessa H, Mikutta R, Dreves A, Ludwig B. 2007. Comparison of chemical fractionation methods for isolating stable soil organic carbon pools. European Journal of Soil Science 58, 1316-1329.

IUSS Working Group WRB. 2007. World reference base for soil resources. World Soil Resources Reports, Vol. 103. FAO: Rome. 145 p.

Janssen M, Lennartz B. 2007. Horizontal and vertical water and solute fluxes in paddy rice fields. Soil Till. Res. 94, 133–141.

Kaiser K, Kalbitz K. 2012. Cycling downwards - dissolved organic matter in soils. Soil Biology and Biochemistry 52, 29-32.

Kaiser K, Guggenberger G. 2000. The role of DOM sorption to mineral surfaces in the preservation of organic matter in soils. Organic Geochemistry 31, 711-725.

Kaiser K, Zech W. 1997. Competitive sorption of dissolved organic matter fractions to soils and related mineral phases. Soil Sci Soc Am J 61, 64-69.

Katoh M, Murase J, Hayashi M, Matsuya K, Kimura M. 2004. Nutrient Leaching from the Plow Layer by Water Percolation and Accumulation in the Subsoil in an Irrigated Paddy Field. Soil Science and Plant Nutrition 50, 721-729.

Kirk G, Olk, DC. 2000. Carbon and Nitrogen Dynamics in Flooded Soils. IRRI, Los Banos, Philippines, p. 194.

Kleja DB, Svensson M, Majdi H, Jansson PE, Langvall O, Bergkvist B, Johansson MB, Weslien P, Truusb L, Lindroth A, Ågren GI. 2007. Pools and fluxes of carbon in three Norway spruce ecosystems along a climatic gradient in Sweden. Biogeochemistry 89, 7-25.

Kögel-Knabner I, Amelung W, Cao Z, Fiedler S, Frenzel P, Jahn R, Kalbitz K, Kölbl A, Schloter M. 2010. Biogeochemistry of paddy soils. Geoderma 157, 1-14.

Kondo M, Uchida M, Shibata Y. 2010. Radiocarbon-based residence time estimates of soil organic carbon in a temperate forest: Case study for the density fractionation for Japanese volcanic ash soil. Nuclear Instruments and Methods in Physics Research Section B: Beam Interactions with Materials and Atoms 268 (7-8), 1073-1076.

Krull ES, Skjemstad JO. 2003. $\delta^{13}C$ and $\delta^{15}N$ profiles in ^{14}C-dated Oxisol and Vertisols as a function of soil chemistry and mineralogy. Geoderma 112, 1-29.
Kuzyakov Y, Domanski G. 2000. Carbon input by plants into the soil - Review. Journal of Plant Nutrition and Soil Science 163, 421-431.

Laskar A, Yadava M, Ramesh R. 2012. Radiocarbon and stable carbon isotopes in two soil profiles from northeast india. Radiocarbon 54, 81-89.

Lavelle P, Gignell D, Lepage M, Wolters V, Roger P, Ineson P, Heal OX, Dhillion OW. 1997. Soil function in a changing world: the role of invertebrate ecosystem engineers. Eur J Soil Sci 33, 159-193.

Lennartz B, Horn R, Duttmann R, Gerke HH, Tippkötter R, Eickhorst T, Janssen I, Janssen M, Rüth B, Sander T, Shi X, Sumfleth K, Taubner H, Zhang B. 2009. Ecological safe management of terraced rice paddy landscapes. Soil and Tillage Research 102, 179-192.

Li ZP, Zhang TL, Li DC, Velde B, Han FX. 2005. Changes in soil properties of paddy fields across a cultivation chronosequence in subtropical China. Pedosphere 15, 110-119.

Liu CW, Cheng SW, Yu WS, Chen SK. 2003. Water infiltration rate in cracked paddy soil. Geoderma 117, 169-181.

Lu Y, Watanabe A, Kimura M. 2003. Carbon dynamics of rhizodeposits, root- and shoot-residues in a rice soil. Soil Biology and Biochemistry 35, 1223-1230.

Maie N, Watanabe A, Kimura M. 2004. Chemical characteristics and potential source of fulvic acids leached from the plow layer of paddy soil. Geoderma 120, 309-323.

Michalzik B, Kalbitz K, Park J, Solinger S, Matzner E. 2001. Fluxes and concentrations of dissolved organic carbon and nitrogen - a synthesis for temperate forests. Biogeochemistry 52, 173-205.

Moore TR, Dalva M. 2001. Organic controls on the release of dissolved organic carbon by plant tissues and soils. Soil Science 166, 38-47.

Neue HU, Gaunt J, Wang Z P, Becker-Heidmann P, Quijano C. 1997. Carbon in tropical wetlands. Geoderma 79, 163-185.

O´Brien BJ, Stout JD. 1978. Movement and turnover of soil organic matter as indicated by carbon isotope measurements. Soil Biology and Biochemistry 10, 309-317.

Paton TR, Humphreys GS, Mitchell PB. 1995. Soils: a new global view. UCL, London, pp. 213.

Paul EA, Collins HP, Leavitt SW. 2001. Dynamics of resistant soil carbon of Midwestern agricultural soils measured by naturally occurring ^{14}C abundance. Geoderma 104, 239-256.

Paul EA, Follett RF, Leavitt SW, Halvorson A, Petersen GA, Lyon DJ. 1997. Radiocarbon dating for determination of soil organic matter pool sizes and dynamics. Soil Science Society of America Journal 61, 1058-1067.

Ponnamperuma FN. 1972. The chemistry of submerged soils. Advanced Agron. 24, 29-96.

Qualls RG, Haines BL. 1992. Biodegradability of dissolved organic matter in forest throughfall, soil solution and stream water. Soil Sci Soc Am J 56, 578-586.

Rasse DP, Mulder J, Moni C, Chenu C. 2006. Carbon Turnover Kinetics with Depth in a French Loamy Soil. Soil Science Society of America Journal 70, 2097-2105.

Rethemeyer J, Kramer C, Gleixner G, John B, Yamashita T, Flessa H, Andersen N, Nadeau MJ, Grootes PM. 2005. Transformation of organic matter in agricultural soils: radiocarbon concentration versus soil depth. Geoderma 128, 94-105.

Rumpel C, Kögel-Knabner I, Bruhn F. 2002. Vertical distribution, age, and chemical composition of organic carbon in two forest soils of different pedogenesis. Organic Geochemistry 33, 1131-1142.

Rumpel C, Ba A, Darboux F, Chaplot V, Planchon O. 2009. Erosion budget of pyrogenic carbon at meter scale and process selectivity. Geoderma 154, 131-137.

Rumpel C, Kögel-Knabner I. 2011. Deep soil organic matter - a key but poorly understood component of terrestrial C cycle. Plant and Soil, 338(1-2), 143-158.

Rumpel C, Chabbi A, Marschner B. 2012. Carbon storage and sequestration in subsoil horizons: Knowledge, gaps and potentials. In: Lal R, Lorenz K, Hüttl RF, Schneider BU, von Braun J. (Eds.), Recarbonization of the Biosphere: Ecosystems and the Global Carbon Cycle. Springer Dordrecht, Heidelberg, New York, London. p. 444-464.

Sahrawat KL. 2004. Organic matter accumulation in submerged soils. Adv. Agron. 81, 169-201.

Sander T, Gerke HH. 2007. Preferential Flow Patterns in Paddy Fields Using a Dye Tracer. Vadose Zone Journal 6, 105-115.

Sanderman J, Amundson R. 2008. A comparative study of dissolved organic carbon transport and stabilization in California forest and grassland soils. Biogeochemistry 89 (3), 309-327.

Scharpenseel HW, Becker-Heidmann P, Neue HU, Tsutsuki K. 1989. Bomb-carbon, ^{14}C-dating and ^{13}C-measurements as tracers of organic matter dynamics as well as of morphogenetic and turbation processes. Science of the Total Environment 81/82, 99-110.

Scharpenseel HW, Pfeiffer EM, Becker-Heidmann P. 1996. Organic carbon storage in tropical hydromorphic soils. In: Carter MR, Stewart BA. (Eds.), Structure and organicmatter storage in agricultural soils. Adv. Soil Sci. Lewis Publishers, Boca Raton, pp. 361-392.

Schimel JP, Wetterstedt JÅM, Holden P, Trumbore SE. 2011. Drying/rewetting cycles mobilize old C from deep soils from a California annual grassland. Soil Biology and Biochemistry 43 (5), 1101-1103.

Singh BK, Milard P, Whitely AS, Murrell JC. 2004. Unravelling rhizospheremicrobial interactions: opportunities and limitations. Trends Plant Sci. 12, 386-393.

Sollins P, Homann P, Caldwell B. 1996. Stabilization and destabilization of soil organic matter: mechanisms and controls. Geoderma 74, 65-105.

Stevenson FJ. 1994. Humus Chemistry - Genesis, composition, reactions. 2nd edition. John Wiley, New York.

Strahm BD, Harrison RB, Terry T, Harrington TB, Adams AB, Footen PW. 2009. Changes in dissolved organic matter with depth suggest the potential for postharvest organic matter retention to increase subsurface soil carbon pools. Forest Ecology and Management 258, 2347-2352.

Tanji KK, Gao S, Scardaci SC, Chow AT. 2003. Characterizing redox status of paddy soils with incorporated rice straw. Geoderma, 114 (3-4), 333-353.

Trumbore SE, Vogel JS, Southon JR. 1989. AMS ^{14}C measurements of fractionated soil organic matter: an approach to deciphering the soil carbon cycle. Radiocarbon 31 (3), 644-654.

Trumbore S. 2009. Radiocarbon and Soil Carbon Dynamics. Annual Review of Earth and Planetary Sciences 37, 47-66.

von Lützow M, Kögel-Knabner I, Ekschmitt K, Matzner E, Guggenberger G, Marschner B, Flessa H. 2006. Stabilization of organic matter in temperate soils: Mechanisms and their relevance under different soil conditions - a review. European Journal of Soil Sciences 57, 426-445.

Vranova V, Rejsek K, Skene KR, Janous D, Formanek P. 2013. Methods of collection of plant root exudates in relation to plant metabolism and purpose: A review. Journal of Plant Nutrition and Soil Science 176, 175-199.

Wang H, Yang Z, Wang Y, Saito Y, Liu JP. 2008. Reconstruction of sediment flux from the Changjiang (Yangtze River) to the sea since the 1860s. Journal of Hydrology 349, 318-332.

Wilkinson MT, Richards PJ, Humphreys GS. 2009. Breaking ground: pedological, geological and ecological implications of soil biotrubation. Earth Sci Rev 97, 257-272.

Wissing L, Kölbl A, Vogelsang V, Fu JR, Cao ZH, Kögel-Knabner I. 2011. Organic carbon accumulation in a 2000-year chronosequence of paddy soil evolution. Catena, 87 (3), 376-385.

Wopereis MCS, Bouma J, Kropff MJ, Sanidad W. 1994. Reducing bypass flow through a dry, cracked and previously puddled rice soil. Soil and Tillage Research 29, 1-11.

Zhang M, He Z. 2004. Long-term changes in organic carbon and nutrients of an Ultisol under rice cropping in southeast China. Geoderma 118, 167-179

Appendix

Table A1: Radiocarbon data of bulk soil samples from paddy and non-paddy soils of different ages

Sample ID	Depth (cm)	Horizon	sampled depth (cm)	TOC (%)	^{14}C (pMC)	±	Conventional ^{14}C Age (BP)	±
Paddy soil (50 years)								
KIA 41465	0-7	Alp	3.5	1.20	101.99	0.43	modern	34
KIA 39160	7-14	Arp	12.5	1.13	101.48	0.25	modern	19
KIA 39161	14-23	Ardp	15	0.49	92.36	0.24	638	21
KIA 39162	14-23	Ardp	22	0.19	57.92	0.20	4387	28
KIA 39163	23-38	Bwg1	31	0.17	49.81	0.22	5599	36
KIA 39164	38-50	Bwg2	39.5	0.19	46.98	0.19	6068	32
KIA 39165	50-70	Bwg3	51.5	0.15	48.87	0.20	5752	33
KIA 39166	70-100	Blg	71.5	0.13	50.48	0.20	5492	32
KIA 39167	70-100	Blg	91.5	0.15	49.42	0.19	5662	31
Paddy soil (100 years)								
KIA 41468	0-9	Alp1	4.5	1.10	105.62	0.27	modern	20
KIA 39168	9-15	Alp2	12	1.76	107.01	0.27	modern	20
KIA 40286	15-21	Ardp	16	0.92	104.27	0.25	modern	20
KIA 40287	15-21	Ardp	20	0.51	92.76	0.32	603	28
KIA 40288	21-30	Bwg1	29	0.20	78.00	0.26	1996	27
KIA 40289	30-50	Bwg2	39	0.20	56.55	0.19	4579	27
KIA 40290	50-75	Bwlg1	51.5	0.21	54.57	0.18	4865	27
KIA 40291	50-75	Bwlg1	73.5	0.18	48.94	0.17	5741	29
KIA 40292	75-100	Bwlg2	98.5	0.17	54.16	0.20	4927	30
Paddy soil (300 years)								
KIA 40298	0-18	Alp	16.5	3.56	101.46	0.32	modern	25
KIA 40299	18-24	Ardp	19	1.99	103.34	0.33	modern	26
KIA 40300	18-24	Ardp	21	0.88	87.23	0.30	1097	28
KIA 40301	18-24	Ardp	23	0.54	80.13	0.29	1779	29
KIA 40302	24-30	Bwdl	28.5	0.28	66.63	0.25	3261	30
KIA 40303	30-50	Bwl	41.5	0.33	53.54	0.23	5018	34
KIA 40304	50-70	Bwlg1	52.5	0.23	59.77	0.28	4134	37
KIA 40305	50-70	Bwlg1	68.5	0.43	67.79	0.25	3123	29
KIA 40306	70-100	Bwlg2	88.5	0.14	50.54	0.21	5482	33
Paddy soil (500 years)								
KIA 38975	0-15	Alp	13.5	0.84	109.39	0.38	modern	28
KIA 38976	15-19	Ardp	16	1.31	110.38	0.27	modern	20
KIA 38892	19-25	Brdp	20	0.45	96.83	0.24	259	20
KIA 38977	25-48	Bwg1	24	0.36	91.08	0.27	751	24
KIA 38893	48-75	Bwg2	41.5	0.19	71.10	0.23	2740	26
KIA 38978	48-75	Bwg2	61.5	0.16	46.65	0.23	6125	39
KIA 38894	75-100	Bwlg	81.5	0.11	44.90	0.23	6433	41
KIA 38979	75-100	Bwlg	101.5	0.14	50.44	0.23	5498	36

Sample ID	Depth (cm)	Horizon	sampled depth (cm)	TOC (%)	^{14}C (pMC)	±	Conventional ^{14}C Age (BP)	±
Paddy soil (700 years)								
KIA 39169	0-10	Alp1	9	3.30	98.60	0.28	113	22
KIA 39170	10-16	Alp2	11.5	1.88	99.62	0.24	31	19
KIA 39486	16-22	Ardp	17	2.04	107.48	0.26	modern	19
KIA 39487	16-22	Ardp	21	1.03	101.80	0.24	modern	19
KIA 39488	22-45	Bg	23	0.74	94.52	0.23	453	19
KIA 39489	22-45	Bg	33.5	0.38	82.22	0.22	1573	21
KIA 39490	45-69	2Ahgb	46.5	0.49	78.85	0.22	1909	22
KIA 39491	45-69	2Ahgb	56.5	0.53	72.21	0.21	2616	23
KIA 39492	45-69	2Ahgb	67.5	0.37	65.75	0.20	3368	25
KIA 39493	69-106	2Blg1	88.5	0.28	49.71	0.17	5614	28
KIA 39494	106-116	3Ahlgb	107.5	1.03	64.06	0.29	3577	36
KIA 39495	116-130	3Blg	117.5	0.24	49.99	0.18	5569	28
KIA 39496	116-130	3Blg	128.5	0.16	38.42	0.16	7685	34
Paddy soil (1000 years)								
KIA 40312	0-10	Alp	9	1.22	103.05	0.26	modern	20
KIA 40313	10-16	Al(d)p1	11	1.05	100.82	0.24	modern	20
KIA 40314	10-16	Al(d)p1	15	0.44	103.72	0.29	modern	22
KIA 40315	16-21	Aldp2	20	0.55	92.72	0.24	607	21
KIA 40316	21-40	2Ahgb	22.5	0.43	87.27	0.23	1094	21
KIA 40317	21-40	2Ahgb	30	0.40	76.09	0.23	2195	24
KIA 40318	21-40	2Ahgb	38.5	0.33	69.18	0.22	2960	26
KIA 40319	40-55	2Bg	41.5	0.26	59.16	0.23	4217	31
KIA 40320	55-80	2Bl1	56.5	0.28	48.28	0.19	5849	31
KIA 40321	55-80	2Bl1	78.5	0.98	52.94	0.21	5109	31
KIA 40322	80-93	3Ahlb	85.5	1.97	62.54	0.20	3771	25
KIA 40323	80-93	3Ahlb	90.5	1.68	62.34	0.20	3796	25
KIA 40324	93-110	3Bl	108.5	0.49	55.28	0.21	4761	30
Paddy soil (2000 years)								
KIA 39171	0-15	Alp	13.5	3.30	112.25	0.25	modern	18
KIA 39986	15-20	Ar(d)p	16	3.01	113.67	0.30	modern	21
KIA 39987	15-20	Ar(d)p	19	1.51	107.74	0.41	modern	31
KIA 39988	20-27	Bdg	26	0.40	87.32	0.25	1090	23
KIA 39989	27-35	2Ahgb	28	0.40	81.73	0.26	1621	26
KIA 39990	27-35	2Ahgb	34	0.35	73.54	0.22	2469	24
KIA 39991	35-50	2Bg1	41.5	0.25	60.18	0.26	4079	35
KIA 39992	50-70	2Bg2	51.5	0.20	55.85	0.20	4680	29
KIA 39993	70-100	2Blg	71.5	0.13	36.70	0.17	8051	38
KIA 39994	70-100	2Blg	91.5	0.06	29.08	0.21	9923	57

Sample ID	Depth (cm)	Horizon	sampled depth (cm)	TOC (%)	^{14}C (pMC)	±	Conventional ^{14}C Age (BP)	±
Non-Paddy soil (50								
KIA 41466	0-9	Ap	4.5	0.67	101.07	0.39	modern	31
KIA 41467	9-17	ABw	13	0.54	102.06	0.35	modern	27
KIA 39481	17-24	Bw	22.5	0.27	82.86	0.22	1510	21
KIA 39482	24-45	BCg	43.5	0.18	71.39	0.22	2707	25
KIA 39483	45-70	CBg	63.5	0.15	67.29	0.27	3182	33
KIA 39484	70-100	CBlg	81.5	0.15	47.30	0.18	6014	31
KIA 39485	70-100	CBlg	101.5	0.16	45.75	0.18	6281	32
Non-Paddy soil (100 years)								
KIA 41469	0-14	Ap1	7	0.58	98.19	0.32	147	26
KIA 40293	14-25	Ap2	21	0.38	82.31	0.24	1564	24
KIA 40294	25-30	Bw	28.5	0.31	72.82	0.22	2548	24
KIA 40295	30-38	BCwg1	36.5	0.32	71.59	0.24	2685	27
KIA 40296	38-70	BCwg2	62.5	0.31	70.87	0.22	2766	25
KIA 40297	70-100	BCwlg	98.5	0.27	67.42	0.20	3167	24
Non-Paddy soil (300 years)								
KIA 43094	0-11	Ap	5.5	0.93	100.55	0.34	modern	27
KIA 40307	11-22	Bw1	20.5	0.38	86.18	0.29	1195	27
KIA 43095	22-32	Bw2	28	0.37	81.96	0.27	1598	26
KIA 40308	32-50	Bwg1	41.5	0.25	63.49	0.29	3649	37
KIA 40309	50-70	Bwg2	61.5	0.19	57.15	0.25	4494	35
KIA 40310	70-100	Bwlg	81.5	0.13	46.47	0.28	6155	48
KIA 40311	70-100	Bwlg	101.5	0.19	46.38	0.23	6172	40
Non-Paddy soil (700 years)								
KIA 41470	0-11	Ap1	5.5	0.90	103.27	0.28	modern	21
KIA 39497	11-17	Ap2	15.5	0.50	93.75	0.24	518	21
KIA 41471	17-23	Bw1	20	0.35	102.10	0.26		21
KIA 39498	23-45	Bw2	24.5	0.33	86.34	0.23	1180	21
KIA 39499	23-45	Bw2	43.5	0.23	75.66	0.27	2240	28
KIA 39500	45-70	Bwl1	68.5	0.10	53.94	0.21	4959	31
KIA 39501	70-100	Bwl2	91	0.14	50.70	0.18	5456	28
Fresh water wetland								
KIA 39995			1	1.44	104.85	0.29	modern	22
KIA 39996			19	0.57	105.75	0.41	modern	31
Marsh wetland								
KIA 39999			1.5	0.64	94.41	0.27	462	23
KIA 40000			19	0.54	82.83	0.25	1513	24

Sample ID	Depth (cm)	Horizon	sampled depth (cm)	TOC (%)	^{14}C (pMC)	±	Conventional ^{14}C Age (BP)	±
Tidal wetland								
KIA 39997			1	0.33	61.78	0.19	3869	25
KIA 39998			19	0.31	61.32	0.21	3928	28
KIA 39913			117.5	0.18	48.74	0.20	5773	33

Table A2: Radiocarbon data of macro-fossils separated from paddy soils of different ages

sample ID	Sample	sampled depth (cm)	Horizon	TOC (%)	^{14}C (pMC)	±	Conventional ^{14}C Age (BP)	±
Paddy soil (50 years)								
KIA 39161 b	charcoal	15	Ardp	27.46	93.44	0.27	545	23
KIA 39163 b	roots	31	Bwg1	22.75	106.36	0.31	modern	
KIA 39164 b	roots	39.5	Bwg2	32.68	113.96	0.56	modern	
KIA 39164 c	roots	39.5	Bwg2	52.34	112.08	0.47	modern	
KIA 39166 b	roots	71.5	Blg	48.44	119.57	1.03	modern	
Paddy soil (100 years)								
KIA 39168 b	charcoal	12	Alp2	44.95	120.18	0.34	modern	
KIA 40288 b	plant	29	Bwg1	31.61	104.44	0.38	modern	
KIA 40290 b	roots	51.5	Bwlg1	41.93	110.57	0.37	modern	
KIA 40291 b	roots	73.5	Bwlg1	37.11	110.08	0.46	modern	
KIA 40292 b	roots	98.5	Bwlg2	41.88	127.57	0.75	modern	
Paddy soil (300 years)								
KIA 40303 b	plant	41.5	Bwl	21.82	97.08	0.38	238	31
KIA 40303 c	roots	41.5	Bwl	25.36	105.59	0.33	modern	
Paddy soil (700 years)								
KIA 39169 b	wood	9	Alp1	38.59	133.76	0.34	modern	
KIA 39170 b	charcoal	11.5	Alp2	34.94	112.12	0.34	modern	
KIA 39486 b	charcoal	17	Ardp	33.36	109.69	0.28	modern	
KIA 39488 b	roots	23	Bg	21.76	105.65	0.31	modern	
KIA 39489 b	charcoal	33.5	Bg	31.62	97.91	0.39	169	32
KIA 39489 c	roots	33.5	Bg	29.35	104.68	0.27	modern	
KIA 39490 b	charcoal	46.5	2Ahgb	24.06	90.33	0.38	817	27
KIA 39491 b	roots	56.5	2Ahgb	40.14	110.83	0.45	modern	
KIA 39492 b	roots	67.5	2Ahgb	50.46	119.21	0.57	modern	
KIA 39494 b	plant	107.5	3Ahlgb	33.89	82.9	0.28	1506	28
KIA 39495 b	plant	117.5	3Blg	33.85	104.15	0.50	modern	
Paddy soil (1000 years)								
KIA 40316 b	charcoal	22.5	2Ahgb	21.81	90.54	0.48	798	43
KIA 40316 c	roots	22.5	2Ahgb	52.13	101.4	0.46	modern	
KIA 40318 b	charcoal	38.5	2Ahgb	39.69	79.6	0.23	1833	23
KIA 40318 c	roots	38.5	2Ahgb	51.49	107.08	0.50	modern	
KIA 40321 b	roots	78.5	2Bl1	43.33	101.62	1.24	modern	
KIA 40324 b	roots	108.5	3Bl	49.28	118.34	0.33	modern	
Paddy soil (2000 years)								
KIA 39988 b	roots	26	Bdg	9.18	102.93	0.34	modern	

Table A3: Basic properties of bulk soil samples from paddy and non-paddy soils of different ages. *Texture data for paddy soils originate from Wissing et al. (2010) and texture data for non-paddy profiles were provided by Ingrid Kögel-Knabner (Institute for Soil Sciences, Center of Life and Food Sciences Weihenstephan, TUM Munich). **Data about particle sizes were kindly provided by Ingrid Kögel-Knabner (Institute for Soil Sciences, Center of Life and Food Sciences Weihenstephan, TUM Munich).

					Particle-size classes**				
Sample ID	**Depth**	**Horizon**	**Texture***	**Clay**	**Fine silt**	**Medium silt**	**Coarse silt**	**Fine sand**	**Medium /coarse sand**
	(cm)			**(%)**	**(%)**	**(%)**	**(%)**	**(%)**	**(%)**
Paddy soil (50 years)									
KIA 41465	0-7	Alp	SiCL	29.0	13.7	38.4	15.1	1.0	2.8
KIA 39160	7-14	Arp	SiCL	29.7	13.7	37.1	14.5	1.0	4.0
KIA 39161	14-23	Ardp	SiCL	32.1	18.9	36.5	8.7	1.0	2.8
KIA 39163	23-38	Bwg1	SiCL	28.3	13.5	39.9	16.0	0.8	1.5
KIA 39164	38-50	Bwg2	SiL	22.0	12.9	44.7	17.4	0.8	2.2
KIA 39165	50-70	Bwg3	SiCL	29.8	15.5	40.3	11.0	0.8	2.6
KIA 39166	70-100	Blg	SiCL	31.4	16.4	38.2	10.9	0.8	2.3
Paddy soil (100 years)									
KIA 41468	0-9	Alp1	SiCL	27.9	15.3	36.5	12.9	3.4	4.0
KIA 39168	9-15	Alp2	SiCL	28.1	15.0	36.9	15.6	2.0	2.4
KIA 40286	15-21	Ardp	SiCL	28.1	15.1	36.6	14.9	1.0	4.3
KIA 40288	21-30	Bwg1	SiCL	32.9	17.2	35.1	12.8	1.4	0.6
KIA 40289	30-50	Bwg2	SiCL	33.3	14.8	36.6	13.1	0.8	1.4
KIA 40290	50-75	Bwlg1	SiCL	29.3	12.8	36.9	18.5	1.4	1.1
KIA 40292	75-100	Bwlg2	SiCL	28.6	13	37.2	18.3	1.4	1.5
Paddy soil (300 years)									
KIA 40298	0-18	Alp	SiL	24.5	13.1	40.5	16.4	1.8	3.7
KIA 40299	18-24	Ardp	SiCL	29.2	13.9	37.8	16.2	2	0.9
KIA 40302	24-30	Bwdl	SiL	24.3	12.6	41.6	17.9	0.4	3.2
KIA 40303	30-50	Bwl	SiCL	28.4	13.2	39.9	15.2	1.2	2.1
KIA 40304	50-70	Bwlg1	SiCL	31.3	13.4	35.8	13.6	3.4	2.5
KIA 40306	70-100	Bwlg2	SiCL	32.7	14.1	35.6	13.5	1.6	2.5
Paddy soil (500 years)									
KIA 38975	0-15	Alp	SiL	18.5	9.9	42.2	26.0	1.4	2.0
KIA 38976	15-19	Ardp	SiL	19.8	10.9	41.4	24.2	1.6	2.1
KIA 38892	19-25	Brdp	SiL	20.2	12.1	43.8	20.1	0.6	3.2
KIA 38977	25-48	Bwg1	SiL	22.8	11.4	41.9	18.9	2.8	2.2
KIA 38893	48-75	Bwg2	SiL	11.5	5.7	49.0	32.0	1.6	0.2
KIA 38894	75-100	Bwlg	SL	20.6	9.4	43.6	23.3	0.6	2.5

Sample ID	Depth (cm)	Horizon	Texture*	Particle-size classes** Clay (%)	Fine silt (%)	Medium silt (%)	Coarse silt (%)	Fine sand (%)	Medium /coarse sand (%)
Paddy soil (700 years)									
KIA 39169	0-10	Alp1	SiCL	28.6	15.6	39.4	13.2	2.0	1.2
KIA 39170	10-16	Alp2	SiCL	27.7	15.9	41.5	11.4	0.6	2.9
KIA 39486	16-22	Ardp	SiCL	28.4	16.1	41.3	8.9	1.4	3.9
KIA 39488	22-45	Bg	SiCL	27.5	17.6	40.5	11.0	0.8	2.6
KIA 39492	45-69	2Ahgb	SiC	49.0	19.7	25.3	3.7	0.2	2.1
KIA 39493	69-106	2Blg1	SiC	49.1	19.0	26.2	4.0	0.6	1.1
KIA 39494	106-116	3Ahlgb	SiCL	27.7	10.5	41.0	19.6	0.2	1.0
KIA 39495	116-130	3Blg	SiL	23.8	10.4	41.6	22.9	0.8	0.5
Paddy soil (1000 years)									
KIA 40312	0-10	Alp	SiCL	27.7	16.3	43.1	11.9	0.6	0.4
KIA 40313	10-16	Al(d)p1	SiCL	26.8	16.0	42.8	11.0	0.6	2.8
KIA 40315	16-21	Aldp2	SiCL	30.6	16.9	40.4	8.7	0.2	3.2
KIA 40316	21-40	2Ahgb	SiC	41.2	18.2	33.0	5.7	0.2	1.7
KIA 40319	40-55	2Bg	SiC	48.6	19.3	27.0	2.0	1.0	2.1
KIA 40321	55-80	2Bl1	SiC	49.1	21.7	25.6	0.7	0.6	2.3
KIA 40322	80-93	3Ahlb	SiC	44.1	16.9	32.9	4.8	0.2	1.1
KIA 40324	93-110	3Bl	SiC	39.3	16.3	33.7	6.5	1.8	2.4
Paddy soil (2000 years)									
KIA 39171	0-15	Alp	SiL	24.2	17.1	40.4	10.7	3.2	4.4
KIA 39987	15-20	Ar(d)p	SiL	25.6	17.2	40.0	11.7	3.4	2.1
KIA 39988	20-27	Bdg	SiL	27.8	18.9	37.9	11.4	2.0	2.0
KIA 39989	27-35	2Ahgb	SiCL	35.9	16.1	37.3	7.8	0.6	2.3
KIA 39991	35-50	2Bg1	SiC	47.4	14.7	30.5	4.7	0.8	1.9
KIA 39992	50-70	2Bg2	SiCL	37.5	14.4	36.7	9.6	1.2	0.6
KIA 39993	70-100	2Blg	SiCL	32.4	13.9	37.0	10.8	1.6	4.3
Non-Paddy soil (50years)									
KIA 41466	0-9	Ap	SiL	20.8	10.8	46.4	18.5	2.4	1.1
KIA 41467	9-17	ABw	SiL	23.2	11.7	45.0	17.1	1.4	1.6
KIA 39481	17-24	Bw	SiL	24.1	11.0	45.2	17.2	1.0	1.5
KIA 39482	24-45	BCg	SiL	22.6	10.3	43.4	15.7	3.8	4.2
KIA 39483	45-70	CBg	SiL	26.8	12.1	42.3	15.5	1.8	1.5
KIA 39484	70-100	CBlg	SiL	22.3	10.1	46.3	19.0	0.6	1.7

Sample ID	Depth (cm)	Horizon	Texture*	Particle-size classes**					
				Clay (%)	Fine silt (%)	Medium silt (%)	Coarse silt (%)	Fine sand (%)	Medium /coarse sand (%)
Non-Paddy soil (100 years)									
KIA 41469	0-14	Ap1	SiL	27.2	13.4	41.3	14.0	2.0	2.1
KIA 40293	14-25	Ap2	SiL	26.1	13.4	42.3	16.8	0.6	0.8
KIA 40294	25-30	Bw	SiL	29.1	14.2	39.7	12.7	2.6	1.7
KIA 40295	30-38	BCwg1	SiL	31.9	13.9	38.7	12.3	2.0	1.2
KIA 40296	38-70	BCwg2	SiL	32.8	13.9	39.3	11.7	1.0	1.3
KIA 40297	70-100	BCwlg	SiL	31.1	13.8	40.6	13.0	1.0	0.5
Non-Paddy soil (300 years)									
KIA 43094	0-11	Ap	SiCL	23.7	12.9	44.3	16.3	0.4	2.4
KIA 40307	11-22	Bw1	SiCL	26.2	12.9	44.0	14.4	0.6	1.9
KIA 43095	22-32	Bw2	SiCL	28.6	13.1	42.0	12.4	0.8	3.1
KIA 40308	32-50	Bwg1	SiCL	30.5	13.3	41.1	13.1	0.6	1.4
KIA 40309	50-70	Bwg2	SiCL	28.0	14.3	37.7	17.4	1.4	1.2
KIA 40310	70-100	Bwlg	SiCL	27.6	13.7	38.3	14.6	1.4	4.4
Non-Paddy soil (700 years)									
KIA 41470	0-11	Ap1	SiL	19.0	9.0	45.0	22.3	0.6	4.1
KIA 39497	11-17	Ap2	SiL	22.2	9.3	44.1	22.9	0.4	1.1
KIA 41471	17-23	Bw1	SiL	24.9	9.9	43.3	20.0	0.4	1.5
KIA 39498	23-45	Bw2	SiL	19.2	16.0	44.7	15.5	2.4	2.2
KIA 39500	45-70	Bwl1	SiL	14.6	6.5	45.8	29.0	1.8	2.3
KIA 39501	70-100	Bwl2	SiL	22.8	10.1	42.2	21.0	1.4	2.5
Fresh water wetland									
KIA 39995	0-3	N/A	SiL	17.7	11.9	18.6	12.2	9.8	29.8
KIA 39996	18-20	N/A	SCL	15.8	12.2	18.7	7.2	7.2	38.9
Marsh wetland									
KIA 39999	0-3	N/A	N/A	13.7	7.4	36.1	39.3	1.6	1.9
KIA 40000	18-20	N/A	N/A	12.3	7.2	34.8	40.3	2.2	3.2
Tidal wetland									
KIA 39997	0-3	N/A	N/A	10.6	6.1	34.1	41.7	5.2	2.3
KIA 39998	18-20	N/A	N/A						
KIA 39913	115-120	N/A	N/A						

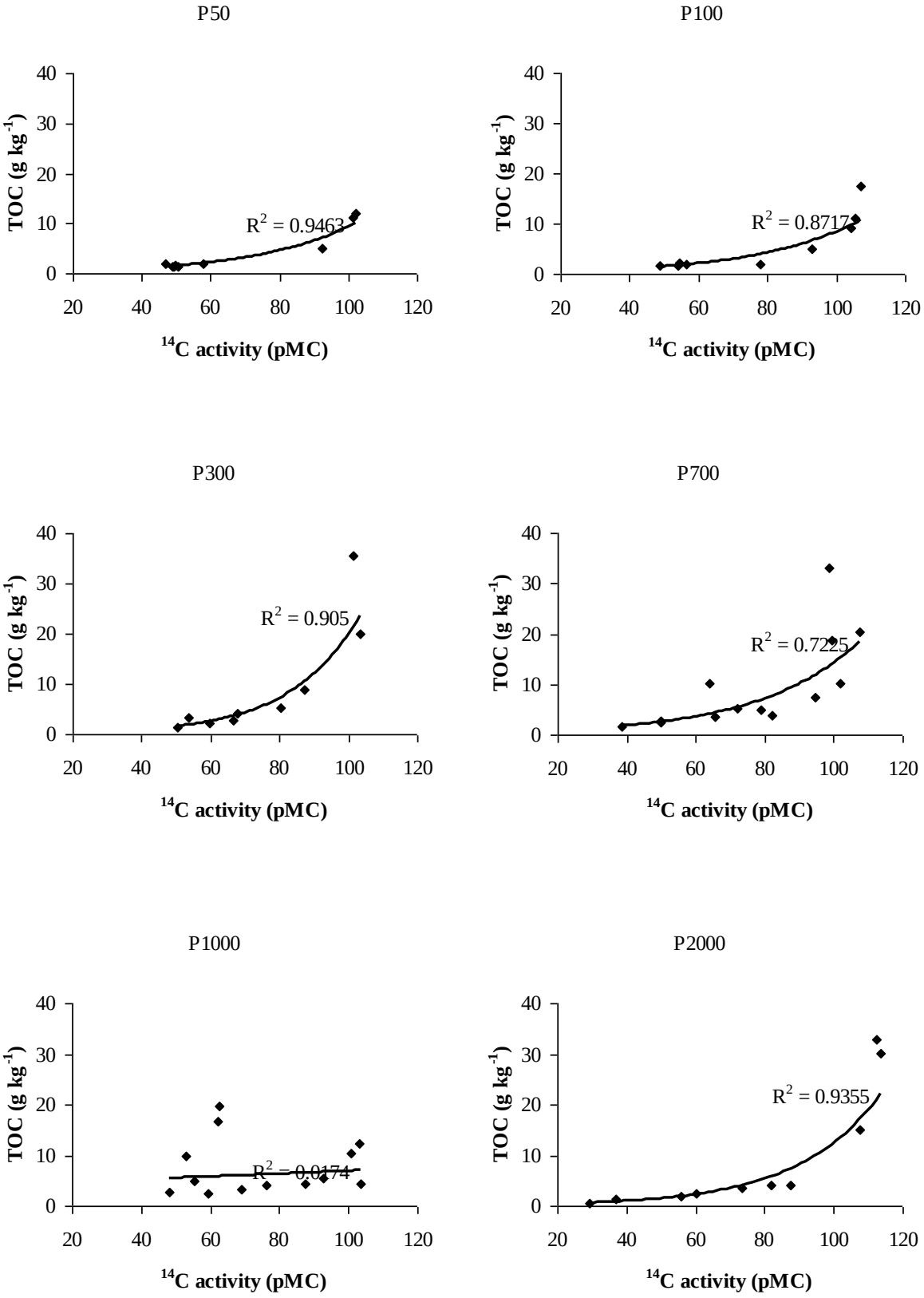

Figure A1: Relationship between the total organic carbon content and the radiocarbon activity in paddy soils of different ages.

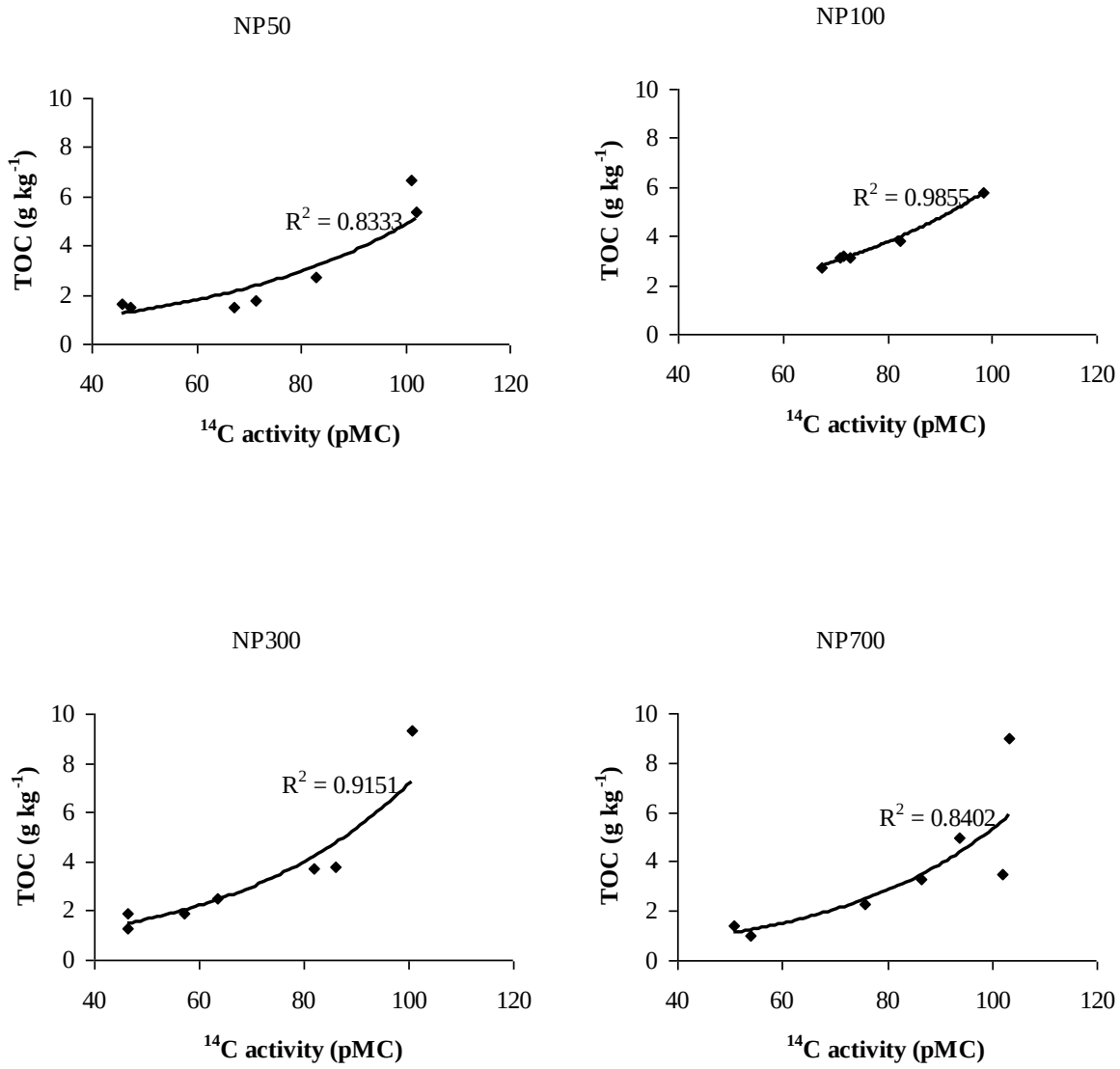

Figure A2: Relationship between the total organic carbon content and the radiocarbon activity in non-paddy soils of different ages.

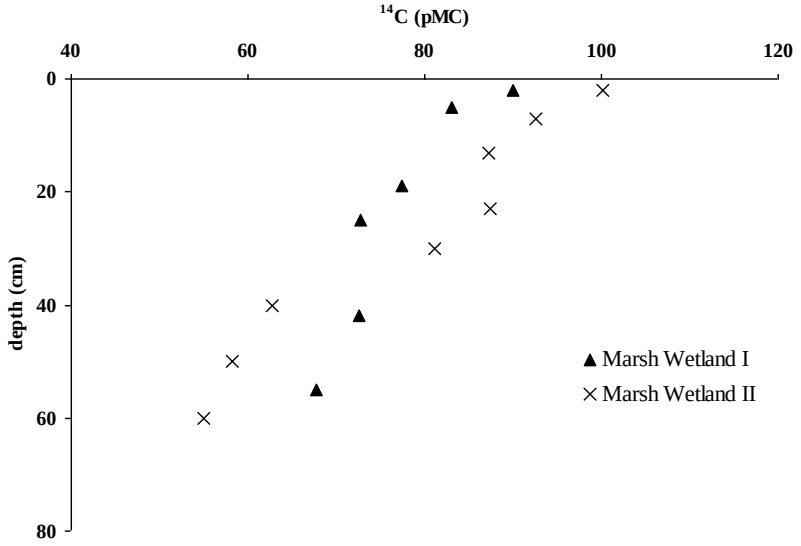

Figure A3: Radiocarbon depth distribution of two additional non-paddy sites located between the '1977' and '1958'-dikes. The graphs illustrate the decline of bulk soil ^{14}C with increasing soil depth.

Erklärung

Hiermit erkläre ich, dass ich die vorliegende Dissertation nach den Regeln guter wissenschaftlicher Praxis der Deutschen Forschungsgemeinschaft selbst verfasst habe. Dabei habe ich keine Hilfe, außer der wissenschaftlichen Beratung durch meine Betreuer in Anspruch genommen. Es wurden keine weiteren als die angegeben Hilfsmittel und Quellen verwendet. Des Weiteren erkläre ich, dass diese Arbeit weder ganz noch zum Teil einer anderen Stelle im Rahmen eines Prüfungsverfahrens vorgelegt wurde. Ich habe bisher keinen anderen Promotionsversuch unternommen.

Teile dieser Arbeit wurden bereits veröffentlicht oder zur Publikation vorbereitet.

Kiel, den

Tino Bräuer